

**Dynamics of partial anaerobiosis, denitrification,
and water in soil: experiments and simulation**

DE WIT, J.



**BIBLIOTHEEK
LANDBOUWUNIVERSITEIT
WAGENINGEN**

Promotoren: dr.ir. C.T. de Wit,
buitengewoon hoogleraar in de theoretische teeltkunde

dr.ir. G.H. Bolt,
hoogleraar in de bodemscheikunde en de bodemnaturkunde

NN08201, 1174

P.A. Leffelaar

**Dynamics of partial anaerobiosis, denitrification,
and water in soil: experiments and simulation**

Proefschrift
ter verkrijging van de graad van
doctor in de landbouwwetenschappen,
op gezag van de rector magnificus,
dr. C.C. Oosterlee,
in het openbaar te verdedigen
op vrijdag 6 november 1987
des namiddags te vier uur in de aula
van de Landbouwuniversiteit te Wageningen

ISBN 299636

This study was carried out at the departments:

Soil Science and Plant Nutrition and Theoretical Production Ecology
De Dreyen 3 Bornsesteeg 65
6703 BC Wageningen 6708 PD Wageningen

of Wageningen Agricultural University, Wageningen, The Netherlands

NN08201, 1174.

Stellingen

1. In grond is geen hoge correlatie te verwachten tussen denitrificatiesnelheid en graad van anaërobie.

Sextone, A.J., N.P. Revsbech, T.B. Parkin, and J.M. Tiedje. 1985. Direct measurement of oxygen profiles and denitrification rates in soil aggregates. *Soil Sci. Soc. Am. J.* 49:645-651.

2. Het gebruik van de "Oxygen Diffusion Rate" methode, om het proces van bodemaëratie in onverzadigde grond te karakteriseren, moet worden afgeraden.

Phene, C.J. 1986. Oxygen electrode measurement. In *Methods of soil analysis*, part 1. A. Klute (ed.). *Agronomy 9*. American Society of Agronomy, Madison, Wis., pp. 1137-1159.

McIntyre, D.S. 1970. The platinum microelectrode method for soil aeration measurement. *Advances in Agronomy* 22:235-283.

3. De stelling "niet simuleren zonder experimenteren" geldt voor bodemecologische studies ook omgekeerd: "niet experimenteren zonder simuleren".

4. Bij het ontwikkelen van programmatuur van computermodellen dient veel meer dan thans het geval is, gelet te worden op de herkenbaarheid en daarmee de overdraagbaarheid van de erin verwerkte proceskennis.

5. In de eerste lijns gezondheidszorg wordt veel te weinig aandacht besteed aan het bestaan van voedselallergie.

6. Het gebruik van gedroogde en gemalen grond voor microbiologische experimenten dient vermeden te worden.

Fillery, L.R.P. 1983. Biological denitrification. In *Gaseous loss of nitrogen from plant-soil systems*.

J.R. Freney and J.R. Simpson (eds.). Martinus Nijhoff, The Hague. pp. 33-64.

Wollum II, A.G. 1982. Cultural methods for soil microorganisms. In *Methods of soil analysis*, pt 1.

A.L. Page (ed.). *Agronomy 9*. American Society of Agronomy, Madison, Wis., pp. 781-802.

7. Stikstofverliezen als gevolg van denitrificatie worden overschat door het meten van alleen nitraatafname, en onderschat door het meten van alleen de produktie van lachgas plus stikstofgas.

dit proefschrift.

Stellingen bij het proefschrift "Dynamics of partial anaerobiosis, denitrification, and water in soil: experiments and simulation" van P.A. Leffelaar.

Wageningen, 6 november 1987.

BIBLIOTHEEK
LANDBOUWUNIVERSITEIT
WAGENINGEN

42400

Aan Ita, Freek en Evelien

DANKWOORD

Velen hebben direct of indirect bijgedragen aan het tot stand komen van dit proefschrift. Mijn dank hiervoor gaat ten eerste uit naar mijn beide promotoren, Prof.Dr.Ir. C.T. de Wit en Prof.Dr.Ir. G.H. Bolt, enerzijds voor de grote vrijheid die zij mij gelaten hebben om het onderzoek naar eigen inzicht aan te pakken, anderzijds voor de opbouwende kritiek die zij leverden op de teksten.

Met betrekking tot het experimentele werk gaat mijn dank uit naar:

- Th. J. Jansen (voormalig CABO-medewerker), voor het deskundig vervaardigen van de vele onderdelen die tesamen de meetopstelling vormden, en voor de prettige samenwerking.
- W. Ch. Melger en G.P. Lelyveld (vakgroep Organische Chemie), voor de ondersteuning die zij hebben geboden bij het werken met de gaschromatograaf en voor het vervaardigen van de kolommen.
- H. Vrijmoeth, voormalig student RMHAS te Wageningen, voor het bepalen van de optimale samenstelling van het ijkasmengsel voor de gaschromatograaf.
- Dr.Ir. H.P. Kimmich, J.G. Spaan, Ir. J. de Koning en A. Lamboo van de Katholieke Universiteit te Nijmegen, voor de hulp bij het werken met catheter zuurstofelectroden.
- Ing. J.G. de Swart en G.L. Jupijn (ITAL), voor het vervaardigen van de versterkers voor de zuurstofelectroden.
- C. Rijpma, M. Schimmel, J. van der Goor en A. van Wijk (Centrale dienst De Dreijen), voor het goed verzorgde tekenwerk en het vervaardigen van het besturingssysteem voor het meten van bodemvocht.
- P.J.M. ten Have (voormalig medewerker vakgroep Theoretische produktie-ecologie), voor de hulp bij de eerste bodemvochtmetingen.
- S. Maasland, C.A. Kok, W. van Barneveld en W.C. Nieuwboer, voor de hulp bij het oplossen van vele technische zaken.
- Dr.Ir. V.J.G. Houba en A. van den Berg, voor het uitvoeren en bespreken van de chemische analyses.
- D.P. van den Akker, J.D. Wouda, J.C.M. Lambert, J.F.M. Wacki, H. van den Heuvel, G.E. van der Weerthof, H. Lindeman, E.B. Tijssen Jr., J.M. Kuster, P.H.F.M. van Twist, J. Treur en M.R. Kuijk, allen voormalige studenten aan de HTS te Arnhem, voor hun inzet bij het uitvoeren van deelexperimenten, het maken van schakelingen voor de meetopstelling en het helpen ontwikkelen van rekenprogramma's voor de verwerking van de experimentele gegevens.

Met betrekking tot het theoretische werk gaat mijn dank uit naar:

- Prof.Dr.Ir. H.J. Merk (Technische Universiteit Delft) en Prof.Dr.Ir. J. Schenk (vakgroep Natuur- en weerkunde), voor de stimulerende discussies met betrekking tot

gasdiffusie in multinaire gasmengsels.

- Ir. J.H.G. Verhagen, in het bijzonder voor zijn hulp bij het opstellen van de vergelijkingen om gelijke gasdrukken te handhaven in aan elkaar grenzende gas-continue bodemlagen waarin verschillende productiesnelheden optreden.
- Prof.Dr. A.J.B. Zehnder, Dr.Ir. J.L.M. Huntjens (vakgroep Microbiologie) en Dr.Ir. B.H. Janssen, voor het bediscussieren van de lange lijst vooronderstellingen die ten grondslag ligt aan het denitrificatiesubmodel.
- Dr.Ir. C. Dirksen, in het bijzonder voor het op leerzame wijze verbeteren van een aantal van mijn engelse teksten.
- Dr.Ir. J. Goudriaan, Dr.Ir. H. van Keulen (CABO), Ir. J.A. den Dulk en Ir. P. Koorevaar, die altijd bereid waren tijd vrij te maken voor het oplossen van problemen.
- P. Keizer, L. Verheyen, H. Tuinhof, R. Baas, J. Reijerink, D. van den Tillaart, M.P. van der Maas, W. Otten, W. Wessel en E. Korzilius, allen (voormalige) studenten aan de Landbouwuniversiteit te Wageningen, voor hun inbreng bij de ontwikkeling van de submodellen aangaande waterherverdeling, respiratie en denitrificatie in grond.

Verder gaat mijn dank uit naar:

- Prof.Dr.Ir. R. Rabbinge, voor zijn fijne hulp bij alle zaken die geregeld dienden te worden voor de voortgang van het onderzoek.
- Mw. H.H. van Laar, en G.J. van Hoof, Ir. G.J. Lokhorst, A.J. Koster en G. Klein (Rekencentrum), voor de hulp bij het werken met de computer.
- Mw. C.G. Uithol-van Gulijk en B.H.J. van Amersfoort, voor het typen van een aantal van de teksten.
- Ir. D.W.G. van Kraalingen, voor zijn hulp bij het werken met de laserprinter.
- de vakgroep Bodemkunde en Plantenvoeding, voor het langdurig beschikbaar stellen van laboratorium- en bureauruimten.
- de anonieme medewerkers van de hoofdbibliotheek, voor de vlotte toezending van de vele door mij aangevraagde literatuur.
- het Nederlands Meststoffen Instituut, voor de bescheiden, maar daarom niet minder nuttige, subsidie, die zij aan het project toekenden.
- alle anderen die hebben bijgedragen aan het onderzoek, maar hier niet genoemd zijn.

Tenslotte wil ik Ita hartelijk bedanken voor het geduldig aanhoren van alle verhalen over anaërobie, moeilijke metingen en computers die "plat" gaan, en voor het vertrouwen dat zij had in de goede afloop van dit werk.

CONTENTS

Abstract	10
1. General introduction	11
2. Simulation of partial anaerobiosis in a model soil in respect to denitrification (P.A. Leffelaar. 1979. <i>Soil Sci.</i> 128:110-120)	15
3. Dynamics of partial anaerobiosis, denitrification, and water in a soil aggregate: experimental (P.A. Leffelaar. 1986. <i>Soil Sci.</i> 142:352-366)	27
4. Dynamic simulation of multinary diffusion problems related to soil (P.A. Leffelaar. 1987. <i>Soil Sci.</i> 143:79-91)	43
5. Denitrification in a homogeneous, closed system: experiment and simulation (P.A. Leffelaar, and W.Wessel. Submitted)	57
6. Dynamics of partial anaerobiosis, denitrification, and water in a soil aggregate: simulation (P.A. Leffelaar. Submitted)	79
Summary	109
Samenvatting	113
Curriculum vitae	117

ABSTRACT

Leffelaar, P.A. 1987. Dynamics of partial anaerobiosis, denitrification, and water in soil: experiments and simulation. Doctoral thesis, Agricultural University Wageningen, Wageningen, The Netherlands, p.117.

Dynamic interactions between biological respiration and denitrification, and physical transport processes that modify the abiotic soil environment in which bacteria live, were studied through the development of a new type of experimental respirometer system and an explanatory simulation model.

The respirometer system enables one to measure simultaneously the distribution of water, oxygen, nitrate, ammonium, and pH as a function of space and time in an unsaturated, artificially made, homogeneous, cylindrical soil aggregate. The coherent data sets that were obtained by this experimental system served to test the explanatory simulation model.

The simulation model comprises four submodels: 1) biological respiration and denitrification, 2) water transport including a description to account for hysteresis, 3) solute transport, and 4) gas transport including a new description to simulate the integral soil atmosphere. Besides evaluation of the integral model with the results of the respirometer system, three of the submodels were also separately tested, either by means of experiments (submodel 1 and 2) or by analytical solutions (a special case of submodel 4).

It was found that the new respirometer system yields valuable data to test the simulation model, and that the simulation model gives a fair description of the measured data. However, it appears that only the combined study of the results of experiments and simulations will deepen the understanding of the complicated interactions that occur in this soil biological ecosystem.

It was the objective of this study to describe the respirometer system, the explanatory simulation model, and the tests that were done to evaluate the integral model and the separate submodels.

Additional index words: respirometer, gamma radiation, gas chromatography, polarographic Clark-type oxygen electrodes, Stefan-Maxwell equations, ordinary diffusion, binary diffusion coefficients, microbial growth, Monod equation, Pirt equation, maximum growth yield, maintenance coefficient, gas-continuous pores, soil atmospheric pressure, CSMP-III

CHAPTER 1

General introduction

Soil nitrogen is essential for plant growth and the formation of proteins required by living matter. Often crop yields are restricted by lack of nitrogen. Then, productivity may be strongly increased by nitrogen inputs from fertilizers. Much of the fertilizer nitrogen added to the soil is not used by the crop, however, since it can be lost from the root zone by e.g. volatilization of ammonia, and nitrification of ammonium to nitrate with subsequent denitrification or leaching (Stevenson 1982). These losses form a waste of energy, labour, and money for the agricultural practice, whilst they also form a threat for the environment: leached nitrate can contaminate groundwaters from which drinking water is prepared (van Kessel 1976), nitrous oxide from denitrification may affect the protective ozone layer of the stratosphere (Crutzen 1981).

Estimates of nitrogen losses by microbial denitrification from aerated, structured, partially saturated soils are reported to be substantial and to vary tremendously: Colbourn and Dowdell (1984) reported that 0-20 % of the added fertilizer was lost from arable soils, and 0-7 % from grassland soils, whereas Firestone (1982) cited studies where the average nitrogen losses were estimated between 25 and 30 %. The variation in the estimates of these nitrogen losses can partly be ascribed to indirect assessment of denitrification, for instance by N-balance methods, and partly by the complex nature of the process, resulting in statements that "denitrification appears the least understood of all the N-transformation processes" (Tanji and Gupta 1978; Colbourn and Dowdell 1984). A better understanding of the dynamic interactions between the biological and physical processes determining denitrification is expected to eventually lead to improved management practices involving timing and intensity of fertilizer application and irrigation, form of N-fertilizer, and tillage techniques.

Therefore, this study aimed at integrating existing knowledge about the major processes that were known to cause and affect denitrification by means of a mathematical explanatory dynamic simulation model, and at developing capability to test such a model by experiments in which denitrification could be assessed directly. The resulting investigations are reported in the present study.

Denitrification refers to the process in which nitrate serves as an electron acceptor for essentially aerobic microorganisms at low oxygen concentrations, with the result that nitrous oxide and molecular nitrogen are produced (Delwiche 1981). Denitrification in soil thus occurs when the interactions between biological and physical processes result in locations where oxygen is absent, and bacteria capable of denitrification, nitrate, decomposable organic matter, and water are present.

A low oxygen concentration is considered a prerequisite for the occurrence of denitrification (Woldendorp 1981; Knowles 1982), though some reports indicate that the process may also take place at higher oxygen concentrations (Robertson and Kuenen 1984). In structured soil low oxygen concentrations are mainly confined to the aggregates (Currie, 1961; Greenwood, 1961). First, therefore, the dynamic behaviour

of the anaerobic soil fraction as a function of respiratory activity and water distribution was theoretically investigated in a model soil consisting of spherical aggregates in a hexagonal packing (chapter 2). It appeared that anoxity, and thus possibly denitrification, was nearly always present inside aggregates, while interaggregate pores had approximately atmospheric oxygen concentrations. The major difficulty of the model was to test it. As a consequence, the interactions between biological and physical processes were further experimentally (chapter 3) and theoretically (chapter 6) studied in a single cylindrical soil aggregate, in which transport processes were radial. This geometry is a model representation of a spherical soil aggregate from which the upper and lower sides are removed. The tested model may be converted to a spherical geometry and be used in a field model describing the spatial arrangement of aggregates and the interaggregate transport processes, e.g. a model resembling the one described in chapter 2. The experimental respirometer system (chapter 3) enables one to measure simultaneously the state variables water, oxygen, nitrate, nitrite, ammonium, and pH as a function of space and time, and atmospheric composition in the chamber that contains the aggregate as a function of time. The system allows to largely avoid other N-transformations in soil so that attention can be restricted to the process of denitrification. Though the experimental system yielded coherent data sets to evaluate the simulation model, it was clear that a full explanation of the relationships among the measured data required a theoretical framework, i.e. the same simulation model.

The final simulation model (chapter 6) comprises four submodels, each containing the differential equations that are solved to obtain a particular state variable as measured in the respirometer. In principle, each submodel should be tested separately, to judge its quality before it is used in the final model. This testing of submodels was achieved as follows.

The major transport mechanism in the removal of gaseous denitrification products is diffusion. Therefore, the interdiffusion of gases in complex systems where respiration and denitrification take place was studied in chapter 4. Here, results of Fick's first law with an extension to maintain isobaric conditions are compared with results from the rigorous gas kinetic theory.

The microbial processes of respiration and denitrification were studied in chapter 5. Here, the results of the submodel that calculates microbial activity in a thin, homogeneous soil layer, are compared with experiments carried out in gastight petri dishes.

The final simulation model (chapter 6) also contains a submodel for water redistribution including hysteresis in the soil water characteristic, and a submodel describing the transport of nitrate and nitrite. The former submodel could be tested directly against the experimental data from the respirometer system. The latter submodel was not tested separately: nitrate and nitrite distributions were only compared with the respirometer data from chapter 3. Therefore, this submodel may contain larger errors compared with the results of the separately tested submodels, since the distributions of nitrate and nitrite are the result of the integrated effect of other submodels as well.

REFERENCES

Colbourn, P., and R.J. Dowdell. 1984. Denitrification in field soils. In Biological processes and soil fertility. J. Tinsley and J.F. Darbyshire (eds.). Martinus Nijhoff, The Hague, pp. 213-226.

Crutzen, P.J. 1981. Atmospheric chemical processes of the oxides of nitrogen, including nitrous oxide. In Denitrification, nitrification, and atmospheric nitrous oxide. C.C. Delwiche (ed.). Wiley, New York, pp. 17-44.

Currie, J.A. 1961. Gaseous diffusion in the aeration of aggregated soils. *Soil Sci.* 92:40-45.

Delwiche, C.C. (ed.). 1981. Denitrification, nitrification, and atmospheric nitrous oxide. Wiley, New York, p. 286.

Firestone, M.K. 1982. Biological denitrification. In Nitrogen in agricultural soils. F.J. Stevenson (ed.). Agronomy 22. American Society of Agronomy, Madison, Wis., pp. 289-326.

Greenwood, D.J. 1961. The effect of oxygen concentration on the decomposition of organic materials in soil. *Plant Soil* 14:360-376.

Kessel, J.P. van. 1976. Influence of denitrification in aquatic sediments on the nitrogen content of natural waters. *Agricultural Research Reports* 858, PUDOC, Wageningen, p. 104.

Knowles, R. 1982. Denitrification. *Microbiological reviews* 46:43-70.

Robertson, L.A., and J.G. Kuenen. 1984. Aerobic denitrification - old wine in new bottles? *Antonie van Leeuwenhoek* 50:525-544.

Stevenson, F.J. 1982. Origin and distribution of nitrogen in soil. In Nitrogen in agricultural soils. F.J. Stevenson (ed.). Agronomy 22. American Society of Agronomy, Madison, Wis., pp. 1-42.

Tanji, K.K., and S.K. Gupta. 1978. Computer simulation modeling for nitrogen in irrigated croplands. In Nitrogen in the environment, vol. 1. D.R. Nielsen and J.G. MacDonald (eds.). Academic Press, New York, pp. 79-130.

Woldendorp, J.W. 1981. Nutrients in the rhizosphere. Agricultural yield potentials in continental climates. *Proc. 16th Coll. Int. Potash Institute, Bern*, pp. 99-125.

CHAPTER 2

SIMULATION OF PARTIAL ANAEROBOSIS IN A MODEL SOIL IN RESPECT TO DENITRIFICATION

P. A. LEFFELAAR

Department of Theoretical Production Ecology, Bornsesteeg 65, Wageningen, The Netherlands

Received for publication November 10, 1978; revised February 13, 1979

ABSTRACT

Factors affecting anaerobiosis in soil have been studied by means of computer simulation applied to a model soil composed of spherical aggregates in a hexagonal packing. This schematized geometry implies that two different types of pores are distinguished: intra- and interaggregate pores. The moisture characteristics for the interaggregate water and the non-water-covered area of the aggregates, the so-called air-exposed area, were calculated in general terms. The results give a tool to derive curves for a certain aggregate radius. The interaggregate water content is used to calculate the diffusion properties of the model soil down the profile. The diffusion from interaggregate pores into the aggregates is taken proportional to the air-exposed area of the aggregates.

Results of the model are given for an aggregate radius of 0.5 centimeters. They indicate anaerobiosis to occur below a depth of 10 centimeters and in the profile as a whole, before and during rainfall, respectively. The anaerobic soil volume rapidly responds to a shower of rain. However, it is not affected as seriously by the water regime as it is by the magnitude and distribution of the respiratory activity or the diffusion coefficient in the aggregates. The model soil was also used to derive, for a particular case, a soil anaerobiosis characteristic relating soil moisture suction to the anaerobic soil fraction. Some indications are given for further experimental research.

INTRODUCTION

Oxygen deficiency is a prerequisite for the occurrence of denitrification in soil.¹ However, denitrification has been reported to occur in well-aerated soils too (Broadbent 1951). This suggests the existence of anaerobic locations in soils normally considered well-aerated. Such anaerobic pockets could be due to the presence of structural elements in the soil. Currie (1961) states that soil microorganisms and plant roots require intimate contact with the soil particles for satisfactory uptake of nutrients and water and, therefore, are predominantly found in the finer pores of the soil. Consequently, respiration tends to take place within the aggregates rather than between them. Centers of aggregates thus may become anaerobic, introducing spatial differences in oxygen status. This variability is a major problem in interpreting soil aeration mea-

surements (Flühler et al. 1976). These authors therefore consider the approach of Currie (1961) and Greenwood (1961), who described the aeration status within spherical soil aggregates, as a key for eliminating existing misinterpretations of soil aeration measurements.

Some attempts to model anaerobiosis are reported by van Veen (1977)² and Smith (1977). The former regarded the soil as a bundle of capillaries, whereas the latter considered spherical aggregates having a certain size distribution but did not take into account their spatial arrangement.

The subject of this study is the dynamic behavior of the anaerobic soil fraction in a model soil, consisting of spherical aggregates, by a computer simulation technique. Evaluation of the model may lead to increased insight into the relative importance of the variables incorporated. Results thus obtained can be used to

¹ J. W. Woldendorp, 1963, The influence of living plants on denitrification, Ph.D. thesis, Wageningen, The Netherlands.

² H. van Veen, 1977, The behavior of nitrogen in soil—a simulation study, Ph.D. thesis, Vrije University, Amsterdam.

SIMULATION OF PARTIAL ANAEROBIOESIS

indicate subjects that should be investigated experimentally.

DESCRIPTION OF THE MODEL SOIL

Basic considerations

Many soil types show structural units, in the centers of which anaerobiosis may be found. The oxygen status of a particular aggregate in a soil is governed by its dimensions, the oxygen concentration at the outside, the oxygen consumption rate, and the diffusion coefficient in the interior. The latter is largely determined by the water content and the solubility of oxygen in water. The oxygen concentration at the outside is governed by the macrodiffusion process of oxygen from the atmosphere into the soil, which mainly takes place through the interaggregate pores. Because the diffusion coefficient of oxygen is about 10^4 times smaller in water than in air, the diffusion rate of oxygen from an interaggregate pore into an aggregate is reduced when water partially covers the aggregate, as may occur at contact points. Thus the moisture characteristics of a soil are important in determining its oxygen status. These considerations have resulted in a model soil consisting of spherical aggregates in a hexagonal packing, enabling us to perform calculations concerning interaggregate moisture content and oxygen transport in aggregated soils.

Geometry

The model soil is composed of spherical aggregates of three sizes. The largest aggregates are arranged in a hexagonal packing, and the smaller aggregates fit exactly in the tetrahedral and octahedral voids of this packing. A unit hexagonal packing contains 6, 12, and 6 equidimensional, tetrahedral, and octahedral spheres, respectively. Their radii are in the proportion of

$$R:R_4:R_8 = R:R \frac{2^{1/2}}{3} \left(\frac{3}{2} - \frac{3^{1/2}}{2} \right) : R(2^{1/2} - 1) \\ = 1:0.2247:0.4142$$

The total height of such a unit is $2/3^{1/2} \times 4R$, and it has a volume of $2^{1/2} \times 24R^3$. It has a porosity of 19.0083 percent with and 25.952 percent without inscribed spheres. A detailed description of the model soil is given by Leffelaar (1977). Slichter (1899) and Azároff (1960) give extensive descriptions of the equidimensional sphere packing without inscribed spheres.

Physical characteristics of the model soil

Volume of the pendular water ring

In the model soil the water in the interaggregate pores is present in the form of annuli of wedge-shaped cross section around the points of contact of the aggregates (pendular rings). The volume of water held at given suctions may be calculated for equidimensional aggregates (Wilsdon 1921). However, the model soil contains aggregates of different sizes, which requires a more general formula for unequal spheres. This formula was derived using the coordinate system of Fig. 1.

The volume of the pendular water ring V_{pr} may be calculated as the difference between the volumes of a truncated cone V_c and the two spherical segments V_R and V_{R_s} , and the fraction of a torus V_t included by the cone, Eq. (1).

$$V_{pr} = V_c - (V_R + V_{R_s} + V_t) \quad (1)$$

where

$$V_c = \frac{\pi}{3} \{ R_x(1 - \cos \alpha) \\ + R(1 + \cos(\alpha + \beta)) \} \quad (2)$$

$$\cdot (R^2 \sin^2(\alpha + \beta) + R_x^2 \sin^2 \alpha \\ + R_x \sin \alpha R \sin(\alpha + \beta))$$

$$V_R = \frac{\pi}{12} R^3 \{ 8 + 9 \cos(\alpha + \beta) \\ - \cos 3(\alpha + \beta) \} \quad (3)$$

$$V_{R_s} = \frac{\pi}{12} R_x^3 \{ 8 - 9 \cos \alpha + \cos 3\alpha \} \quad (4)$$

$$V_t = \pi \left\{ r^2 \sin \alpha (r + R_x) \left(\frac{2\pi\beta}{360} - \sin \beta \right) \right. \\ \left. - \frac{4}{3} r^3 \cos \left(\alpha + \frac{1}{2} \beta - 90 \right) \sin^3 \frac{1}{2} \beta \right\} \quad (5)$$

A number of assumptions were made to develop Eqs. (1) to (5): (1) gravitational distortion was ignored; (2) the properties of the solid-fluid interface were assumed to be uniform with a contact angle of zero degrees, as made plausible

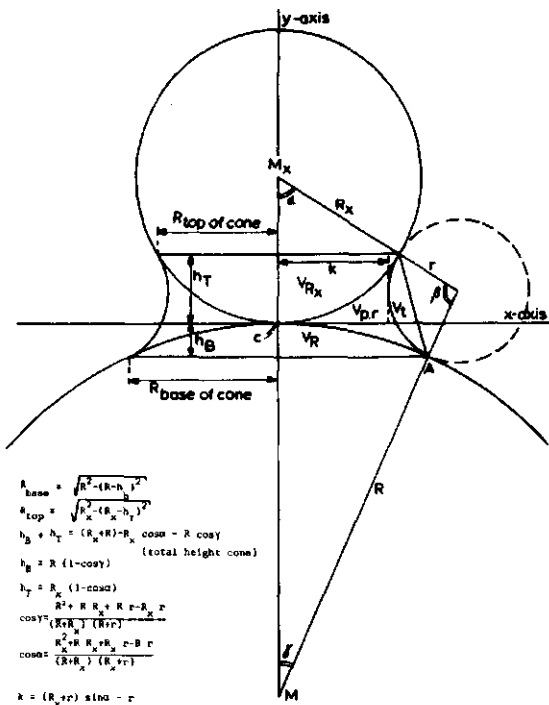


FIG. 1. General coordinate system to calculate pendular ring volume.

by Kruyer (1958); (3) the surface free energy of the air-water interface is supposed to be equal in each point. Though this condition is not met in the case of a toroidal surface, comparison with exact data presented by Kruyer (1958) for an equidimensional system showed this approximation to introduce a maximum positive absolute and relative error in the volumetric moisture content of 0.21 percent and 3.39 percent, respectively. Numerical results obtained with Eqs. (1) to (5) were favorably compared with Wilsdon's (1921) formula for equidimensional spheres ($\alpha = \gamma$).

Relationship between suction and pendular water volume

The relation between matric suction Sm and surface tension σ may be described by

$$Sm = \frac{\sigma}{\rho g} \left(\frac{1}{r_1} + \frac{1}{r_2} \right) \quad (6)$$

The radii of the pendular water rings are of opposite sign and are given by $r_1 = r$ and

$$r_2 = -$$

$$\left\{ (R_x + r) \frac{2((R + R_x + r)RR_xr)^{1/2}}{R_x(R + R_x + r) + Rr} - r \right\} \quad (7)$$

At a given suction the radii of curvature belonging to equal and unequal spheres are different. Therefore, the radii were calculated for appropriate suction values and were subsequently used to calculate the corresponding water volumes. The volumetric moisture content θ_v (%) for a hexagonal packing was obtained by Eq. (8)

$$\theta_v (\%) = \frac{36V_{pr} + 48V_{pr4} + 36V_{pr8}}{2^{1/2} \times 24R^3} \times 100 \quad (8)$$

The relation between volumetric water content and suction for the model soil, containing nonporous aggregates, may now be calculated using Eqs. (1) to (8). The result is presented in Fig. 2 in terms of the dimensionless quantities $Sm R \rho g / \sigma$ and θ_v . Taking a value of 13.4 cm^{-2} for $\rho g / \sigma$ and 0.5 cm for R , which radius is assumed to be a fair estimate for the largest aggregates in a well-prepared seed bed, the suction

SIMULATION OF PARTIAL ANAEROBIOSIS

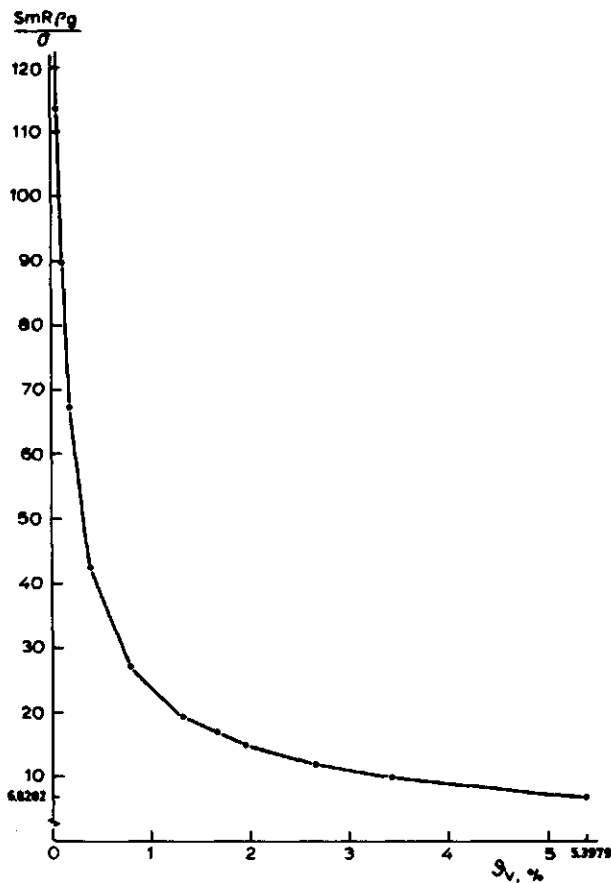


FIG. 2. Moisture characteristic of hexagonal.

can be calculated as 2.18 cm H₂O when θ_v = 2 percent. The low maximum moisture content of 5.3979 percent results from the fact that, at still higher moisture contents, neighboring water rings coalesce, and Eqs. (1) to (8) no longer hold (Haines 1927; Keen 1924). The angle γ at which this process starts amounts to 30, 19.47, and 13.27° for R = R₁, R = R₈, and R = R₄ spheres, respectively.

It should be pointed out that the hexagonal closest sphere packing is not isotropic;³ each sphere has a different number of water rings. This complication was not considered; instead

an average number of different rings per sphere was calculated.

The model soil aggregates were next assigned a porosity according to the soil properties of a sandy loam soil (Stroosnijder 1976, p. 87), resulting in a total porosity of 65.51 percent. The hydraulic properties of the complete model soil were obtained by simply adding the two moisture characteristics. Thus, the moisture characteristic of the sandy loam uniquely refers to the intraaggregate pores. This procedure could be repeated for other soil types to provide information on the relative importance of moisture depletion within the aggregates at different suc- tions on anoxia. It is not intended to simulate the hydraulic properties of a sandy loam soil. However, the procedure indicates the need of

³ J. van Brakel, 1975, Capillary liquid transport in porous media, Ph.D. thesis, University of Technology, Delft, Pasman, 's-Gravenhage.

quantitative knowledge of how different pore types drain and moisten when suction is changed (Stolzy and Flühler 1978).

Air-exposed area of aggregates

Diffusion of oxygen from interaggregate pores into the aggregates, is taken proportional to the air-exposed area of the aggregates. This area is complementary to the area covered by the pendular water rings and can be calculated by Eq. (9)

$$AEA(\%) =$$

$$\left\{ 1 - \frac{C}{2} \left(1 - \frac{R_x(R_x + R) + r(R_x - R)}{(R_x + R)(R_x + r)} \right) \right\} \times 100 \quad (9)$$

The relation between moisture content θ_v and air exposed area AEA is shown in Fig. 3. We

explain below how this parameter is applied in the calculations.

The ratio D/D_0 pertaining to the oxygen macrodiffusion process

Millington and Shearer (1971) advanced an equation to calculate the ratio of the diffusion coefficient of molecules D in a porous system having intra- and interaggregate pores, to the diffusion coefficient in the same medium (water or air) without any solid obstacles D_0 . Their equation was used to describe the oxygen diffusion process in the model soil, the result being shown in Fig. 4. Obviously, the ratio D/D_0 is much less affected by filling of intraaggregate pores than by filling of interaggregate pores. The ratio D/D_0 thus calculated ($0.04 < D/D_0 < 0.18$) is in the expected order of magnitude when compared to data from Currie (1965): $0.025 <$

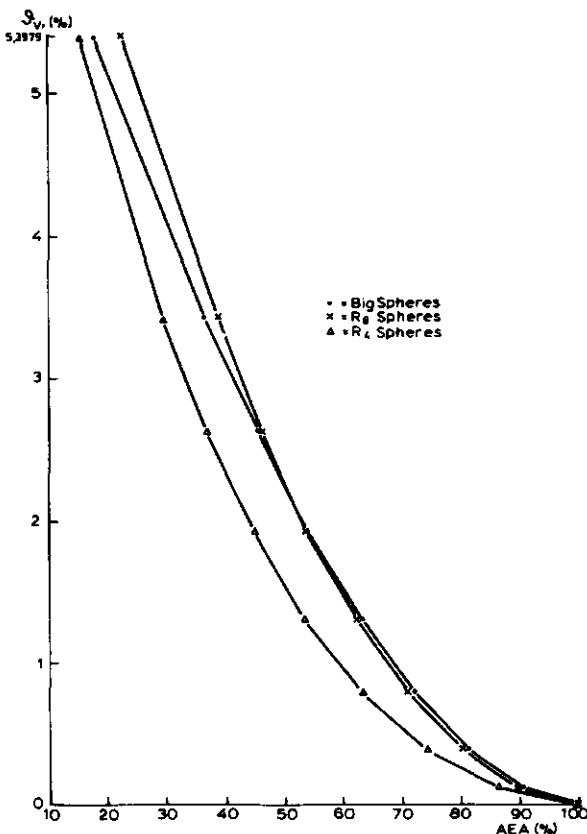


FIG. 3. The relation between air-exposed area of spheres and moisture content.

SIMULATION OF PARTIAL ANAEROBOSIS

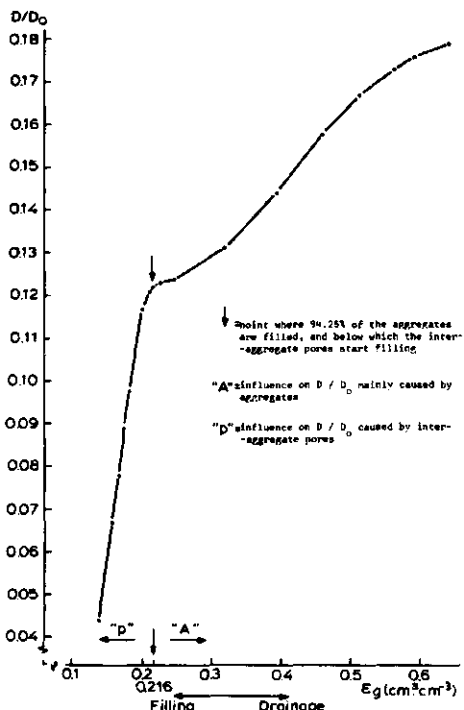


FIG. 4. The relation between D/D_0 and gas-filled porosity ϵ_g .

$D/D_0 < 0.156$, measured for eight soils with aggregate porosities in the range of 25 to 41 percent.

Diffusion within an aggregate

Oxygen diffusion within the aggregates is described by an analytical solution to the diffusion equation (Currie 1961), assuming steady-state conditions. This assumption is supported by Radford and Greenwood (1970), who found simulated concentrations of oxygen to reach at least 95 percent of their equilibrium values within 3 min.

Diffusion coefficients pertaining to the water-filled part of the aggregates were calculated according to Millington and Shearer (1971), multiplied by the air-exposed area (AEA) of the appropriate aggregate size, and used in the diffusion equation.

The distribution of the respiratory activity over the aggregates will be discussed in the section about the computer model.

The maximum radius at which an aggregate is still fully aerobic, called critical radius, is strongly dependent on moisture content. Therefore, the water distribution within the aggregates should be known. As a first approximation it was supposed to be accumulated in a concentric sphere. The equivalent radii of such water spheres, was calculated by Eq. (10)

$$r_{eq} = R \left(\frac{\theta_v}{\epsilon} \right)^{1/3} \quad (10)$$

The ratio of the equivalent and critical radii was converted to the anaerobic aggregate volume as described by Currie (1961, Eq. (16)).

Hydraulic conductivity

The hydraulic conductivity of the model soil was calculated by the procedure of Green and Corey (1971) on the basis of the soil moisture characteristic given by Stroosnijder (1976). The moisture characteristic was divided into 20 classes of $\Delta\theta_v = 0.0135$ each, ranging from $\theta_v = 0.465$ to 0.195 or from $Sm = 0.0$ to $-200 \text{ cm H}_2\text{O}$. Beyond this value the moisture transport was assumed to be negligible. The curve was matched with the measured hydraulic conductivity, amounting to 16.5 cm day^{-1} (Stroosnijder, 1976), and it was linearly extrapolated to account for higher suction values. The results of the calculations are shown in Fig. 5.

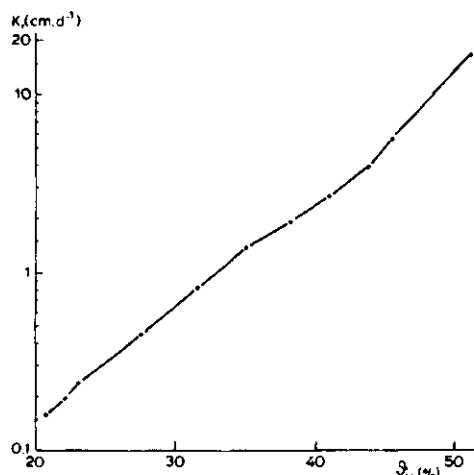


FIG. 5. The relation between hydraulic conductivity and moisture content.

THE COMPUTER MODEL

The computer model was written in CSMP-III and executed on a DEC 10 machine. Basic principles of the language are discussed by de Wit and Goudriaan (1978) and de Wit and van Keulen (1975). The latter report deals especially with transport processes in soils. The computer program will not be discussed in detail, but additional assumptions used to develop the program are enumerated.

The soil considered is made up of 15 layers, each having a thickness of a unit hexagonal sphere packing. The radius of the largest aggregates was taken as 0.5 cm, resulting in a total soil depth of 24.495 cm. The upper layer is exposed to air.

The main cause of oxygen transport through the soil is molecular diffusion. However, mass flow of oxygen takes place complementary to the mass flow of water. This process is also taken into account.

The oxygen consumption rate, including both root and microbial respiratory activity, and the rate of moisture extraction by the roots are distributed homogeneously over the aggregates in the rooted profile and are proportional to the aggregate volumes, as long as no anaerobiosis occurs. However, when anaerobic microsites develop, these rates are reduced in proportion to the anaerobic aggregate fraction. The oxygen-consumption rate is taken as constant down to a critical oxygen concentration denoting effective anaerobic conditions.

The flow rate of oxygen out of the last compartment is taken as zero, as no oxygen is consumed beyond that depth. For water flow the transport is governed by the average hydraulic conductivity and the matric suction in the last compartment and the depth where the groundwater table is projected. The water flow sub-model is based on the model of van Keulen and van Beek (1971). Rain is introduced in the model by means of a block function, with an intensity of 9 cm day⁻¹ and durations of 3 or 6 h.

Model parameters

Grable (1966) reported values for oxygen consumption ranging from 5 to 10 liters O₂ m⁻² soil surface day⁻¹. Bakker and Hidding (1970) reported this value to be about 9 liters for microorganisms only, and Woldendorp¹ showed that the ratio of respiratory activity of roots to microorganisms was 2 to 1. From these estimates

it is concluded that the lowest and highest oxygen consumption rates would be about 10 and 27 liters O₂ m⁻² soil surface · 25 cm depth⁻¹ day⁻¹.

The diffusion coefficient of oxygen in free water is 2.24 cm² day⁻¹ at T = 25°C, P = 1 bar (Lemon and Wiegand 1962). D/D₀, calculated according to Millington and Shearer (1971) for a water-filled part of an aggregate with porosity of 0.465 cm³ cm⁻³, equals 0.0566, resulting in D = 0.1272 cm² day⁻¹. The diffusion coefficient of oxygen in free air was reported to be 19,526 cm² day⁻¹. The relative solubility of oxygen in water at 25°C is 2.98 × 10⁻² (Grable 1966).

The critical oxygen concentration was taken as 2.24 × 10⁻⁸ g O₂ cm⁻³ (Greenwood 1961).

MODEL EVALUATION

Evaluation of the model was performed by studying the relative influence of changes in input data on the anaerobic volume fraction (sensitivity analysis). Therefore, results of simulation runs differing in one parameter or function, are compared with a so-called basic run (run no. 1). The schedule of simulation runs is presented in Table 1. Results in terms of the fractional anaerobic volume (FANVOL) plotted against time are shown for some simulation runs in Figs. 6 through 10, for soil layers 1, 7, and 15 corresponding to average depths of 0.8, 10.6, and 23.7 cm, respectively. The parameters tested may be divided in two categories: those directly affecting oxygen status (runs 2, 3, 4, and 5), and those indirectly affecting it by governing the water regime of the soil (runs 6, 7, and 8).

At the onset of the simulations, about 0.05 day is needed to adjust FANVOL to its right initial value. This adjustment is particularly clear in Figs. 7 and 8. At that time, Figs. 6 to 10 indicate the presence of anaerobic microsites in the soil layers below 10 cm. So, the soil is a source for continuous denitrification, provided no other limitations prevail. Further, these figures show a rain of 11.25 mm to affect anaerobiosis for about 1 day.

Figure 7 shows the respiration to have a pronounced effect on anaerobiosis. Initially in the upper layer an anaerobic soil fraction of about 11 percent is calculated, and the maximum after 3 h rain (11.25 mm) is 8.7 times that, in case the consumption rate is a factor of 2.7 lower. The model soil is thus very sensitive to changes in respiratory activity.

Results of run 3 can be visualized by adjusting

SIMULATION OF PARTIAL ANAEROBOSIS

TABLE 1
Schedule of simulation runs

Parameter	Run 1 (Fig. 6)	Run 2 (Fig. 7)	Run 3	Run 4	Run 5	Run 6 (Fig. 8)	Run 7 (Fig. 9)	Run 8 (Fig. 10)
Oxygen consumption $\times 10^{-3} \text{ g O}_2 \text{ cm}^{-2} \cdot 25 \text{ cm depth}^{-1} \text{ d}^{-1}$	1.3089	<i>3.4904^a</i>	1.3089 ^b	1.3089	1.3089	1.3089	1.3089	1.3089
Diffusion coefficient in an aggregate $\text{cm}^2 \text{ d}^{-1}$	0.1272	0.1272	0.1272	0.1272	0.0636	0.1272	0.1272	0.1272
Ratio interaggregate porosity to intraaggregate porosity	0.408	0.408	0.408	<i>0.204^b</i>	0.408	0.408	0.408	0.408
Depth of groundwater table, cm	100	100	100	100	100	50	100	100
Rain intensity, $\text{cm d}^{-1} /$ duration, h	9/3	9/3	9/3	9/3	9/3	9/6	9/2-2.2	

^aItalic parameters are changed as compared to simulation run 1.

^bHalf the aggregates respire, while total oxygen consumption rate is the same as in simulation run 1.

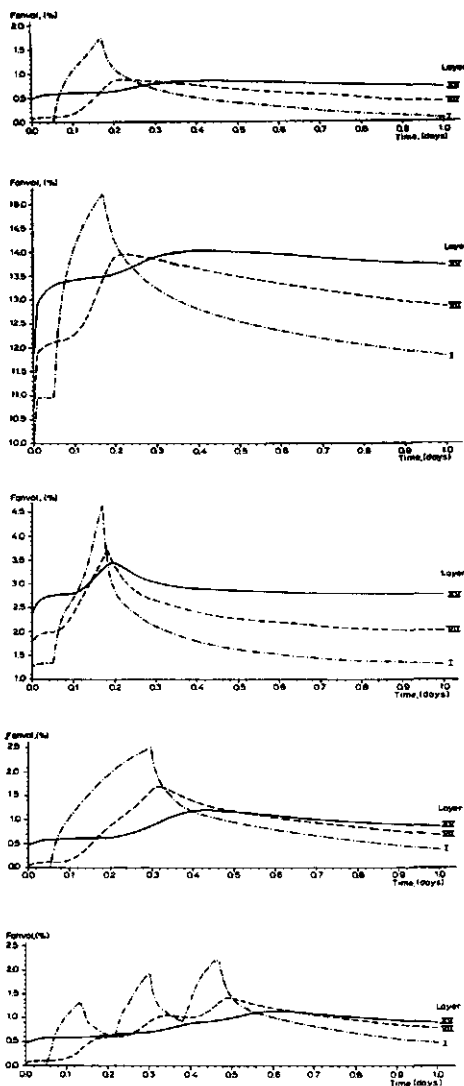


FIG. 6-10. FANVOL as a function of time for three layers. From top to bottom, 6: basic program, run 1; 7: oxygen consumption 26.7 liters $\text{O}_2 \text{ m}^{-2} \cdot 25 \text{ cm depth}^{-1} \text{ day}^{-1}$, run 2; 8: depth of groundwater table 50 cm, run 6; 9: rain duration 6 h, run 7; 10: rain intermittently applied in periods of 2 h interchanged with 2-h drought, run 8.

the origin of the ordinate of Fig. 6 to 3.8 percent. Then it follows that the spatial distribution of the respiratory activity is important, too. When, in each soil layer, the respiration is assumed to

take place in 50 percent of the aggregates, the anoxic volume increases by a factor of 3 for the top layer.

In run 4 the ratio of inter- to intraaggregate pores was decreased from 0.4 to 0.2, and D/D_0 was recalculated. Anaerobiosis was somewhat less affected than by halving the diffusion coefficient in the aggregates, run 5. The latter change was made to simulate the presence of slacksides on aggregates, which are expected to impair oxygen transport. Anaerobiosis in the case of runs 4 and 5 can be visualized by diminishing the values of FANVOL of Fig. 7 by 6.6 and 4.4 percent, respectively.

From the results presented it may be concluded that the model is very sensitive to parameters directly affecting oxygen status; the change in FANVOL in all cases was greater than the twofold change in the value of a particular parameter. Further experimental work is needed, however, to test whether the calculated anaerobic volumes do occur in reality. Some evidence that mathematical equations, very similar to the ones used in this study, hold for saturated soil aggregates was reported by Greenwood and Goodman (1967).

Figure 8 demonstrates the influence of depth of the groundwater table on anaerobiosis, which in this case was 50 cm below the soil surface instead of 100 cm. FANVOL increases more than proportionally with the ratio of the water table depths. This implies that in most of the Dutch grassland area, where shallow water table depths prevail during the greater part of the year, anaerobic conditions could easily occur.

Rain duration (Fig. 9) and distribution (Fig. 10) have a minor impact on soil anaerobiosis. It is remarked, however, that no very extreme circumstances were simulated, e.g., the minimum gas-filled pore fraction was $0.23 \text{ cm}^3 \text{ cm}^{-3}$ in run 7. Comparing this value with Fig. 4, we learn that it is on the safe side: D/D_0 is still large. This is also the reason that pendular water rings did not seriously affect the anaerobic soil volume. The difference between the influence of normal water regimes and parameters directly affecting soil anaerobiosis may also be demonstrated by the ratio of the average FANVOL for the whole soil profile in the different simulation runs, to that in the basic run. For runs 7 and 8 this ratio is about 1.1, for run 6 it is about 1.3, and for runs 2, 3, 4, and 5 it is about 3.4. These values stress the importance of experiments to determine the

parameters that directly affect the oxygen status of the soil.

The value of the critical oxygen concentration hardly affected anaerobiosis, even when it was set 10 times higher. This was also true for the rate of water extraction (transpiration), normally 0.3 cm day^{-1} , when tripled to 0.9. Therefore no separate figures are presented.

The instantaneous increase of anaerobiosis in the surface soil after the onset of rain suggests the possibility that denitrification occurs directly, too. This was reported by Burford and Greenland (1970).

Figure 11 shows curves relating the anaerobic soil fraction to suction for three interaggregate oxygen concentrations, e.g., 21, 19, and 17 percent, using the values of the parameters of the basic run (Table 1, first three lines). A soil in which aggregate size does not exceed 1 cm should hardly suffer from anaerobiosis at suctions above $100 \text{ cm H}_2\text{O}$. The smaller aggregates did not contribute to the anaerobic soil volume. The rapid increase in anaerobic volume with decreasing moisture tension occurs because the degree of water saturation has a strong impact on the diffusion coefficient of oxygen. The curves presented in Fig. 11 might be called "soil anaerobiosis characteristics," analogous to the term "soil moisture characteristic" (Childs 1940).

It was not attempted to use the model for predictive purposes, as experimental data of the anaerobic soil fraction should be obtained first to verify whether the right order of magnitude is being calculated.

DISCUSSION

The computer model presented probably tends to underestimate occurrence of anaerobiosis. First, rather small principal aggregate sizes have been chosen. Secondly, the total soil porosity is high, facilitating oxygen diffusion, with the result that the lowest interaggregate concentration calculated was 19.9 percent, for the deepest soil layer in run 2. Thirdly, oxygen diffusion may be impaired by incomplete wetting of soil aggregates. Emerson (1955) reported some evidence for this. It was shown that the process of water uptake by soil aggregates was delayed for some time. One can derive from his Fig. 2 that it takes about 6.6 and 17.2 days to absorb 90 and 97.5 percent of the total water uptake by a grassland surface aggregate, respectively. Stroosnijder and Koorevaar (1972) reported that soil air pressure

SIMULATION OF PARTIAL ANAEROBOSIS

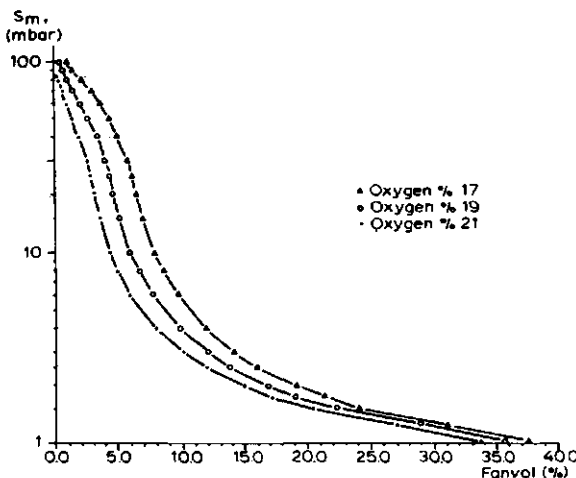


FIG. 11. The relation between suction and FANVOL for three oxygen concentrations for the model soil.

inside the elements increased to values above atmospheric pressures upon the entrance of water into soil aggregates. Based on these findings, one would expect that, after the onset of rain, mainly the outer shell of an aggregate would be directly wetted, possibly resulting in blocking of the pores and impaired oxygen transport. Air is enclosed then, the oxygen is readily consumed, and hence a greater anaerobic soil volume will result than when water is located in the center of the aggregates. Fourth, pool and/or crust formation will also increase anaerobiosis. However, replacing the top soil layer in the simulation model by an empirical equation for crust formation, as reported by Bakker and Hidding (1970), did not confirm that oxygen diffusion was impaired and anaerobiosis enhanced. This result is in accordance with a theoretical analysis by van Bavel (1951).

Conditions that positively influence soil anaerobiosis in the field are the possible presence of soil cracks and soil surface evaporation, which have not been taken into account in the simulation model.

This modeling actively proved to be useful to unite existing knowledge, to discover deficiencies in this knowledge, and to estimate the relative importance of the variables used. Future research will, to a large extent, be based on the results presented in this paper. In particular, attention will be paid to the distribution of water and oxygen in individual soil aggregates.

LIST OF SYMBOLS

- α, β, γ angles expressed as degrees, Fig. 1
- ϵ void fraction of an aggregate, $\text{cm}^3 \text{cm}^{-3}$
- θ_v volumetric moisture fraction pertaining to the complete soil or to the aggregates (Eq. 10), $\text{cm}^3 \text{cm}^{-3}$ or percent
- ρ density of water, g cm^{-3}
- σ surface tension of water, dynes cm^{-1}
- g acceleration due to gravity, cm s^{-2}
- r_1, r_2 radii of curvature of air-water interface of pendular rings, cm
- r_{eq} equivalent radius of water-filled sphere in an aggregate, cm
- AEA air-exposed area of an aggregate, percent
- C number of contact points between aggregates
- FANVOL fraction anaerobic volume of soil, $\text{cm}^3 \text{cm}^{-3}$ or percent
- R radius of a big aggregate, cm
- R_x when $x = 4$, the radius of an inscribed aggregate in a tetrahedral void, and when $x = 8$, the same for an octahedral void, cm
- $R - R_x$ the contact between equidimensional aggregates
- $R - R_x$ the contact between unequal aggregates where x can either be 4 or 8
- V volume of water, cm^3 , Fig. 1
- indexes to V :
- c truncated cone
- pr pendular water ring
- prx pendular water ring between an inscribed aggregate R_x and a big one

P. A. LEFFELAAR

R refers to a spherical segment of one base of the big aggregates

R_x refers to the same of inscribed aggregates
 t the fraction of the torus included by the cone

NOTE

A listing of the computer program that produced these results is available from the author.

ACKNOWLEDGMENTS

The helpful suggestions of Dr. J. Goudriaan and Dr. H. van Keulen are kindly acknowledged. Assistance in drawing the figures by Mr. G. C. Beekhof and the typing of the manuscript by Mrs. C. G. Uithol is appreciated.

REFERENCES

Azároff, L. V. 1960. Introduction to solids. McGraw-Hill, New York.

Bakker, J. W., and A. P. Hidding. 1970. The influence of soil structure and air content on gas diffusion in soils. *Neth. J. Agric. Sci.* 18: 37-48.

Bavel, C. H. M., van. 1951. A soil aeration theory based on diffusion. *Soil Sci.* 72: 33-46.

Broadbent, F. E. 1951. Denitrification in some California soils. *Soil Sci.* 72: 129-137.

Burford, J. R., and D. J. Greenland. 1970. Denitrification under an annual pasture. *Proc. XIth Int. Grasslands Congr. Australia*, pp. 458-461.

Childs, E. C. 1940. The use of soil moisture characteristics in soil studies. *Soil Sci.* 50: 239-252.

Currie, J. A. 1961. Gaseous diffusion in the aeration of aggregated soils. *Soil Sci.* 92: 40-45.

Currie, J. A. 1965. Diffusion within soil micro-structure, a structural parameter for soils. *J. Soil Sci.* 16: 279-289.

Emerson, W. W. 1955. The rate of water uptake of soil crumbs at low suctions. *J. Soil Sci.* 6: 147-159.

Flühler, H., L. H. Stolzy, and M. S. Ardakani. 1976. A statistical approach to define soil aeration in respect to denitrification. *Soil Sci.* 122: 115-123.

Grable, A. R. 1966. Soil aeration. *Adv. Agron.* 18: 57-106.

Green, R. E., and J. C. Corey. 1971. Calculation of hydraulic conductivity: A further evaluation of some predictive methods. *Soil Sci. Soc. Am. Proc.* 35: 3-7.

Greenwood, D. J. 1961. The effect of oxygen concentration on the decomposition of organic materials in soil. *Plant Soil* 14: 360-376.

Greenwood, D. J., and D. Goodman. 1967. Direct measurements of the distribution of oxygen in soil aggregates and in columns of fine soil crumbs. *J. Soil Sci.* 18: 182-196.

Haines, W. B. 1927. Studies in the physical properties of soils: 4. A further contribution to the theory of capillary phenomena in soil. *J. Agric. Sci.* 27: 264-290.

Keen, B. A. 1924. On the moisture relationships in an ideal soil. *J. Agric. Sci.* 14: 170-177.

Keulen, H., van, and C. G. E. M. van Beek. 1971. Water movement in layered soils. *Neth. J. Agric. Sci.* 19: 138-153.

Kruyer, S. 1958. The penetration of mercury and capillary condensation in packed spheres. *Trans. Faraday Soc.* 54: 1758-1767.

Leffelaar, P. A. 1977. A theoretical approach to calculate the anaerobic volume fraction in aerated soil in view of denitrification. A computer simulation study. Report no. 9, Dept. of Theoretical Production Ecology, Agricultural University, Wageningen, The Netherlands (available on request).

Lemon, E. R., and C. L. Wiegand. 1962. Soil aeration and plant root relations: 2. Root respiration. *Agron. J.* 54: 171-175.

Millington, R. J., and R. C. Shearer. 1971. Diffusion in aggregated porous media. *Soil Sci.* 111: 372-378.

Radford, P. J., and D. J. Greenwood. 1970. The simulation of gaseous diffusion in soils. *J. Soil Sci.* 21: 304-313.

Slichter, C. S. 1899. Theoretical investigation of the motion of ground waters. 19th Annual report U.S. Geol. Survey, part II, pp. 295-328.

Smith, K. A. 1977. Soil aeration. *Soil Sci.* 123: 284-291.

Stolzy, L. H., and H. Flühler. 1978. Measurement and prediction of anaerobiosis in soils. In *Nitrogen in the environment*, vol. 1, D. R. Nielsen and J. G. McDonald (eds.). Academic, New York, pp. 363-426.

Stroosnijder, L. 1976. *Infiltratie en herverdeling van water in grond*. Pudoc, Wageningen, The Netherlands.

Stroosnijder, L., and P. Koorevaar. 1972. Air pressure within soil aggregates during quick wetting and subsequent "explosion": 1. Preliminary experimental results. *Meded. Fac. Landbouwwet. Rijksuniv. Gent* 37: 1095-1106.

Wilsdon, B. H. 1921. Studies in soil moisture, part I. *Memoirs of the department of agriculture in India. Chemical Series* 6: 155-186.

Wit, C. T., de, and J. Goudriaan. 1978. Simulation of ecological processes. Pudoc, Wageningen, The Netherlands.

Wit, C. T., de, and H. van Keulen. 1975. Simulation of transport processes in soils. Pudoc, Wageningen, The Netherlands.

CHAPTER 3

0038-075X/86/1426-0352\$02.00/0
SOIL SCIENCE
Copyright © 1986 by The Williams & Wilkins Co.

December 1986
Vol. 142, No. 6
Printed in U.S.A.

DYNAMICS OF PARTIAL ANAEROBOSIS, DENITRIFICATION, AND WATER IN A SOIL AGGREGATE: EXPERIMENTAL

P. A. LEFFELAAR¹

A respirometer system was developed to study the dynamics of partial anaerobiosis and denitrification in unsaturated soil. The system enables one to measure simultaneously the distribution of water, oxygen, nitrate, nitrite, ammonium, and pH as a function of space and time in an unsaturated, artificially made, homogeneous, cylindrical aggregate and the changes in atmospheric composition as a function of time in the chamber that contains the aggregate. Except for water transport, these processes are caused by microbial activity, because roots are not present in the aggregate.

The respirometer system was especially designed to generate coherent data sets to evaluate a simulation model that calculates the development of denitrification products as a function of environmental conditions. Nondestructive measurements during an experiment involve gamma-ray attenuation, gas chromatography, and polarography. Destructive measurements are executed at the end of an experiment in the form of chemical analyses of soil.

The reported experiment shows that hysteresis in the soil water characteristic strongly affects the water distribution in the aggregate. As a result, the oxygen supply to the interior of the aggregate is decreased to such an extent that anaerobiosis is maintained there after the oxygen is consumed. The respiratory quotient and the release of denitrification products are underestimated in the partially wet soil because of the high solubilities of carbon dioxide and nitrous oxide in soil moisture. Large amounts of nitrite have been found. Therefore, assessment of denitrification through the measurement of nitrate alone will overestimate nitrogen losses, while the measurement of nitrous oxide and molecular nitrogen alone will give an underestimation. The consumption rate of oxygen and the production rates of carbon dioxide, nitrous oxide, and molecular ni-

rogen compare well with field data. This is the result of the pretreatment of the soil, which aimed at avoiding the flush of microbial activity upon wetting. The results support the thesis that denitrification will occur in soil when at a certain place and time oxygen is absent and bacteria capable of denitrification, water, nitrate, and decomposable organic compounds are present.

The respirometer system yields valuable data to evaluate the simulation model. However, full account of the interrelationships among the generated data can be achieved only by the same simulation model, because the measured variables reflect the integrated effect of biological activity and transport processes.

The objective of this paper is to describe the respirometer system and its measuring devices and to report some of the measurements.

The release of nitrous oxide and molecular nitrogen by biological denitrification occurs when bacteria capable of denitrification colonize a location where oxygen is absent and water, nitrate, and decomposable organic compounds are present (Delwiche 1981; Ingraham 1981). In aggregated unsaturated soils anaerobiosis, and hence denitrification, is mainly confined to the aggregates (Currie 1961; Greenwood 1961). In principle, therefore, denitrification losses from aggregated field soils can be predicted when denitrification losses from individual aggregates and their size distribution are known (Smith 1977 and 1980). Denitrification from a single aggregate can be predicted successfully only when the spatial distributions of denitrifiers, oxygen, water, nitrate, and decomposable organic compounds can be measured or calculated as a function of time and when these distributions are subsequently combined so that zones of denitrification show up.

Figure 1 depicts some schematic oxygen and water distributions as expected in field aggregates under the assumption of a homogeneous distribution of bacteria and organic compounds

¹ Dept. of Theoretical Production Ecology, Bornseweg 65, 6708 PD Wageningen, The Netherlands.

Received for publication 6 May 1986; revised 11 Aug. 1986.

PARTIAL ANAEROBOSIS AND DENITRIFICATION

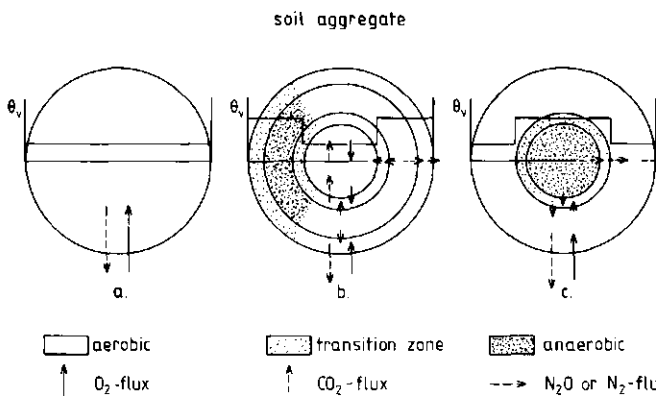


FIG. 1. Schematic of water and oxygen distributions in soil aggregates. a, in a dry period; b, just after a rain shower; c, some time after rainfall. Lengths of arrows indicate relative magnitudes of molar source or sink terms.

and a negligible nitrate production due to nitrification. When oxygen consumption rate does not exceed oxygen supply rate, no anoxic conditions develop, and equimolar respiration occurs as indicated by arrows (Fig. 1a). Just after rainfall, mainly the outer shell of an aggregate will be wetted (Leffelaar 1979). In the outer shell oxygen diffusion rate is then seriously impeded, and when oxygen consumption rate exceeds oxygen supply rate, anoxic conditions occur there (Fig. 1b). When nitrate from fertilizer has been absorbed with the rainwater, denitrification occurs in the wetted shell. In the center of the aggregate equimolar respiration continues to take place until the oxygen from the enclosed air has been consumed. Then most of the aggregate volume is anaerobic, but denitrification does not necessarily increase, for the nitrate is mainly concentrated in the wetted shell. The arrows in Fig. 1b indicate a net gas production caused by denitrification. Subsequent redistribution of water may result in a decrease of the anaerobic aggregate volume, and hence of denitrification, when the water content in the wetted shell becomes low enough to get continuous gas-filled pores that permit rapid oxygen diffusion into the aggregate. The distribution of oxygen as depicted in Fig. 1c will be found in initially water-saturated aggregates that are drying. Upon further drying their oxygen distributions will adjust to that of Fig. 1a.

These complicated dynamic interactions between biological and physical processes determining denitrification are studied in a most comprehensive way through the development of an explanatory simulation model that describes microbial activity; movement of gases, water,

and nitrate; and decomposition of organic compounds in an individual aggregate. It appeared that coherent data sets to evaluate such a comprehensive model did not exist. It is the objective of this paper to describe a new type of respirometer system designed especially to generate such coherent data sets and to report some of the measurements.

MATERIALS AND METHODS

The experimental soil aggregate on which the measurements of the spatial distribution of oxygen, water, nitrate, and decomposable organic compounds as a function of time are performed is a short cylinder of homogeneously packed soil material in which transport processes are radial. This geometry is a model representation of a soil aggregate from which the upper and lower sides are removed and originates directly from Fig. 1. For the same geometry a simulation model is developed that can thus be evaluated. The evaluated model may then be converted to a spherical geometry and be used in a field model describing the spatial arrangement of aggregates and the interaggregate transport processes. Thus, the interaction between microbial activity and the movement of gases, nitrate, and water and with this denitrification in real situations can be simulated. A scheme of the experimental installation is given in Fig. 2.

Soil

A sandy loam soil from Lelystad was taken from the surface 25-cm layer and stored under field-moist conditions. Some characteristics are: pH (measured in 4 g of soil suspended in 10 ml of liquid) in H_2O and KCl : 7.8 and 7.4, respec-

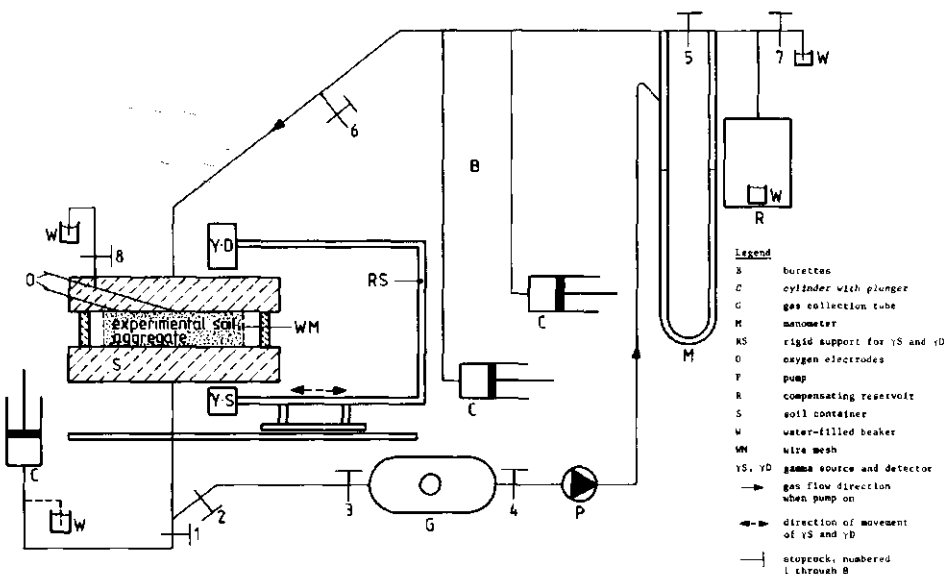


FIG. 2. Diagram of respirometer system showing soil container, gas collection circuit (stopcocks 1 through 7 and attached devices), oxygen electrodes, and gamma-ray attenuation apparatus with rigid support. Spatial arrangement of oxygen electrodes is correctly shown in Fig. 3.

tively; CaCO_3 (Scheibler's method described by Allison and Moodie 1965); 6%; organic carbon (Meibius 1960); 1.2%; total nitrogen (Novozamsky et al. 1984); 0.09%; CEC- BaCl_2 (Bascomb 1964); 10.1 cmol(+) per kg of soil and soil texture (pipette method described by Day 1965) $<2\text{ }\mu\text{m}$, $<20\text{ }\mu\text{m}$, and $<50\text{ }\mu\text{m}$: 13, 27, and 32%, respectively. The soil is air-dried, pulverized to pass a 0.5-mm sieve, directly remoistened to about 0.1 to 0.15 g g⁻¹, and left in a closed container for at least 6 wk to let the metabolism of microorganisms recover (Birch 1958, 1959; Fillery 1983). Remoistening is attained by adding an appropriate amount of ice scrapings to soil and mixing in a mortar with a pestle.

Measuring system

The measuring system (Fig. 2) was mounted in a constant-temperature room ($22.7 \pm 1.5^\circ\text{C}$) and is composed of the following subsystems

1. container (S), which holds the experimental soil aggregate and the oxygen electrodes
2. a closed gas collection circuit (stopcocks 1 through 7 and attached devices), which serves three purposes
 - it contains enough oxygen to meet the

respiratory demand of the microorganisms in the soil aggregate during one experiment

—it functions as volumeter to determine net changes in the total volume of gas resulting from respiration and denitrification

- it is used to withdraw gas samples to assess gaseous composition by gas chromatography
3. two polarographic Clark-type oxygen electrodes to measure oxygen pressure at two locations in the experimental soil aggregate
4. a gamma-ray attenuation apparatus to measure the radial distribution of soil water content

Technical details, comments on procedures, and calculations to obtain data are given below for each subsystem. Table 1 summarizes the course of an experiment.

Soil container

Technical description

Figure 3 depicts the Perspex soil container in which the cylindrical soil aggregate is radially

TABLE 1
Course of experiment

Initial

Preparation

1. Weigh (W1) empty soil container (S); pack experimental soil aggregate in container and weigh (W2) again. Connect container to gas collection circuit, of which stopcocks 1 through 7 (glass) are greased by vacuum grease (Dow Corning). (W2 - W1) gives amount of initially moist soil.
2. Leave soil aggregate alone for at least 1 wk to let metabolism of microorganisms recover; closed stopcocks: 1, 5, 6, 7, 8. Stopcocks not mentioned are open.
3. Replace air by a mixture of neon-oxygen (about 0.2 ml O₂ ml⁻¹) (Matheson Gas Products, Oevel, Belgium) during this week by periodic flushing through stopcock 6 while pump is switched on; closed stopcock: 8, water-sealed stopcocks: 1, 7.
4. Record gamma-ray attenuation reference scans for moisture calculations and for assessing homogeneity of packing. Record at least five scans with a measurement every third millimeter.
5. Test (qualitatively) whether soil respiration occurs through gas analysis for carbon dioxide. If no respiration takes place, experiment may be stopped.
6. Determine initial moisture content and NO₃⁻, NO₂⁻, NH₄⁺, and pH on separate amount of soil.

Start

7. Calibrate polarographic oxygen electrodes by bathing them in gas mixtures (Matheson Gas Products) containing known volume fractions of oxygen in nitrogen (about 0.0, 0.05, 0.1, and 0.2 ml ml⁻¹) and noting the mV signal.
8. Adjust burettes to half of their maximum volume.
9. Install oxygen electrodes with pump switched on, and flush system with Ne-O₂ mixture through stopcock 6 to prevent air entry; closed stopcock: 8, water-sealed stopcocks: 1, 7. Leak-proof connections are attained by piercing the electrodes through greased rubber stoppers fitting into the borings of the top cover of the soil container.
10. (Partially) wet experimental soil aggregate via cylinder with plunger near stopcock 1 with solution either with or without nitrate and/or glucose added; closed stopcock: 2, water-sealed stopcock: 7. Enclosed air in soil is allowed to escape via tube containing central oxygen electrode and water-sealed stopcock 8.
11. When solution has penetrated to desired depth into soil aggregate, excess water is removed by withdrawing plunger of cylinder near stopcock 1; closed stopcocks: 2, 8, water-sealed stopcock: 7.
12. Continue to flush system with Ne-O₂ mixture for about 1 min; closed stopcocks: 1, 8, water-sealed stopcock: 7.
13. Time is zero when stopcocks are closed in the sequence 6, 7, 5, and pump is switched off.

Time elapsed from step 8 through step 13 is about 8 min.

Dynamic

Measurements as a function of time and place

14. Oxygen pressure by polarography.
15. Moisture by gamma-ray attenuation.

Measurements as a function of time

16. Gas analysis for Ne, CO₂, N₂O, O₂, and N₂ by gas chromatography. Before moment of gas sampling: adjust system pressure via burettes and manometer and switch on pump for 10 min. At moment of sampling: switch off pump, readjust system pressure if necessary, and close stopcocks 3 and 4. Analyze gas sample from gas collection tube. If gas analysis seems not trustworthy, a new gas sample can be taken. Open stopcocks 3 and 4. Calibration chromatograms are recorded regularly.
17. Read volume of burettes.
18. Read temperature.

Steps 14 through 18 can be taken as simultaneous, as the rate of measuring is much faster than the rate of change of the state variables measured.

Gamma-ray attenuation measurements take 20 min and are started 10 min before the moment that the other readings are performed.

Terminal

Preparation

19. Take out oxygen electrodes and weigh container with soil (W3). (W3 - W2) gives amount of water added during wetting.
20. Calibrate oxygen electrodes.

Measurements as a function of place

21. Partition soil aggregate into five concentric layers of 1-cm thickness each.
22. Determine gravimetric water content and NO₃⁻, NO₂⁻, NH₄⁺, and pH in each layer.

Steps 19 through 21 take less than 1 h. Soil samples for chemical analyses are put into extraction solutions within 2 to 3 h to prevent further microbial conversions of nitrogenous and carbonaceous materials. Gravimetric water contents are used to express chemical data on an over-dry basis.

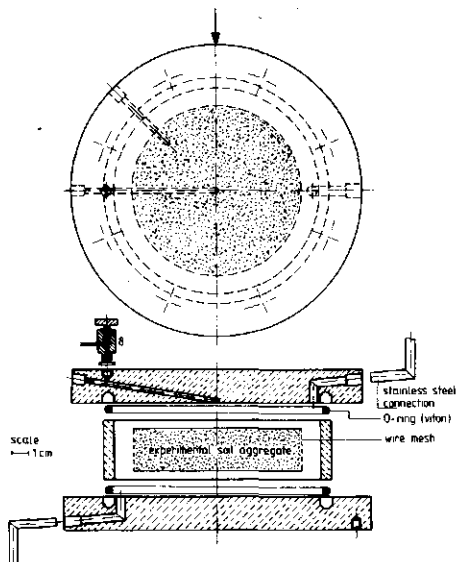


FIG. 3. Top cover of soil container seen from above and expanded transect through container center. Drawn to scale. Arrow indicates direction of movement of gamma-ray source and detector.

supported by a wire mesh of 72.7% porosity. The upper and lower sides of the aggregate are covered by two disks that are kept apart by a cylinder of 12-cm internal diameter. The aggregate has a height and diameter of about 2.5 and 10 cm, respectively, to provide enough soil for chemical analyses on concentric rings of 1-cm thickness each. Nuts to tighten the disks with the soil in between have been sunk into the Perspex to minimize the distance between the source and detector of the gamma-ray attenuation apparatus. In the upper disk two 2.1-mm-diameter holes were drilled from the circumference to the center of the soil container and to a place 4 cm from the center, respectively. Each hole may accommodate a 2-mm-diameter Clark-type oxygen electrode and slants toward the inner part of the soil container to keep the head space between the electrode tip and the soil surface as small as possible. A brass stopcock (no. 8) with a small dead volume is connected with the central electrode hole to let enclosed gases escape from the soil aggregate when it is partially wetted at the start of an experiment. Each Perspex disk has one 5-mm-diameter hole that connects the gaseous atmosphere around the aggregate with the gas collection circuit via

a stainless steel tube glued into the Perspex. The holes are placed opposite one another with respect to the center of the container to force the gases in the system around the soil aggregate to mix thoroughly before gas samples are taken. In the bottom disk two holes (one visible in transect in Fig. 3) are drilled from below to fasten the soil container onto a steady support.

Comment on procedures (Table 1, item 1)

The experimental soil aggregate is prepared in an auxiliary cylinder, which is placed into the previously weighed (W1) soil container. The wire mesh for radial support of the aggregate fits loosely into this auxiliary cylinder, which has a height and internal diameter of 2.5 and 9.8 cm, respectively. A quantity of sieved moist soil, sufficient for an aggregate with a dry bulk density of 1.4 g cm^{-3} , is weighed. A small amount of this soil is then added to the auxiliary cylinder and tapped as homogeneously as possible, before the next amount of soil is added. This process is repeated until the appropriate height has been reached. Then the auxiliary cylinder is pulled up, excess soil is removed, and the container is assembled and weighed (W2).

Gas collection and analysis

Technical description

The gas collection circuit contains the following parts (Fig. 2)

1. a volumeter composed of a manometer (glass, internal diameter 0.4 cm), two calibrated burettes (glass, 50- and 100-ml capacity) of which the water levels can be adjusted by cylinder-plunger arrangements (Perspex), and a compensation reservoir (Perspex, 2500-ml capacity).

The initial volume of the gas circuit (about 550 ml, including the space around the soil aggregate) is determined by the sum of the differences in weight of each part when filled with water and when dry, respectively.

Pressure differences between the gas circuit and the compensation reservoir are eliminated by adjusting the water levels in the burettes. The change in burette volume is a measure for the net change in gas volume due to respiration and denitrification in the soil aggregate. The compensation reservoir is added to avoid the

PARTIAL ANAEROBOSIS AND DENITRIFICATION

influence of barometric pressure changes on the burette volume readings during an experiment. To maintain similar water vapor pressures at both sides of the manometer, a beaker filled with water is placed in the compensation reservoir (Scholander 1942).

2. a gas collection unit composed of a small pump (aluminum pump head, viton diaphragm, and valves, modified to reduce pressure buildup to 5 cm H₂O, flow rate 170 ml min⁻¹; Charles Austen Pumps Ltd., Surrey, England) to homogenize the gases evolved in the gas circuit and a gas collection tube (glass, 75-ml capacity, Subaseal septum), in which the mixture is trapped by closing stopcocks 3 and 4 at the moment that gas composition is to be determined.

A preliminary experiment showed that gases are well mixed after 10 min of pumping. Gas samples are withdrawn from *G* through the septum by a 0.1-ml Hamilton 1710 RN gas syringe (Hamilton Co., Reno, Nevada, U.S.A.), which is previously flushed with carrier gas from the gas chromatograph to remove traces of air.

The different parts of the gas collection circuit are connected by glass tubes with internal diameters between 0.4 and 0.8 cm. Transitions between different parts are bridged by short pieces of gas-tight rubber tubes (viton and butylene tube), which are additionally tightened by Unex hose clips (Uniclip Ltd., Surrey, England).

Gas samples are injected in a Packard-Becker 427 gas chromatograph, which contains a Porapak (stainless steel, 400 cm long and 2-mm internal diameter, packed with 80–100 mesh Porapak Q; Supelco, Inc., Bellefonte, U.S.A.) and a Mol Sieve (SS, 400 cm × 2 mm, packed with 60–80 mesh Mol Sieve 5A; Supelco) column in a series/bypass configuration with restrictor (McNair and Bonelli 1969; Thompson 1977). The system is equipped with a thermal conductivity detector (TCD) with constant filament temperature (Packard Becker, Type 903 with Type 303 detector controller). Operating temperatures of injection port, column oven, valve, detector block, and filament are 70, 50, 70, 70, and 200°C, respectively. Hydrogen carrier gas (Matheson Gas Products, 99.999% purity) with a flow velocity of 20 ml min⁻¹ is routed to the

columns via a drying tube (15 cm × 10 mm) packed with granular Mol Sieve 5A (8–12 mesh; Supelco). A fast recovery of the base line after switching of the valve, is obtained by pressure control.

A gas analysis takes about 7 min, peaks are completely separated, and the minimal detectable volume fraction equals about 0.0003 ml ml⁻¹ for CO₂ from air.

Calibration of the system is performed by analysis of a gas mixture (L'air Liquide Belge, Schelle, Belgium) containing known volume fractions of Ne, CO₂, N₂O, O₂, and N₂ (about 0.75, 0.05, 0.05, 0.1, and 0.05 ml ml⁻¹, respectively; relative accuracy 3%).

Comment on procedures (Table 1, item 3)

Replacement of air-N₂ by a gas of the helium group serves to overcome the experimental problem to determine small amounts of N₂ from denitrification in an atmosphere in which this gas is the major constituent. A gas of the helium group does not significantly affect denitrification (Blackmer and Bremner 1977) and, in addition, is used to indicate leaks in the gas collection circuit during an experiment by following its time course. Neon gas has been chosen because of its easy separation from oxygen and molecular nitrogen at temperatures slightly above room temperature.

Calculations

Gas percentages of the sample are calculated using peak areas and calibration chromatograms before and after sampling. Gas percentages are converted to milliliters of gas using the volume of the gas collection circuit as adjusted by the volumeter. These state variables are further used to calculate production (CO₂, N₂O, N₂) and consumption (O₂) rates by numerical differentiation.

Oxygen pressure

Technical description

Oxygen pressure is measured in the center and 4 cm from the center of the experimental soil aggregate by means of Clark-type oxygen electrodes. The electrodes were purchased from the Department of Physiology, Faculty of Medicine, University of Nijmegen, The Netherlands, which also supplied the amplifier scheme. Electrode construction, operation, and characteris-

tics have been described by Kimmich and Kreuzer (1969) and Kreuzer et al. (1980). General schemes for amplification of oxygen electrode currents have been published by, among others, Prazma et al. (1978) and Fatt (1976).

The electrodes were selected for their small oxygen consumption, compared with that of soil. Typical values for the electrode and soil are $7.8 \cdot 10^{-11} \text{ mol s}^{-1}$ (using Faraday's law, Gleichmann and Lübbbers 1960, and a current of 300 nA as measured at an oxygen pressure of 20 kPa with a 12- μm Teflon membrane mounted) and $9.6 \cdot 10^{-6} \text{ mol m}^{-3} \text{ soil s}^{-1}$ (assuming that $5 \text{ L O}_2 \text{ m}^{-2} \text{ d}^{-1}$, Grable 1966, is uniformly consumed over a depth of 0.25 m)². Further criteria to select the electrodes were stability (usually less than 10% variation in sensitivity over 1 to 7 d of use), linearity (correlation coefficients of calibration lines before and after experiments up to 7 d were always significant at the 1% level), and smallness (2-mm diameter).

Electrode currents are preamplified and converted to voltages to yield a signal of 1 mV per nA. This signal is further processed by an electrical circuit that is used to select the appropriate polarization voltage of the electrode (adjustable between 0 and -1.56 V), to adjust its sensitivity (1 to 22 times) and its zero current (up

to 1000 nA), and to suppress the signal as a whole (0 to -2 V) to record small changes in signal at high oxygen pressures. The electrode signal is read from a digital voltmeter and is continuously recorded on a strip chart recorder to note any sudden changes in signal.

Preliminary electrode experiments

Two gases in the soil system may seriously interfere with the oxygen measurement, namely N_2O and CO_2 . Nitrous oxide may be reduced at a platinum cathode (Johnson and Sawyer 1974; Eberhard and Mindt 1979), resulting in too high a reading.

An experiment, however, in which an electrode equipped with a 6- μm Teflon membrane was exposed to mixtures containing volume fractions of O_2 (0, 0.05, 0.1, and 0.2) and N_2O (0, 0.2, 0.4, and 1.0) in N_2 prepared in a 30-ml gas syringe showed a maximum relative increase of about 4% at an $\text{O}_2\text{-N}_2\text{-N}_2$ mixture of 0.2-0.4-0.4. Another experiment showed that polarograms (from -0.3 to -1.2 V) prepared in $\text{O}_2\text{-N}_2\text{-N}_2$ mixtures containing volume fractions of 0.1-0.2-0.7 and 0.1-0.0-0.9, respectively, were similar, and an interference peak of N_2O around -0.7 V , as reported by Eberhard and Mindt (1979), was not found.

The other gas, CO_2 , may reduce oxygen measurements (Küchler et al. 1978). Carbon dioxide may lower the pH in the buffered electrolyte that electrically bridges the cathode and anode. This could result in a less efficient reduction of hydrogen peroxide (Kreuzer et al. 1980) and thus in a (partial) shift from a four-electron oxygen reduction reaction to a two-electron reaction (Lee and Tsao 1979).

To evaluate this effect, an electrode was exposed to $\text{O}_2\text{-CO}_2\text{-N}_2$ mixtures (prepared as described above) with volume fractions of 0.2-0.25-0.55 and 0.2-0.5-0.3, respectively. The electrode signal at the 0.25 CO_2 fraction showed a maximum relative decrease of 7% after 12 min; it finally (after 2 h) stabilized at this level after an initial recovery. The electrode signal at the 0.5 CO_2 fraction showed a very strong decrease that did not recover.

It is concluded that the electrodes can be used in soil, as the extreme conditions imposed with respect to the volumetric gas fractions will probably not be reached. Moreover, in the soil experiments a 12- μm membrane is used.

² Comparison of these two numbers with different dimensions was done by calculating the time course of oxygen pressure in an air-filled chamber of 0.6-cm diameter and 0.01-cm length. The chamber was sealed at one side by an electrode and at the other side by the end of a soil pillar of similar diameter and a length of 2.5 cm. At time zero, oxygen pressure ($p\text{O}_2$) was $2 \cdot 10^4 \text{ Pa}$, and no oxygen was supplied thereafter. Oxygen consumption of the electrode (O_{2e} , mol) was calculated by integrating $d\text{O}_{2e}/dt = (a p\text{O}_2)/(nF)$, where t is time (s), a is electrode sensitivity (A Pa^{-1}), n is number of moles of electrons involved in the reduction of one mole of oxygen (4), and F is the charge of one mole of electrons (Faraday's constant: $96494 \text{ A s mol}^{-1}$ electrons). Oxygen consumption rate of soil was taken as mentioned above. The effective diffusion coefficient in soil (D) was calculated from $D = D_0 (\epsilon \cdot \theta_e)^{4/3}$ (Millington 1959), where D_0 is oxygen diffusion coefficient in free air, ϵ is soil porosity, and θ_e volumetric water content. Values for these parameters were $0.1987 \cdot 10^{-4} \text{ m}^2 \text{ s}^{-1}$, $0.5 \text{ m}^3 \text{ m}^{-3}$, and $0.48 \text{ m}^3 \text{ m}^{-3}$, respectively. The simulation showed that the electrode did not use more than 10% of the total amount of oxygen consumed from the chamber and that no concentration gradient was induced in the soil pillar.

PARTIAL ANAEROBOSIS AND DENITRIFICATION

Calculations

Oxygen pressure in the pores of the soil aggregate at the two locations during an experiment was calculated assuming that the electrode signal had a linear drift with time. The measured oxygen pressure was not converted to oxygen concentration, because it can be used directly to check the simulation model.

Water content

Technical description

Water content is measured along the diameter of the experimental soil aggregate by means of 60-keV gamma radiation from ^{241}Am . Theory and application of attenuation methods are described by Gardner (1965) and Gardner and Calisendorff (1967). This technique can safely be used here, because the radiation energy of the ^{241}Am source is very low compared with the energy necessary to kill or inactivate microorganisms (Becking 1971)³. The source-detector system used was developed by the Department of Soil Science and Plant Nutrition at the Agricultural University, Wageningen. The system has been described by de Swart and Groenevelt (1971). The transport mechanism to locate the rigid support holding the source and detector (Fig. 2), however, was newly built for the present study. This transport mechanism consists of two stainless steel bars along which the support is guided with ball bushings. Locating is done by a motor-driven precision screw-thread that can be rotated in a female screw attached to the rigid support (detailed drawings available on request). The support can automatically be located at each millimeter or at regular intervals along the diameter of the soil container.

At a source-detector distance of 7.2 cm, typical corrected count rates through air, empty soil container, oven-dry soil, and nearly water-satu-

³ In the worst case, that all microorganisms are situated just above the soil container bottom, that living mass and density of microorganisms are 0.014% of soil mass (derived from Woldendorp 1981) and equal to the density of water, and that the radiation period is 10 min, the radiation absorbed dose is $2.6 \cdot 10^{-4}$ Gy. This number should be compared with D-10 values (radiation dose producing 10% survival or 90% lethality in microorganisms) of the order of 100 Gy (Becking 1971).

rated soil are 35 250, 14 850, 5450, and 4350 counts per second, respectively.

Comment on procedures (Table 1, items 4 and 15)

The counting durations for calculating instrumental dead time (see below), attenuation coefficient of water, reference scans at initial water content, and scans through wetted soil were 30, 60, and 18 s, respectively.

Data are converted to counts per second, corrected for instrumental dead time according to Overman and Clark (1960), and corrected for drift in the electronics (less than 0.5% and not time dependent) using the reference measurements. Instrumental dead time ($2.87 \cdot 10^{-6}$ s per count) was found by a procedure described by Fritton (1969), from which the weighed variance was omitted, however.

The attenuation coefficients of water and soil are needed to calculate water contents and bulk densities. For water it was $0.190 \text{ cm}^2 \text{ g}^{-1}$, assuming a density of 1 g cm^{-3} . This number compared well with the value of $0.196 \text{ cm}^2 \text{ g}^{-1}$ given by Groenevelt et al. (1969). The attenuation coefficient for the sandy loam soil was determined as $0.280 \text{ cm}^2 \text{ g}^{-1}$.

Water contents located symmetrically around the center of the soil container were considered duplicates: when corresponding water contents were plotted against each other, slopes of about unity and intercepts of about zero were obtained. This indicates that the changes in water contents in the soil aggregate were small during the determination of a scan.

The distribution of the volumetric water content in space and time can directly be compared with the results of the simulation model.

Chemical analyses

Comment on procedures (Table 1, items 10, 11, 6, and 22)

The soil is wetted with a solution that may contain potassium nitrate (KNO_3) and/or glucose ($\text{C}_6\text{H}_{12}\text{O}_6$). Concentrations are so chosen that equivalents of about 65 kg NO_3^- -N and 65 kg C per ha are applied to the aggregate.

Nitrate, nitrite, and ammonium are determined in the extract of the soil-KCl mixture used to measure pH. In the nitrate determination, NO_3^- ions are routed through a Cu-Cd

reduction column to form nitrite. This ion is converted into a colored organic complex of which the concentration is measured spectrophotometrically (Novozamsky et al. 1983). Nitrite is determined similarly, but now the reduction column is left out of the measuring system. The determination of ammonium is described by Novozamsky et al. (1974).

Calculations

Chemical data were expressed on an oven-dry basis. The nitrogen species, i.e., NO_3^- , NO_2^- , NH_4^+ , N_2O , and N_2 , were used to calculate the inorganic N balance at the start and the end of an experiment. The difference between the amounts of nitrate before and after an experiment does not necessarily balance with the sum of the amounts of the produced inorganic nitrogen species, because mineralization and/or immobilization of nitrogen may take place.

Error analysis

State variables obtained from experiments result from a combination of a number of differently measured quantities. Reliability of the state variables is assessed by calculating the propagation of the errors in the measured quantities on these final results.

Systematic errors in the measurements are avoided as much as possible by calibrating the various measuring instruments. Random errors, however, remain in each measured quantity. They can be evaluated from knowledge about the measuring instruments. Error propagation is calculated by procedures outlined by Berendts et al. (1973), using partial derivatives with respect to each measured quantity. These calculations yield confidence intervals of one standard deviation.

The equation to calculate water content from gamma-radiation data appeared too complex to obtain the partial derivatives analytically. Therefore, these partial derivatives were evaluated numerically.

The measurements with the polarographic oxygen electrodes yield electrical signals that were converted to oxygen pressures, using calibration lines before and after an experiment. These calibration lines, obtained by linear regression, were also used to calculate confidence limits for oxygen pressure estimates, using Eq. (6.14.2) of Snedecor and Cochran (1974). Errors in the oxygen measurements in the period

between determinations of calibration lines were calculated by linear interpolation.

Values for the errors in individual measurements used in the error propagation calculations are summarized in Table 2. No errors have been assumed in time, molecular weights, and locating the gamma-radiation apparatus.

Errors are indicated as vertical bars in Figs. 4 through 7, when they are larger than the symbols used.

RESULTS AND DISCUSSION

One representative coherent data set on the distribution of water, gases, and nitrogen species is presented in Figs. 4 through 7 and Table 3 for

TABLE 2
Values for errors in individual measurements for error propagation calculations

Measurement	Error	Dimension
Gas chromatography ^a	1.5	%
Particle density ^b	1	%
Chemical analyses ^c	10	%
Volume of gas collection circuit	5	ml
Burette readings	0.2	ml
Amount of wetting solution	2	ml
Concentration of KNO_3 and $\text{C}_6\text{H}_{12}\text{O}_6$ in wetting solution	0.05	g L^{-1}
Weight of initially moist soil	2	g
Initial gravimetric water content ^d	0.001	g g^{-1}
Final gravimetric water content ^e	0.003	g g^{-1}
Diameter of concentric layers (measuring tape, MT)	0.1	cm
Height of sample (vernier callipers)	0.02	cm
Water penetration depth (MT)	0.1	cm
Dead time	$0.05 \cdot 10^{-6}$	s
Water density	0.0001	g cm^{-3}
Gamma radiation measurement	counts ^f count time	s^{-1}

^a Statistical analysis (SA) of calibration chromatograms.

^b Based on analysis of method of determination.

^c Based on analysis of number of data at two locations in layers of concentrically partitioned aggregate.

^d SA of quadruple determination.

^e SA of duplicate determination.

PARTIAL ANAEROBOSIS AND DENITRIFICATION

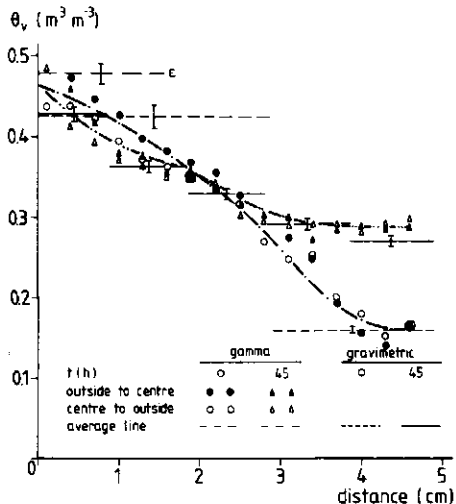


FIG. 4. Volumetric water distribution in soil aggregate (center at distance 4.9 cm) at start and end of experiment.

Lelystad sandy loam soil. In a forthcoming paper other data sets will be discussed in conjunction with the simulation model.

The average density of the Lelystad aggregate was $1.38 \pm 0.03 \text{ g cm}^{-3}$. Variation in densities determined with gamma radiation was well within 5% of the average.

Figure 4 shows the volumetric water distribution at the start of the experiment and at the end, after 45 h. The water volume should be conserved, because no evaporation of water from the aggregate takes place. The volume of water was obtained by summation of the amounts of water in 49 concentric rings of 1-mm thickness each. The water content of each ring was obtained from linear interpolation between the averaged measured water contents. This yielded an initial water volume (V) of $71.2 \pm 0.6 \text{ ml}$. Following the same procedure at 45 h gave $V = 72.0 \pm 0.6 \text{ ml}$. From the gravimetric moisture measurements on the five concentric rings at 45 h, $V = 71.0 \pm 0.7 \text{ ml}$ was calculated. The close agreement among these data shows that the methods to measure water content are satisfactory.

After about 24 h water no longer redistributed (data not shown), even though a homogeneous volumetric water content (0.363 ± 0.008) was not attained. This indicates that a homogeneous

suction distribution was attained in the soil aggregate combined with a heterogeneous water distribution due to hysteresis in the soil water characteristic. In the absence of hysteresis, the air-filled porosity at equilibrium ($0.115 \text{ cm}^3 \text{ cm}^{-3}$) would have been sufficient to let oxygen diffuse into the aggregate and to stop anaerobic processes. In the presence of hysteresis, however, a small amount of added water is sufficient to decrease gaseous diffusion to such an extent that anaerobiosis may occur in soil.

The volume of air-filled pores in the outer shell of the aggregate remained close to zero, even after 45 h. Thus the exchange of gases between the soil and the gas collection circuit took place through the water phase, and it was expected that the aggregate remained anaerobic after the oxygen in its interior was consumed.

Figure 5 confirms this expectation. It shows oxygen pressure in the aggregate center to equal zero after 13 h, while the peripheral oxygen pressure remains about 2 kPa. Outside the aggregate, however, and after 45 h, the amount of oxygen had decreased by only 19.5 ml (Fig. 6), which agrees with an oxygen pressure of 15.7 kPa. Oxygen flux can be obtained by differentiating Fig. 6 with respect to time. Oxygen flux density is obtained by dividing this quantity by

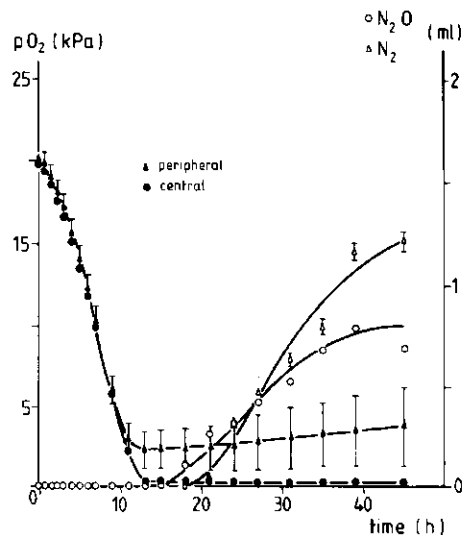


FIG. 5. Oxygen pressure (left y axis) in center and 4 cm from center (peripheral) of soil aggregate and volumes of nitrous oxide and molecular nitrogen in gas collection circuit (right y axis) as function of time.

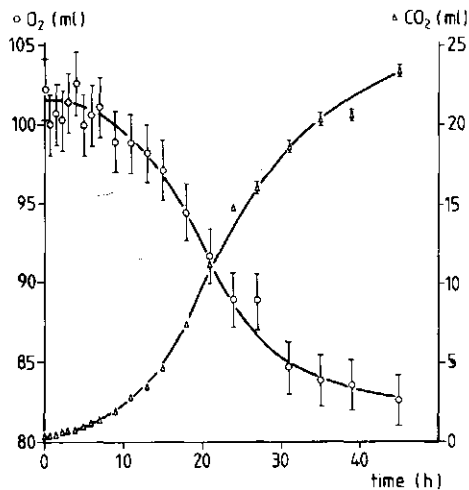


FIG. 6. Volume of oxygen and carbon dioxide in gas collection circuit as function of time.

the surface area of the aggregate ($79.7 \pm 1.0 \text{ cm}^2$). At 21 h the oxygen flux density amounted to $-2.7 \pm 10.8 \text{ L O}_2 \text{ m}^{-2} \text{ d}^{-1}$ (the large confidence interval is discussed below). This value compares favorably with field measurements in bare soil (Russell 1973).

Figure 6 also shows the development of carbon dioxide. The oxygen and carbon dioxide curves form complementary S-shaped curves. The amounts of oxygen consumed ($20 \pm 3 \text{ ml}$) and carbon dioxide produced ($23 \pm 0.5 \text{ ml}$) in 45 h were practically the same. This resulted in a respiratory quotient, defined as the ratio of the volumetric rates of carbon dioxide production and oxygen consumption, of about 1. In a partially anaerobic soil, however, only a portion of the soil is consuming oxygen, while the whole is producing carbon dioxide, and the respiratory quotient should exceed 1. Therefore, the respiratory quotient is not a sensitive measure to decide whether a soil is partially anaerobic. Russell (1973) and Gliński and Stępniewski (1985), however, state the opposite with regard to the sensitivity of the respiratory quotient. The discrepancy between a respiratory quotient of about 1 and the knowledge that soil is partially anaerobic can, at least in part, be explained by the differences in solubility of O₂ and CO₂ in soil water (0.033 and 0.946 ml ml⁻¹, respectively, at 100 kPa and 293 K; Hoeks 1972): when CO₂ is produced at the same rate as O₂ is consumed,

but is released slower, the respiratory quotient will be underestimated as long as no steady rates of exchange of CO₂ and O₂ are established. A possible correction for solubility differences for the production volumes of O₂ and CO₂ is severely hampered by the unknown concentration gradients of these gases inside the aggregate. The CO₂ curve in Fig. 6 was used to calculate the flux density at 21 h and yielded $3.7 \pm 1.3 \text{ L CO}_2 \text{ m}^{-2} \text{ d}^{-1}$. This value is of the same order of magnitude as field data of de Jong et al. (1979), though these authors measured CO₂ evolution in a cropped soil. The confidence interval in the O₂ consumption rate is large compared to that in the CO₂ production rate. This is caused by the propagation of the error in the measured amount of O₂, which is determined by the difference of two large numbers. The reasonable error in the measurement of CO₂ makes it a more appropriate measure to assess soil activity.

Assuming that all carbon dioxide comes from the added glucose ($4.3 \pm 0.2 \text{ mmol}$), and interpreting glucose decay as a first-order rate process, it was calculated that the decay constant is 0.13 h^{-1} . This value is close to the values cited by van Veen and Paul (1981).

Production of nitrous oxide and molecular nitrogen is shown in Fig. 5. These gases occurred in the gas collection circuit a few hours after anaerobiosis was established. The retardation was caused by a combination of adaptation time of the microorganisms to nitrate as new electron acceptor and the time needed for the gas to diffuse through the water phase into the gas collection circuit. Similarly to CO₂, N₂O dissolves well in water (1.1 ml ml⁻¹ at 100 kPa and 298 K; Stolzy and Flühler 1978), whereas N₂ has a low solubility (0.016 ml ml⁻¹ at 100 kPa and 293 K; Hoeks 1972). This will result in an underestimation of the rate of nitrous oxide development when steady rates are not yet reached, especially in very wet soils. Again, solubility corrections for gas production volumes are hampered for reasons explained above. Furthermore, Fig. 5 shows that the rate of release of N₂ is higher than that of N₂O. This will partly be due to the low N₂ solubility in soil water resulting in an exclusion of N₂ from the water phase. On the other hand, nitrous oxide will be reduced further to molecular nitrogen, which decreases its release. These effects agree with findings reported by Letey et al. (1980).

The N₂O and N₂ flux densities derived from

PARTIAL ANAEROBIOESIS AND DENITRIFICATION

Fig. 5 equal 1.3 and 1.9 kg N $ha^{-1} d^{-1}$. Similar values were found in field experiments by Roston et al. (1976 and 1978), but Colbourn and Dowdell (1984) found lower values for the flux densities in field situations. These flux densities illustrate that a flush of microbial activity in soil is effectively avoided through the procedure of wetting and leaving soil at rest for some time prior to its use, and that the small addition of glucose did not cause an unacceptable increase of the rates of gas production and consumption.

Figure 7 depicts the distributions of nitrate and nitrite in the soil aggregate after 45 h. Large amounts of nitrite were formed, particularly in the outer shell of the aggregate. The nitrate concentration in the central portion of the aggregate (with a diameter of 4.16 cm) had risen from 3.4 to 6.7 mmol kg^{-1} dry soil. In principle, nitrate concentration can be changed by denitrification, dissimilatory nitrate reduction to ammonium (Knowles 1982; Tiedje et al. 1982), mineralization with subsequent nitrification and/or transport of nitrate with the water from the wetting solution. However, since minor amounts of ammonium (about 0.2 mmol kg^{-1} dry soil after 45 h) were found in soil, and nitrification is inhibited in the absence of oxygen (Patrick 1982), dissimilatory nitrate reduc-

TABLE 3
Nitrogen balance of the Lelystad soil

Time, h	0.0	45.0
	mmol	
NO_3^-	4.53	0.64
NO_2^-	0.02	3.93
NH_4^+	0.0	0.05
$N_2O + N_2$	0.0	0.21
	4.55 ± 0.19	4.83 ± 0.36

tion to ammonium, mineralization, and nitrification were not important. A calculation using the initial and final water content data from Fig. 4 and the nitrate concentration in the solution ($8.44 \text{ g KNO}_3 \text{ L}^{-1}$) applied to the soil yielded a concentration of 7.6 mmol kg^{-1} dry soil. This value is slightly higher than the 6.7 mmol kg^{-1} dry soil actually found: some nitrate may thus have been denitrified. The large amount of nitrite formed in the outer shell of the aggregate must have been caused by the large initial amount of nitrate and by a larger microbial activity due to a greater glucose concentration. Moreover, the accumulation of nitrite may be due to the high pH of the soil, as suggested by Cooper and Smith (1963). The distributions of water, nitrite, and oxygen at the end of the experiment support the statement made in the introduction, that denitrification will occur only when, at a certain place and time, oxygen is absent and bacteria capable of denitrification, water, nitrate, and decomposable organic compounds are present. Therefore, the magnitude of the rate of denitrification will in principle not correlate with the anaerobic volume in aggregates. This was confirmed by the findings of Sextstone et al. (1985).

Table 3 summarizes the molar balance with regard to inorganic nitrogen in the soil aggregate. The last line shows that the N balance is good. The nitrate that has vanished ($3.9 \pm 0.3 \text{ mmol}$) is quantitatively recovered in the other nitrogen species ($4.2 \pm 0.3 \text{ mmol}$). Because mineralization, nitrification, and dissimilatory nitrate reduction to ammonium were negligible, it is concluded that denitrification was the sole nitrogen transformation process occurring in the soil aggregate.

CONCLUDING REMARKS

The data presented show that the new type of respirometer system makes it possible to meas-

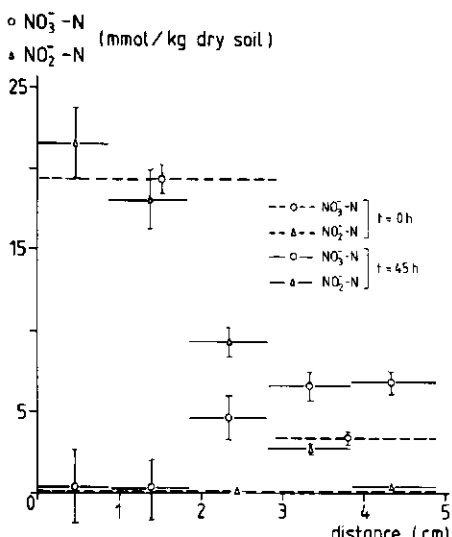


FIG. 7. Distribution of nitrate and nitrite in soil aggregate (center at a distance of 4.9 cm) at start and end of experiment.

LEFFELAAR

ure the course in space and time of the state variables that determine whether anaerobiosis and denitrification occur in soil. A full explanation of the relationships among the measured data, however, requires a simulation model that describes the interactions between the active biomass; transport processes of water, gases, and ions; and such storage factors as different solubilities of gases in soil water. Thus, measurements are gathered to evaluate a simulation model, but a simulation model is needed for a full interpretation of measured data.

It is not unlikely that the simultaneous occurrence of water saturation, anaerobiosis, organic compounds, and nitrate at the same place will have a low frequency in field soil. Therefore, it is possible that actual denitrification in field soils does not correlate with potential denitrification, such as measured with anaerobically incubated soil. Techniques like the one reported here are thus needed for a more realistic approach of the dynamics of partial anaerobiosis and denitrification.

The measuring system described is flexible. For instance, water transport may be excluded by saturating the aggregate, so as to avoid the influence of mass flow of water on the results. Then, only diffusion of ions and gases will take place through the water phase, and their submodels may be checked. On the other hand, the atmosphere in the gas collection circuit may exclusively be replaced by neon, so as to study denitrification under fully anaerobic conditions, while other factors affecting denitrification, such as the living biomass and the flow of water, ions, and gases, are maintained. Also nitrite instead of nitrate can be used as an electron acceptor in the soil.

ACKNOWLEDGMENTS

Thanks are due to Prof. G. H. Bolt and his staff of the Department of Soil Science and Plant Nutrition, who have given me the opportunity to carry out the experimental work in their laboratory. I wish to thank the following people who contributed to various parts of the experimental work: H. P. Kimmich, J. G. Spaan, and J. de Koning of the University of Nijmegen for help with the polarographic oxygen sensors; J. G. de Swart and G. L. Jupijnen of ITAL for manufacturing the amplifiers for the oxygen sensors; D. P. van den Akker, student at the

school for technology at Arnhem (STA), for preparing a manual for these amplifiers; J. D. Wouda (STA) for investigating the influence of nitrous oxide on the performance of the oxygen electrodes; Th. J. Jansen of CABO for manufacturing the soil container and a number of other parts of the respirometer system; M. Schimmel, C. Rijpma, J. van der Goor, and A. van Wijk, who drew and manufactured the support for the gamma system; H. Lindeman (STA) and P. H. F. M. van Twist (STA), for building the power supply for the support, and C. Dirksen and P. Koorevaar for discussions about the gamma measurements; W. Ch. Melger for help with gas chromatographic problems; H. Vrijmoeth (student at the laboratory school RMHAS at Wageningen) for the preliminary experiments to assess the appropriate gas composition for calibrating the gas chromatograph, and J. Treur (STA) for developing a program to calculate peak areas from gas chromatograms; E. B. Tijssen, Jr. (STA) and H. Lindeman (STA) for programming parts of the error analysis; V. J. G. Houba and A. van den Berg for discussing and performing the chemical soil analysis; and S. Maasland, C. A. Kok, W. van Barneveld, and W. C. Nieuwhoer for their assistance in solving many technical problems. The Netherlands Fertilizer Institute (NMI) provided a small subsidy. Prof. C. T. de Wit, Prof. G. H. Bolt, and Dr. B. H. Janssen reviewed the manuscript.

REFERENCES

Allison, L. E., and C. D. Moodie. 1965. Carbonate. In *Methods of soil analysis*, pt. 2. C. A. Black (ed.). *Agronomy* 9. American Society of Agronomy, Madison, Wis., pp. 1379-1396.

Bascomb, C. L. 1964. Rapid method for the determination of cation exchange capacity of calcareous and non-calcareous soils. *J. Sci. Food Agric.* 15:821-823.

Becking, J. H. 1971. Radiosterilization of nutrient media. *Misc. Papers* 9, Landbouwhogeschool Wageningen, The Netherlands, pp. 55-87.

Berendts, B., Th. H. J. A. Blaauw, B. J. M. Harmsen, J. C. Smit, and S. H. Tijs. 1973. *Foutenleer en statistiek*. Agon Elsevier, Amsterdam, p. 141.

Birch, H. F. 1958. The effect of soil drying on humus decomposition and nitrogen availability. *Plant Soil* 10:9-31.

Birch, H. F. 1959. Further observations on humus decomposition and nitrification. *Plant Soil* 11:262-286.

Blackmer, A. M., and J. M. Bremner. 1977. Denitrification of nitrate in soils under different atmospheres. *Soil Biol. Biochem.* 9:141-142.

Colbourn, P., and R. J. Dowdell. 1984. Denitrification

PARTIAL ANAEROBIOESIS AND DENITRIFICATION

in field soils. In *Biological processes and soil fertility*. J. Tinsley and J. F. Darbyshire (eds.). Martinus Nijhoff, The Hague, pp. 213-226.

Cooper, G. S., and R. L. Smith. 1963. Sequence of products formed during denitrification in some diverse western soils. *Soil Sci. Soc. Am. Proc.* 27:659-662.

Currie, J. A. 1961. Gaseous diffusion in the aeration of aggregated soils. *Soil Sci.* 92:40-45.

Day, P. R. 1965. Particle fractionation and particle-size analysis. In *Methods of soil analysis*, pt. 1. C. A. Black (ed.). Agronomy 9. American Society of Agronomy, Madison, Wis., pp. 545-567.

de Jong, E., R. E. Redmann, and E. A. Ripley. 1979. A comparison of methods to measure soil respiration. *Soil Sci.* 127:300-306.

Delwiche, C. C. 1981. The nitrogen cycle and nitrous oxide. In *Denitrification, nitrification, and atmospheric nitrous oxide*. C. C. Delwiche (ed.). Wiley, New York, pp. 1-15.

de Swart, J. G., and P. H. Groenevelt. 1971. Column scanning with 60 keV gamma radiation. *Soil Sci.* 112:419-424.

Eberhard, P., and W. Mindt. 1979. Interference of anesthetic gases at oxygen sensors. *Birth Defects: Orig. Artic. Ser.* 15:65-74.

Fatt, I. 1976. Polarographic oxygen sensors. CRC Press, Cleveland, Ohio, p. 278.

Fillery, I. R. P. 1983. Biological denitrification. In *Gaseous loss of nitrogen from plant-soil systems*. J. R. Freney and J. R. Simpson (eds.). Martinus Nijhoff, The Hague, pp. 33-64.

Fritton, D. D. 1969. Resolving time, mass absorption coefficient and water content with gamma-ray attenuation. *Soil Sci. Soc. Am. Proc.* 33:651-655.

Gardner, W. H. 1965. Water content. In *Methods of soil analysis*, pt. 1. C. A. Black (ed.). Agronomy 9. American Society of Agronomy, Madison, Wis., pp. 82-127.

Gardner, W. H., and C. Calissendorff. 1967. Gamma-ray and neutron attenuation in measurements of soil bulk density and water content. *Proc. symp. isotope and radiation techniques in soil physics and irrigation studies*, Istanbul (IAEA, Vienna).

Gleichmann, U., and D. W. Lubbers. 1960. Die Messung des Sauerstoffdruckes in Gasen und Flüssigkeiten mit der Pt-Elektrode unter besonderer Berücksichtigung der Messung im Blut. *Pflügers Arch. Ges. Physiol.* 271:431-455.

Gliński, J., and W. Stępniewski. 1985. Soil aeration and its role for plants. CRC Press, Boca Raton, Fla., p. 229.

Grable, A. R. 1966. Soil aeration and plant growth. *Adv. Agron.* 18:57-106.

Greenwood, D. J. 1961. The effect of oxygen concentration on the decomposition of organic materials in soil. *Plant Soil* 14:360-376.

Groenevelt, P. H., J. G. de Swart, and J. Cisler. 1969. Water content measurement with 60 keV gamma ray attenuation. *Bull. Int. Assoc. Sci. Hydrol.* 14:67-78.

Hoeks, J. 1972. Effect of leaking natural gas on soil and vegetation in urban areas. PUDOC, Wageningen, p. 120.

Ingraham, J. L. 1981. Microbiology and genetics of denitrifiers. In *Denitrification, nitrification, and atmospheric nitrous oxide*. C. C. Delwiche (ed.). Wiley, New York, pp. 45-65.

Johnson, K. E., and D. T. Sawyer. 1974. The electrochemical reduction of nitrous oxide in alkaline solution. *J. Electroanal. Chem. Interfacial Electrochem.* 49:95-103.

Kimmich, H. P., and F. Kreuzer. 1969. Telemetry of respiratory oxygen pressure in man at rest and during exercise. In *Oxygen pressure recording in gases, fluids, and tissues*. F. Kreuzer (ed.). *Progr. Resp. Res.* H. Herzog (ed.), vol. 3. Karger, Basel, pp. 22-39.

Knowles, R. 1982. Denitrification. *Microbiol. Rev.* 46:43-70.

Kreuzer, F., H. P. Kimmich, and M. Březina. 1980. Polarographic determination of oxygen in biological materials. In *Medical and biological applications of electrochemical devices*. J. Koryta (ed.). Wiley, New York, pp. 173-261.

Küchler, G., W. Wagner, and I. Wolburg. 1978. Experimental study on errors in dynamic measurement of oxygen intake. *Biotelemetry* 4:109-112.

Lee, Y. H., and G. T. Tsao. 1979. Dissolved oxygen electrodes. In *Advances in biochemical engineering*. T. K. Ghose, A. Fiechter, and N. Blakebrough (eds.). Springer-Verlag, New York, pp. 35-86.

Leffelaar, P. A. 1979. Simulation of partial anaerobiosis in a model soil in respect to denitrification. *Soil Sci.* 128:110-120.

Letey, J., W. A. Jury, A. Hadas, and N. Valoras. 1980. Gas diffusion as a factor in laboratory incubation studies on denitrification. *J. Environ. Qual.* 9:223-227.

McNair, H. M., and E. J. Bonelli. 1969. Basic gas chromatography. Varian, U.S.A., p. 306.

Mebius, L. J. 1960. A rapid method for the determination of organic carbon in soil. *Anal. Chim. Acta* 22:120-124.

Millington, R. J. 1959. Gas diffusion in porous media. *Science* 130:100-102.

Novozamsky, I., R. van Eck, J. Ch. van Schouwenburg, and I. Walinga. 1974. Total nitrogen determination in plant material by means of the indophenol-blue method. *Neth. J. Agric. Sci.* 22:3-5.

Novozamsky, I., V. J. G. Houba, D. van der Eijk, and R. van Eck. 1983. Notes on determinations of nitrate in plant material. *Neth. J. Agric. Sci.* 31:239-248.

Novozamsky, I., V. J. G. Houba, E. Temminghoff, and J. J. van der Lee. 1984. Determination of "total" N and "total" P in a single soil digest. *Neth. J. Agric. Sci.* 32:322-324.

Overman, R. T., and H. M. Clark. 1960. Radioisotope techniques. McGraw-Hill, New York, p. 476.

Patrick, W. H., Jr. 1982. Nitrogen transformations in submerged soils. In *Nitrogen in agricultural soil*. F. J. Stevenson (ed.). Agronomy 22. American Society of Agronomy, Madison, Wis., pp. 449-465.

Prazma, J., D. Smith, and W. J. Jochem. 1978. Current-to-voltage converter for measurement of oxygen. *J. Appl. Physiol.: Respirat. Environ. Ex-*

LEFFELAAR

ercise Physiol. 44:977-980.

Rolston, D. E., D. L. Hoffman, and D. W. Toy. 1978. Field measurement of denitrification: 1. Flux of N_2 and N_2O . *Soil Sci. Soc. Am. J.* 42:863-869.

Rolston, D. E., M. Fried, and D. A. Goldhamer. 1976. Denitrification measured directly from nitrogen and nitrous oxide gas fluxes. *Soil Sci. Soc. Am. J.* 40:259-266.

Russell, E. W. 1973. *Soil conditions and plant growth*. Longmans, London, p. 849.

Scholander, P. F. 1942. Volumetric microrespirometers. *Rev. Sci. Instr.* 13:32-33.

Sexstone, A. J., N. P. Revsbech, T. B. Parkin, and J. M. Tiedje. 1985. Direct measurement of oxygen profiles and denitrification rates in soil aggregates. *Soil Sci. Soc. Am. J.* 49:645-651.

Smith, K. A. 1977. Soil aeration. *Soil Sci.* 123:284-291.

Smith, K. A. 1980. A model of the extent of anaerobic zones in aggregated soils and its potential to estimate denitrification. *J. Soil Sci.* 31:263-277.

Snedecor, G. W., and W. G. Cochran. 1974. *Statistical methods*. Iowa State Univ. Press, Ames, p. 593.

Stolzy, L. H., and H. Flühler. 1978. Measurement and prediction of anaerobiosis in soils. *In Nitrogen in the environment*, vol. 1. D. R. Nielsen and J. G. MacDonald (eds.). Academic Press, New York, pp. 363-426.

Tiedje, J. M., A. J. Sexstone, D. D. Myrold, and J. A. Robinson. 1982. Denitrification: Ecological niches, competition and survival. *Antonie van Leeuwenhoek* 48:569-583.

Thompson, B. 1977. *Fundamentals of gas analysis by gas chromatography*. Varian, U.S.A., p. 132.

van Veen, J. A., and E. A. Paul. 1981. Organic carbon dynamics in grassland soils: 1. Background information and computer simulation. *Can. J. Soil Sci.* 61:185-201.

Woldendorp, J. W. 1981. Nutrients in the rhizosphere. Agricultural yield potentials in continental climates. *Proc. 16th Coll. Int. Potash Institute*, Bern, pp. 99-125.

CHAPTER 4

0038-075X/87/1432-0079\$02.00/0

SOIL SCIENCE

Copyright © 1987 by The Williams & Wilkins Co.

February 1987

Vol. 143, No. 2

Printed in U.S.A.

DYNAMIC SIMULATION OF MULTINARY DIFFUSION PROBLEMS RELATED TO SOIL

P. A. LEFFELAAR¹

A dynamic simulation model describing diffusion of gases in multinary gas mixtures was developed to calculate the inter-diffusion of gases in complex systems where respiration and denitrification take place. The model is based on the Stefan-Maxwell equations for concentration diffusion of isothermal, isobaric ideal-gas mixtures and applies to a one-phase system in one dimension. To test the correct implementation of the theory in the model, it was used to calculate the mole fraction distribution in a gas layer for some ternary diffusion problems for which analytical solutions to the steady-state situation are known. Agreement between numerical and analytical solutions was within 1%. Subsequently, the model was used to calculate the dynamic behavior of a gas system in which denitrification takes place and acetylene is used to prevent the conversion of nitrous oxide into molecular nitrogen. When a 2% concentration of acetylene was maintained at the surface of the gas layer, and biological activity was positioned at a depth of 0.25 m, these calculations showed the acetylene concentration to reach 1.8%. This value is sufficiently high to inhibit nitrous oxide conversion into molecular nitrogen, but would be equal to 2% when calculated on the basis of Fick's law. A simplified approach to calculate diffusion in multinary gas mixtures is proposed and tested for the case study of denitrification. It turns out that results of the simplified approach approximate those of the Stefan-Maxwell equations to within 10%. The objectives of this paper are to discuss the model, to compare the results of the numerical and analytical solutions of two ternary diffusion problems, to report the results of the case study of denitrification, and to compare these results with those obtained from simplified diffusion theory.

Exchange of gases between soil and atmosphere is of great importance with regard to biological activity of, for example, (micro-)organisms and plant roots in soil. The physical processes causing gas movement are convection and diffusion. Convection occurs when a spatial difference in absolute gas pressure exists, e.g., after a heavy rainfall (Flühler and Läser 1975) or atmospheric variations in pressure and temperature (Kraner et al. 1964), or due to formation of gaseous products from nongaseous substrates (Stolzy and Flühler 1978). Diffusion occurs when there is a spatial difference in the partial pressures of components in a mixture of gases.

Diffusion in multinary gas mixtures like soil atmosphere cannot exactly be described by Fick's law (Jaynes and Rogowski 1983; Wood and Greenwood 1971). This law assumes that gas fluxes can be calculated independently of each other as concentration gradient times diffusion coefficient. In fact, Fick's law is a special case of the results obtained by the gas kinetic theory for multinary gas mixtures (Hirschfelder et al. 1964, p. 519). Gas kinetic theory shows gas fluxes due to diffusion to be coupled. Thus, gas diffusion of, for example, oxygen and carbon dioxide due to respiration does influence the distribution of an inert gas as nitrogen. As far as is known to the author, no mathematical solutions are available to study the dynamics of the gas phase of soil as a whole. Therefore, a simulation model to describe the dynamics of diffusion in multinary gas mixtures with source/sink terms based on results of the gas kinetic theory as given by Hirschfelder et al. (1964) was developed. This model applies to diffusion processes in soil when the mean free path between intermolecular collisions (a characteristic value is 0.07 μm for air-gases at 293K and 1 atm) is not much more than one-hundredth of the gas-filled pore diameters (Wakao et al. 1965) (a characteristic value is 28 μm for well-drained soils at $\text{pF} = 2$, when calculated from the simple capillary model, Koorevaar et al. 1983). The model does not include the influence of tortuosity and area reduction on diffusion, as these

¹ Agricultural Univ. Wageningen, Dept. of Theoretical Production Ecology, Bornsesteeg 65, 6708 PD Wageningen, the Netherlands.

Received for publication 30 July 1985; revised 19 February 1986.

depend merely on characteristics of the porous medium (Wakao and Smith 1962).

The mathematics of multinary gas diffusion will be seen to be rather involved. Therefore, a simplified approach to calculate diffusion in multinary gas mixtures is proposed.

The objectives of this paper are to describe the multinary dynamic gas diffusion model, to compare some of the model results with known analytical solutions to ternary steady-state diffusion problems, and then to use the model to calculate the dynamic behavior of a gas system in which denitrification takes place and acetylene is used to inhibit the conversion of nitrous oxide into molecular nitrogen. Finally, the simplified description of multinary diffusion is tested for the case study of denitrification.

SIMULATION MODEL BASED ON THE STEFAN-MAXWELL EQUATIONS

The equations describing the diffusion velocity of gas j , \bar{V}_j , relative to the diffusion velocity of gas i , \bar{V}_i , in a v -component isothermal, isobaric ideal-gas mixture for a one-phase system in one dimension for ordinary diffusion are (Hirschfelder et al. 1964, p. 517)

$$\sum_{j=1}^v \frac{n_i n_j}{n^2 D_{ij}} (\bar{V}_j - \bar{V}_i) = \frac{d}{dx} \left(\frac{n_i}{n} \right), \quad \text{for } i = 1, 2, \dots, v \quad (1)$$

All symbols for this and other equations are defined in the appended list of symbols. These v so-called Stefan-Maxwell equations (Cunningham and Williams 1980, p. 109) form a set of $(v - 1)$ independent equations, since

$$\sum_{i=1}^v (n_i/n) = 1$$

Equation (1) can be used to obtain $(v - 1)$ values of the diffusion velocities relative to any particular one. An additional equation that relates all fluxes is necessary to obtain all the diffusion velocities. Equation (1) has been used successfully to describe experimental data (Wilke 1950; Fairbanks and Wilke 1950). Further, a number of analytical solutions for steady-state diffusion problems using various boundary conditions have been published, by, among others, Toor (1957) and Hsu and Bird (1960).

In process calculations it is convenient to relate molar fluxes (N_i) to stationary coordi-

nates, rather than calculating diffusion velocities relative to one another. Further, to calculate the spatial distribution of gases, the space coordinate of the system to be simulated is divided into a number of layers, Fig. 1 (Frissel and Reiniger 1974; de Wit and van Keulen 1975). The principal equation used in the simulation model is obtained as follows. In an isothermal, isobaric ideal-gas mixture, total molecular concentration is constant, so n in the spatial derivative and in the left-hand side of Eq. (1) cancels. Then, replace in Eq. (1) \bar{V}_i by $\bar{v}_i - v_0 = (N_i/c_i) - v_0$, n_i by $c_i \bar{N}$ and n by $c \bar{N}$, write out the v equations for v terms, and rearrange to obtain a set of v linear equations in terms of the products of each individual molar flux (N_i) times its coefficient. Finally, write down the results in matrix notation for a layered system to obtain Eq. (2)

$$\left(\begin{array}{cccc|c|c} \sum_{j=1}^v \frac{\bar{c}_1}{c \bar{b}_{1j}} & \frac{\bar{c}_1}{c \bar{b}_{2j}} & \dots & \frac{\bar{c}_1}{c \bar{b}_{vj}} & \bar{v}_1 & \Delta \bar{v}_1 \\ \frac{\bar{c}_2}{c \bar{b}_{12}} & \sum_{j=2}^v \frac{\bar{c}_2}{c \bar{b}_{2j}} & \dots & \frac{\bar{c}_2}{c \bar{b}_{vj}} & \bar{v}_2 & \Delta \bar{v}_2 \\ \vdots & \vdots & \ddots & \vdots & \vdots & \vdots \\ \frac{\bar{c}_v}{c \bar{b}_{1v}} & \frac{\bar{c}_v}{c \bar{b}_{2v}} & \dots & \frac{\bar{c}_v}{c \bar{b}_{vv}} & \bar{v}_v & \Delta \bar{v}_v \end{array} \right) \left(\begin{array}{c} N_1 \\ N_2 \\ \vdots \\ N_v \end{array} \right) = \left(\begin{array}{c} \Delta \bar{v}_1 \\ \Delta \bar{v}_2 \\ \vdots \\ \Delta \bar{v}_v \end{array} \right)$$

where bars above and Δ 's before symbols indicate, respectively, the arithmetic spatial average and the finite difference of that symbol, both with respect to the layers L and $(L - 1)$ of the system. As only $(v - 1)$ equations are independent, the determinant of the matrix of coefficients in Eq. (2) equals zero. However, the system can be resolved when proper additional equations are defined. For instance, if the sum of the molar

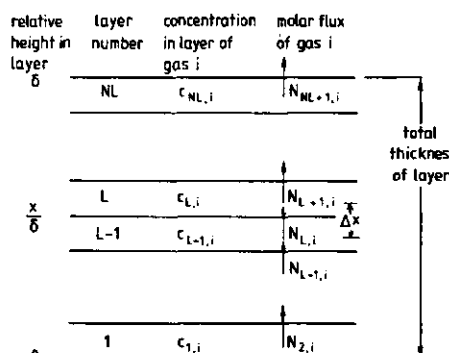


FIG. 1. Geometry of gas layer. Direction of flow is positive upward.

MULTINARY DIFFUSION PROBLEMS

fluxes through each interface is equal to zero, one of the rows (e.g., the first one) in the matrix of coefficients can be replaced by 1s and the corresponding right-hand-side element by 0. The sum of the molar fluxes through each interface is equal to 0 if a soil is exposed at its surface to constant concentrations of O_2 , CO_2 , and N_2 , while at some depth a constant but different concentration of O_2 and CO_2 exists due to equimolar respiration (example 2 in "Model Tests," below).

Essentially, at each time step, the model calculates on the basis of the gas concentrations present at the boundaries and in the layers of the system, the concentration gradients (right-hand side of Eq. (2)) and all the coefficients of the matrix (left-hand side of Eq. (2)), except those in the first row. Then, the Gauss-Jordan elimination method (La Fara 1973, p. 119) is used to obtain the interlayer molar fluxes. From these, the net flux of each gas to each layer is calculated, and the molar equations of continuity with production terms

$$\frac{\partial c_i}{\partial t} = - \frac{\partial N_i}{\partial x} + P_i \quad (3)$$

are solved by integration over a time interval that is sufficiently small to maintain stability. Thus, the new molar distribution of gases over the layers is known. By repeating this procedure, the dynamic behavior of the model can be examined. Equation (2) can not be solved by the Gauss-Jordan algorithm when a certain gas is absent, because a zero pivot element will be found. This occurs when a gas has not yet diffused throughout the layer. Figure 2 gives the flowchart of the heart of the program that processes such zero gas concentrations. First it is checked which gases are present at a layer interface, and second the gases present are rearranged to obtain a matrix of nonzero elements in Eq. (2). Then the Gauss-Jordan elimination method is used to obtain the interlayer molar fluxes, and these results are rearranged in the original storage locations. The process is repeated for each layer interface in case all gases may diffuse throughout the layer; see example 2 in "Model Tests," below. In other options included in the model, the calculations for layer 1 are made differently as discussed in the examples. Other options included are: (1) one gas can diffuse throughout the gas layer; others experience an absorption barrier at the bottom (see

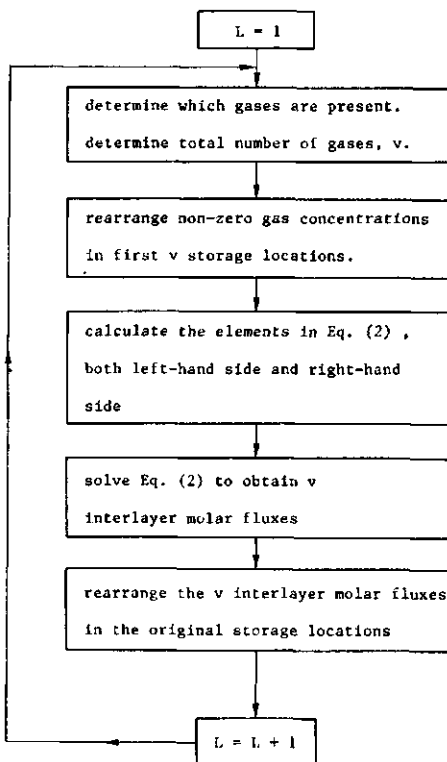


FIG. 2. Flowchart of the program section that processes zero gas concentrations.

example 1 in "Model Tests"); (2) one gas is converted into another gas in the bottom layer by some irreversible reaction, while the other gases cannot diffuse through the bottom layer; stoichiometry of reaction may be chosen as desired; (3) a maximum of six gas fluxes may be imposed to the bottom part of the gas layer; (4) a module containing the kinetics of the case study of denitrification as discussed in this paper.

The gas layer has a linear geometry as depicted in Fig. 1. The binary diffusion coefficients in Eq. (2) are calculated from theoretical equations (Hirschfelder et al. 1964) discussed below.

Numerical calculations are done by a program written in Continuous System Modeling Program III (CSMP III) language (IMB 1975) and executed on a DEC-10 machine. This language was chosen because of the availability of sophisticated methods of integration, e.g., the variable time-step methods that generally combine ac-

curate solutions to the problem and lower computer times compared with fixed time-step methods. All results presented have been obtained by the variable time-step method of Runge-Kutta Simpson.

The program gives results in terms of the distribution in space and time of mole fractions, interlayer molar diffusion fluxes, and cumulative in or outflow of moles of gas at $x = 0$ and $x = \delta$.

BINARY DIFFUSION COEFFICIENTS

Molar diffusion fluxes are directly proportional to binary diffusion coefficients, D_{ij} , thus demanding reliable estimates of these. If possible, accurate measurements of D_{ij} 's should be used in the calculation of fluxes. But even the very extensive compilation of diffusion coefficients by Marrero and Mason (1972) does not give all binary combinations of gas pairs that would be needed, for instance between Ar, O₂, N₂, CO₂, air, H₂O-vapor, NH₃, N₂O, CH₄, and C₂H₂. The Chapman-Enskog theory, however, gives expressions to calculate binary diffusion coefficients under the following assumptions: (1) only binary elastic collisions between molecules, (2) a small mean molecular free path compared with the dimensions of the gas container, and (3) small concentration gradients (Hirschfelder et al. 1964). The composition dependence of binary diffusion coefficients is usually less than 5% (Marrero and Mason 1972). Therefore, this effect is not considered, and the following expression is used (Hirschfelder et al. 1964, p. 539)

$$D_{ij} = \frac{3}{8} \left(\frac{k^3 \bar{N}}{\pi} \right)^{1/2} \frac{[T^3 (M_i + M_j) / (2M_i M_j)]^{1/2}}{p \sigma_{ij}^2 \Omega_{ij}} \quad (4)$$

In Eq. (4) $M_i M_j / (M_i + M_j)$ is the reduced molecular weight of a pair of unlike molecules. The dynamics of collisions between molecules is represented by the dimensionless collision integral Ω_{ij} . The physical meaning of the dimensionless collision integral is that it indicates the deviation of a particular molecular model from the idealized rigid-sphere model. For the numerical evaluation of the collision integral, a relationship between the potential energy of interaction and the intermolecular separation distance is needed. To this purpose the Lennard-Jones potential model is used. This potential model contains two parameters or force constants that are

characteristics of the colliding molecules, i.e., σ_{ii} and ϵ_{ii} . σ_{ii} , with dimension of length, is the value of the intermolecular separation distance where the potential energy is zero and may be considered as the effective molecular size, compared with an ideal rigid-sphere model (Marrero and Mason 1972). ϵ_{ii} is the maximum energy of attraction occurring between molecules. For more details the reader is referred to Hirschfelder et al. (1964). The dimensionless collision integral is dependent on temperature and is usually tabulated as a function of reduced temperature T_{ij} ($= kT/\epsilon_{ij}$). The force constants between unlike nonpolar molecules, σ_{ij} and ϵ_{ij}/k , are obtained from empirical combining laws, i.e., the arithmetic mean for the collision diameter

$$\sigma_{ij} = (\sigma_{ii} + \sigma_{jj})/2 \quad (5)$$

and the geometric mean for the maximum energy of attraction

$$\epsilon_{ij}/k = [(\epsilon_{ii}/k)(\epsilon_{jj}/k)]^{1/2} \quad (6)$$

For all practical purposes, however, Eqs. (5) and (6) may also be used to calculate these values between polar and nonpolar molecules (Mason and Monchick 1962). The constant $\frac{3}{8} (k^3 \bar{N} / \pi)^{1/2}$ in Eq. (4) equals $8.42 \cdot 10^{-24} [J^3 K^{-3} mol^{-1}]^{1/2}$. Equation (4) is symmetrical in i and j and reduces to the equation for a single component when properties of identical molecules are used, thus yielding the coefficient of self-diffusion (Hirschfelder et al. 1964, p. 539). This result is used in the case study of denitrification where nitrogen originating from denitrification is distinguished from atmospheric nitrogen.

Table 1 shows the fair agreement between binary diffusion coefficients calculated from Eqs. (4) through (6) and those calculated by an empirical equation given by Marrero and Mason (1972)

$$\ln(pD_{ij}) = \ln a + b \ln T - c/T \quad (7)$$

Equation (7) is to be used at reduced temperatures above unity. The calculations have been performed at 10 and 20°C for gas pairs that are of interest to soil research. Uncertainty limits given pertain to results of the empirical equation. The last column in Table 1 presents the percentages of deviation of results obtained by Eqs. (4) through (6) with respect to those of Eq. (7) at 10°C; deviations at 20°C are of the same magnitude and are therefore not given. The theoretical values stay within the uncertainty

MULTINARY DIFFUSION PROBLEMS

TABLE 1

Comparison of binary diffusion coefficients obtained from theory with those estimated from regression analysis of experimental data for a number of gas pairs

Gas pair*	Binary diffusion coefficients $D_{ij} \times 10^4 \text{ m}^2 \text{ s}^{-1}$				Uncertainty limits, ^b %	Deviations of results of Eqs. (4) through (6) from those of Eq. (7) at 10°C, %		
	After Hirschfelder et al. (1964) (Eqs. (4) through (6))		After Marrero and Mason (1972) (Eq. (7))					
	10°C	20°C	10°C	20°C				
Ar-CH ₄	0.1909	0.2034	0.1865	0.1985	3	2.4		
Ar-N ₂	0.1763	0.1875	0.1785	0.1897	2	-1.2		
Ar-O ₂	0.1765	0.1879	0.1763	0.1872	3	0.1		
Ar-air	0.1762	0.1876	0.1781	0.1892	3	-1.1		
Ar-CO ₂	0.1272	0.1357	0.1379	0.1476	3	-7.8		
CH ₄ -N ₂	0.1976	0.2103	0.1953	0.2075	3	1.2		
CH ₄ -O ₂	0.1997	0.2128	0.2057	0.2193	3	-2.9		
CH ₄ -air	0.1980	0.2108	0.1977	0.2101	3	0.2		
N ₂ -O ₂	0.1867	0.1987	0.1905	0.2023	3	-2.0		
N ₂ -H ₂ O	0.2065	0.2208	0.2249	0.2417	4	-8.2		
N ₂ -CO ₂	0.1383	0.1473	0.1490	0.1596	2	-7.2		
O ₂ -H ₂ O	0.2079	0.2225	0.2273	0.2442	7	-8.5		
O ₂ -CO ₂	0.1369	0.1460	0.1484	0.1584	3	-7.7		
Air-H ₂ O	0.2067	0.2210	0.2249	0.2417	5	-8.1		
Air-CO ₂	0.1378	0.1469	0.1489	0.1593	3	-7.5		
H ₂ O-CO ₂	0.1461	0.1566	0.1482	0.1620	10	-1.4		
CO ₂ -N ₂ O	0.0982	0.1049	0.1056	0.1127	3	-7.0		
O ₂ -N ₂ O	0.1376	0.1468	-	-	-	-		
O ₂ -C ₂ H ₂	0.1472	0.1569	-	-	-	-		
N ₂ -N ₂ O	0.1391	0.1483	-	-	-	-		
N ₂ -C ₂ H ₂	0.1476	0.1573	-	-	-	-		
C ₂ H ₂ -CO ₂	0.1084	0.1159	-	-	-	-		
C ₂ H ₂ -N ₂ O	0.1082	0.1157	-	-	-	-		

* For the same sequence of gas pairs, Jaynes and Rogowski (1983) have listed the constants a , b , and c of Eq. (7).

^b Uncertainty limits for D_{ij} pertain to results calculated after Marrero and Mason (1972).

limits of the empirical values except for gas pairs involving CO₂ or H₂O, where deviations are larger by a factor of 2 to 3. Nevertheless, all deviations remain well within 10%. Furthermore, the temperature dependence of the reported binary diffusion coefficients in the trajectory 10 to 20°C amounts on the average to 6.7 and 6.9% for the theoretical and empirical values, respectively. The binary diffusion coefficients for the last six gas pairs in Table 1, needed in the case study of denitrification, were not reported by Marrero and Mason (1972).

As the force constants σ_{ii} and ϵ_{ii} are available for many gas molecules, applicability of the theoretical equations is very broad, compared with the experimental data given by Marrero and Mason (1972). Therefore, Eqs. (4) through (6) are used throughout this work.

The force constants and molecular weights for

a number of gases of interest to soil aeration research are listed in Table 2. Numerical values for the dimensionless collision integral are available through Hirschfelder et al. (1964), (Table I-M, pp. 1126-1127, column 1). Thus binary diffusion coefficients may be calculated for all combinations of the gases listed.

SIMPLIFICATION OF THEORY

The mathematics of multinary gas diffusion is rather complicated. Therefore, we have tried to simplify the mathematical description of diffusion by the following reasoning. Assume that gases in a mixture diffuse independently of each other and that each molar flux can be calculated by Fick's first law

$$N_i = -D_{iN_2} c \frac{dX_i}{dx} \quad (8)$$

TABLE 2
Molecular weights and force constants for calculating binary diffusion coefficients according to Eqs. (4) through (6)

Gas	Ne	Ar	Air	N ₂	O ₂	CO ₂
$M \times 10^3 \text{ kg mol}^{-1}$	20.17	39.95	28.97	28.01	32.00	44.01
$\sigma_a \times 10^{10} \text{ m}^a$	2.789	3.418	3.617	3.681	3.433	3.996
$\epsilon_{ii}/k \text{ K}^2$	35.7	124.0	97.0	91.5	113.0	190.0
Gas	CH ₄	C ₂ H ₂	N ₂ O	NH ₃	H ₂ O	
$M \times 10^3 \text{ kg mol}^{-1}$	16.04	26.04	44.01	17.03	18.02	
$\sigma_a \times 10^{10} \text{ m}^a$	3.822	4.221	3.879	3.15	2.71	
$\epsilon_{ii}/k \text{ K}^2$	137.0	185.0	220.0	358.0	506.0	

^a Except for NH₃ and H₂O, from Hirschfelder et al. (1964), pp. 1110-1112. NH₃ and H₂O from Monchick and Mason (1961), Tables 12 and 14, respectively.

The binary diffusion coefficients in Eq. (8) are related to nitrogen, because the main molecular interaction between the different gases will occur with this principal constituent of soil atmosphere. Different binary diffusion coefficients will give different gas fluxes at similar concentration gradients, in principle causing gradients in absolute pressure. However, gradients in absolute pressure in diffusing gas mixtures are usually immeasurably small (Marrero and Mason 1972), and the effect is that the total molar flow $\sum_{i=1}^v N_i$ is zero, thus maintaining isobaric conditions. But when N_i is computed according to Eq. (8) their sum is not zero. Therefore, the corrected flux $N_{i,\text{corr}}$ is computed as follows

$$N_{i,\text{corr}} = N_i - \left(\sum_{j=1}^v N_j \right) X_i \quad (9)$$

By the minus sign in Eq. (9) and the fact that $\sum_{i=1}^v X_i = 1$, the mass balance is maintained. A possible additional convective flux, N_{conv} , from gas production is added to this diffusive flux to obtain total flux $N_{i,\text{tot}}$.

$$N_{i,\text{tot}} = N_{i,\text{corr}} + N_{\text{conv}} X_i \quad (10)$$

In the simplified mathematical description of diffusion, Eqs. (8) through (10) in finite difference form replace Eq. (2) in the simulation model. This simplified theory is tested for the case study of denitrification.

MODEL TESTS

The correct implementation of the theory in the dynamic simulation model was ascertained by comparing its numerical results, obtained for particular sets of boundary conditions and at steady state, to corresponding analytical solutions. Steady-state analytical solutions to iso-

thermal, isobaric, ordinary diffusion problems for ternary idea-gas mixtures for one-phase systems in one dimension have been given by, among others, Toor (1957) and Hsu and Bird (1960). To give examples of importance for soil research, gas mixtures are composed of the following gases: O₂, N₂, CO₂, H₂O-vapor, N₂O, or C₂H₂.

Diffusion of H₂O-vapor through stagnant O₂ and N₂

When water vapor diffuses away from a water table through a sterile soil, the other gases, O₂ and N₂, experience an absorption barrier (Toor 1957) at the water table due to their low solubility in water. Hence, the water table is considered impermeable to oxygen and nitrogen. At the onset of diffusion of water vapor into initially dry O₂-N₂ atmosphere, these gases will be pushed upward by the water vapor, because the system remains isobaric. Fairbanks and Wilke (1950) measured the time course of such displaced volumes of gas mixtures at the end of a long tube from the bottom of which a liquid was allowed to evaporate upward. From these data they derived the diffusion coefficient of the vapor in the mixture. Eventually, equal molar amounts of water vapor will enter and leave the gas layer, while oxygen and nitrogen are stagnant.

The molar water vapor flux into the first layer adjacent to the water table is calculated according to

$$N_1 = (\Delta c_1 / \Delta x) / \left(- \sum_{j=1}^v (\bar{c}_j / (\bar{c} \bar{D}_{1j})) \right) \quad (11)$$

This equation is obtained from Eq. (2) if the oxygen and nitrogen fluxes equal zero. The gra-

MULTINARY DIFFUSION PROBLEMS

dients of oxygen ($i = 2$) and nitrogen ($i = 3$) in that layer may be calculated from $\Delta c_i / \Delta x = N_i \dot{c}_i / (\dot{c} \bar{D}_{ii})$. Through the remaining part of the gas layer all gases can diffuse freely, but as the system will remain isobaric, the sum of the molar fluxes through all interfaces should equal the molar water vapor flux through the bottom of the gas layer. Thus, the additional equation necessary to solve Eq. (2) at each layer interface, except the first one, becomes $\sum_{i=1}^3 N_i = N_1$. This is attained in the model by replacing the first row in the matrix of coefficients by 1s and the corresponding right-hand-side element by N_1 from Eq. (11).

The analytical solution with respect to the steady-state molar water vapor flux, N_1 , is implicitly given in

$$X_2^0 = \left[1 - \frac{1}{r} \left(\frac{\exp(\alpha_{12}r) - 1}{\exp(\alpha_{12}r) - Q} \right) \left(\frac{\exp(\alpha_{12} - Q)}{\exp(\alpha_{12} - 1)} \right) \right]^{-1} \quad (12)$$

(Hsu and Bird 1960), where $\alpha_{12} = N_1 \delta / (cD_{12})$, $r = D_{12}/D_{13}$, $Q = (1 - X_{1s})/(1 - X_{10})$, and X_2^0 is the average mole-fraction of gas 2, oxygen, before any water vapor has diffused into the gas layer. Equation (12) was solved for N_1 by an iterative procedure using as a first guess the steady-state flux from the simulation model. The analytical solution with respect to the steady-state mole-fraction profiles of the stagnant gases oxygen, $i = 2$, and nitrogen, $i = 3$, are obtained through integration of the Stefan-Maxwell equations $dX_i/dx = (N_i/(cD_{ii})) X_i$, subject to the boundary condition $X_i = X_i^0$ at $x = \delta$, yielding

$$X_i = X_i^0 \exp[N_1(x - \delta)/(cD_{ii})] \quad (13)$$

Equation (13) shows that the mole-fraction profiles decrease exponentially from the top, $x = \delta$, to the bottom, $x = 0$, of the gas layer.

The molar water vapor flux and mole-fraction profiles obtained by simulation after about 300 s, and analytically by Eqs. (12) and (13), are reported in Table 3 for the following conditions: 293K, 1 atm, $X_{10} = 2.3094 \times 10^{-2}$, $X_{1s} = 0.0$, $X_2^0 = X_{2s} = 0.2$, $X_3^0 = X_{3s} = 0.8$, $D_{12} = 2.2251 \times 10^{-5} \text{ m}^2 \text{ s}^{-1}$, $D_{13} = 2.2082 \times 10^{-5} \text{ m}^2 \text{ s}^{-1}$, $c = 41.5696 \text{ mol m}^{-3}$, $\delta = 0.05 \text{ m}$. The binary diffusion coefficients between water vapor and oxygen and between water vapor and nitrogen, respectively, are almost equal, making the analytical solutions of Eqs. (12) and (13) sensitive to slight changes in the input parameters. Table 3 shows that results of the mole-fraction profiles and the molar water vapor flux as calculated by the simulation model and the analytical solution, respectively, do not differ more than 0.1%. Note that although O_2 and N_2 possess concentration gradients, they are stagnant. This result indicates that if concentration profiles are used to predict fluxes, the interpretation of results in terms of Fick's first law would not be correct. As a consequence, calculations of gas fluxes from measured oxygen concentration profiles by means of Fick's first law, and soil respiration rates from the differences between these fluxes at different depths in soil as proposed by de Jong and Schappert (1972) for carbon dioxide, would result in overestimates of soil activity. To give an order of magnitude, oxygen consumption was calculated from the steady-state profile given in Table 3 as $3.5 \times 10^{-5} \text{ mol O}_2 \text{ m}^{-3} \text{ s}^{-1}$ using the binary diffusion coefficient between oxygen and nitrogen from Table 1. This value may be compared to respiration figures of de Jong and

TABLE 3

Comparison between model results and analytical results with respect to the steady-state mole-fraction profiles and the molar water vapor flux, respectively

Relative height in gas layer x/δ	Simulation model		Analytical solution	
	O_2	N_2	O_2	N_2
0.95	0.199768	0.799064	0.199768	0.799065
0.65	0.198379	0.793468	0.198381	0.793475
0.35	0.197000	0.78791	0.197004	0.78792
0.05	0.195631	0.78239	0.195636	0.78241
$\text{mol m}^{-2} \text{ s}^{-1}$				
Molar water vapor flux	0.4301×10^{-3}		0.4296×10^{-3}	

Schappert based on carbon dioxide profiles. The average value read from their Fig. 3 is about 1×10^{-5} mol $\text{CO}_2 \text{ m}^{-3} \text{ s}^{-1}$. Thus the evaporating water already causes an oxygen profile that suggests a respiration rate much greater than that found in practice.

Equimolar counterdiffusion through a stagnant third gas

When steady-state conditions prevail in soil with respect to the exchange of carbon dioxide ($i = 1$) and oxygen ($i = 2$) with the atmosphere, the third gas, nitrogen ($i = 3$), is stagnant when Eqs. (14) and (15) are simultaneously satisfied (Toor 1957).

$$N_1 = -N_2 = \frac{1}{\left(\frac{1}{D_{13}} - \frac{1}{D_{23}}\right)} \frac{p}{RTx} \ln \left(\frac{X_{36}}{X_{30}} \right) \quad (14)$$

$$\left(1 - \frac{D_{12}}{D_{23}}\right) (X_{10} - X_{1s}) + \left(1 - \frac{D_{12}}{D_{13}}\right) (X_{20} - X_{2s}) = \ln \left(\frac{X_{36}}{X_{30}} \right) \quad (15)$$

Equation (14) gives the molar fluxes N_i of components CO_2 ($i = 1$) and O_2 ($i = 2$) when the molar nitrogen flux ($i = 3$) equals 0, but $N_3 = 0$ only when the mole fractions are related so as to satisfy Eq. (15). For a numerical evaluation of Eq. (15) the mole fractions of carbon dioxide, oxygen, and nitrogen at the surface of the gas layer, i.e., at $x = \delta$, are set equal to 0.0, 0.2, and 0.8, respectively, and at depth $x = 0$ the mole fraction of carbon dioxide is set equal to 0.1. The binary diffusion coefficients for the relevant gas pairs, as obtained from the theoretical equations at 20°C , are taken from Table 1. The mole fraction of nitrogen at depth $x = 0$, X_{30} , may be expressed as $1 - X_{10} - X_{20}$. Subsequently, Eq. (15) may be solved by an iterative procedure, because the mole fraction of oxygen at $x = 0$, X_{20} , is the only unknown left. For this example it is found that $X_{20} = 0.1204$, and $X_{30} = 0.7796$. The diffusion fluxes of carbon dioxide and oxygen can now be calculated from Eq. (14). At atmospheric pressure, a temperature of 20°C , and a layer thickness of 0.05 m, this yields $N_1 = -N_2 = 0.12236 \text{ mol m}^{-2} \text{ s}^{-1}$. In this example all gases can diffuse freely through the gas layer, while the sum of the molar fluxes equals zero

$$\sum_{i=1}^v N_i = 0$$

To compare the performance of the simulation model with the analytical solution, Eq. (2) was solved using this additional equation by replacing the first row in the matrix of coefficients by 1s and the corresponding right-hand side by 0. The model was run with the above-mentioned conditions.

The molar flux established for carbon dioxide was $N_1 = 0.12226 \text{ mol m}^{-2} \text{ s}^{-1}$, which is but 0.08% lower than the analytical result. By this time, (after about 300 s) the flux of molecular nitrogen was about $10^{-9} \text{ mol m}^{-2} \text{ s}^{-1}$. Nevertheless, this gas shows a concentration gradient of 17 mol m^{-4} . Interpretation of this concentration gradient in terms of Fick's first law would cause a flux of $-0.25 \text{ mol m}^{-2} \text{ s}^{-1}$ when the binary diffusion coefficient of the gas pair nitrogen-carbon dioxide is used. Nitrogen experiences a so-called diffusion barrier (Toor 1957), indicating that the resistance of the gas layer to the transfer of nitrogen is infinite.

A third example (data not reported), where oxygen diffuses through the gas layer to form carbon dioxide at $x = 0$, while nitrogen is stagnant after some time, also compared well to the appropriate analytical solution given by Hsu and Bird (1960).

From the good agreement between numerical and analytical solutions and the fact that the method of solving Eq. (2) is identical when more than three components are involved, it is concluded that the model can be used to study the dynamic behavior of more complex systems for which no analytical solutions are available.

DENITRIFICATION; A CASE STUDY

During denitrification nitrate serves as an electron acceptor for microorganisms at low oxygen concentrations, with the result that the gases N_2O and N_2 can be produced (Delwiche 1981). Direct field estimation of N_2 emission is difficult because of the large concentration of N_2 in the atmosphere. However, acetylene (C_2H_2) inhibits the reduction of nitrous oxide to molecular nitrogen (Yoshinari et al. 1977). Therefore, estimates of nitrogen losses from soil can be obtained by measuring nitrous oxide, while acetylene is supplied to the soil atmosphere through probes inserted into soil (Ryden et al. 1979). From these probes acetylene has to diffuse through the macropore space and from there into the soil crumbs where denitrification is expected to occur (Leffelaar 1979; Smith 1980).

MULTINARY DIFFUSION PROBLEMS

The major question of interest in this case study is whether calculations of gas diffusion according to the Stefan-Maxwell equations yield significantly different results for respiration and denitrification compared with Fick's law. To assess this difference, acetylene is chosen as a measure because its dynamic behavior can also be calculated by an analytical solution (Crank 1975). As production of gases causes convection (Stolzy and Flühler 1978), acetylene will be pushed away from the sites where denitrification takes place. Therefore, subquestions of interest are: (1) can effective concentrations of acetylene be reached at locations in soil where denitrification takes place to inhibit the conversion of nitrous oxide to molecular nitrogen, without severely disturbing the soil atmosphere?; if so (2) what time does it take to reach such effective concentrations compared with estimates based on Fick's law?; and (3) what overall gas movement takes place in the profile due to net production of gases?

To investigate these questions the following system is studied. A soil layer 0.25 m thick and having linear geometry as depicted in Fig. 1 is subdivided into 10 equal layers. The soil surface, i.e., at $x = \delta$, is continuously supplied with a mixture of air and 2% of acetylene, while gaseous products of denitrification, nitrous oxide and molecular nitrogen, released from soil are continuously removed. Thus the gas composition at the soil surface for O_2 , CO_2 , N_2 from the atmosphere (subsequently called N_2^{at}), C_2H_2 added, N_2O , and N_2 from denitrification is 20.0, 0.03, 77.97, 2.0, 0.0, and 0.0%, respectively. As a first approximation biological activity is located in the deepest sublayer, i.e., layer 1. Below this layer soil is impermeable to gases. The overlaying nine inert sublayers serve as a resistance to diffusion. The production terms (P_i) in layer 1 are defined by Eqs. (16) through (22)

$$P_{O_2} = -k_1 r_{O_2} \quad (16)$$

$$P_{CO_2} = -P_{O_2} + k_2 c_{NO_3} (1 - r_{O_2}) \quad (17)$$

$$P_{N_2^{at}} = 0.0 \quad (18)$$

$$P_{C_2H_2} = 0.0 \quad (19)$$

$$P_{N_2O} = 0.5 k_3 c_{NO_3} (1 - r_{O_2}) - P_{N_2} \quad (20)$$

$$P_{N_2} = k_4 c_{N_2O} (1 - r_{O_2}) (1 - r_{C_2H_2}) \quad (21)$$

$$P_{NO_3} = -k_3 c_{NO_3} (1 - r_{O_2}) \quad (22)$$

where k_1 and k_2 , k_3 , k_4 are zeroth-order and first-

order rate constants, respectively. Rate-limiting concentrations of oxygen and acetylene may occur. This is introduced in the equations by r_i , where i refers to either oxygen or acetylene. It is assumed that r_i is a linear function of gas concentration between a lower, l_i , and a higher, h_i , limit, as depicted in Fig. 3. When nitrate is present and $l_{O_2} < c_{O_2} < h_{O_2}$, both aerobic respiration and denitrification occur. Increasing denitrification activity with decreasing oxygen tension in continuous culture studies of *Hyphomicrobium X* was reported by Meiberg et al. (1980). When $k_{C_2H_2} < c_{C_2H_2} < h_{C_2H_2}$, the conversion of nitrous oxide to molecular nitrogen, Eq. (21), is partially inhibited. Partial inhibition of nitrous oxide reduction below 1% of acetylene in anaerobic moist soil was reported by Yoshinari et al. (1977). When $c_{O_2} > h_{O_2}$, r_{O_2} equals unity, and equimolar respiration takes place as shown by Eqs. (16) and (17).

Molecular nitrogen occurs both as the gas produced by denitrification, Eq. (21), and as atmospheric nitrogen. These gases with different origins are separately followed in the model. The additional equation to solve Eq. (2) at each sublayer interface except the first one is

$$\sum_{i=1}^n N_i = N_1$$

where N_1 is calculated from the net specific production rate ($\text{mol m}^{-3} \text{ s}^{-1}$), as obtained by the sum of P_i of Eqs. (16) through (21) times the volume of the biologically active layer and divided by the surface area between layers 1 and 2.

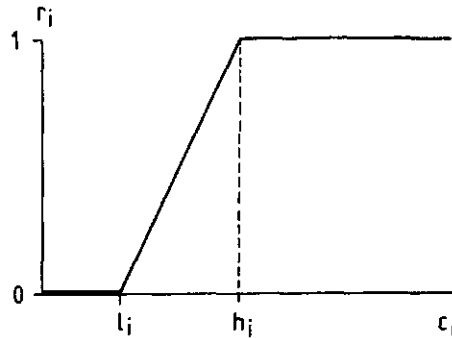


FIG. 3. General relationship between reduction factor and gas concentration. For numerical values of l_i and h_i see text.

Model parameters

The zeroth-order rate constant $k_1 = 3.95 \cdot 10^{-4}$ mol O₂ m⁻³ s⁻¹ is based on work by Greenwood and Goodman (1964). These authors also indicated that respiration remains constant down to low values of oxygen concentration, thus supporting the assumption of a zeroth-order process. The first-order rate constant k_3 in Eq. (22) equals $6.53 \cdot 10^{-6}$ s⁻¹. This value is derived from Avnimelech (1971), who reported nitrate disappearance as a function of initial concentration and temperature under conditions favorable for denitrification. Following Eq. (1) from Yoshinari et al. (1977), the reduction of 1 mole of nitrate will result in the production of 1 mole of carbon dioxide and 0.5 mole of nitrous oxide. Therefore k_2 in Eq. (17) is taken equal to k_3 , and k_3 in Eq. (20) is multiplied by 0.5. Also, as a first approximation, rate constant k_4 is taken equal to k_3 . The initial amount of nitrate is 88.6 g NO₃⁻ m⁻² (200 kg NO₃⁻-N ha⁻¹) located in the deepest soil layer. Nitrate is assumed to be effectively depleted when 0.5% of the initial amount is left. The lower and upper values of the concentrations of oxygen and acetylene in Fig. 3 are taken equivalent to 0.1 and 1.0%, respectively. The gas fluxes defined in Eqs. (16) through (21) refer to the surface area of soil as a whole. To satisfy these fluxes at a gas-filled porosity of ϵ , the fluxes inside the pores must be approximately $\epsilon^{(4/3)}$ times as large (Millington 1959), where the factor 4/3 combines both area reduction and tortuosity. To incorporate this effect on gas fluxes for $\epsilon = 0.05$, the rate constants k_1 , k_2 , and k_4 were set higher by a factor of 50. Rate constant k_3 was also multiplied by 50 to reduce computer time by increasing the nitrate depletion rate.

Results and discussion of case study

Figure 4 depicts the dynamics of the relative mole fraction of each gas and the relative convective flow in the biologically active deepest sublayer, i.e., layer 1. Absolute values of mole fraction or convective flow may be calculated from the curves by multiplying a specific value by its maximum, also given in Fig. 4. The arrow in Fig. 4 separates two periods. In the first period O₂, CO₂, N₂^{at} and added C₂H₂ diffuse in the soil layer, while oxygen and carbon dioxide are involved in equimolar respiration. In the second period the oxygen concentration is smaller than 1% and denitrification occurs. Nitrous oxide and

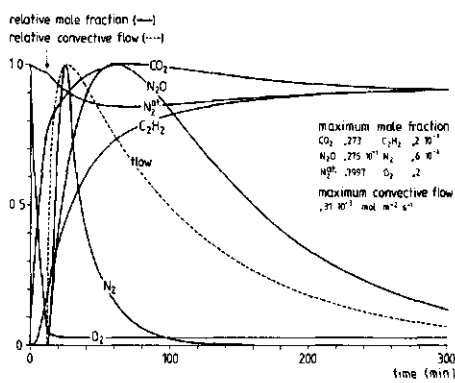


FIG. 4. Relative mole fractions of O₂, CO₂, N₂^{at}, C₂H₂, N₂O, and N₂ (full lines) in sublayer 1 and relative convective flow (dashed line) through gas layer as a function of time.

molecular nitrogen are formed and cause a gas flow away from the active layer, because below this layer soil is impermeable. The influence of this convective flow on acetylene diffusion was evaluated by comparing its time course to results obtained by Eq. (4.17) of Crank (1975) (data not shown) using $D_{C_2H_2-N_2}$ from Table 1. This reveals that at the time of maximum convective flow the relative mole fraction of the simulated curve is about 14% lower. Furthermore, it takes 12% longer to reach the level of 1% acetylene. After the time of maximum convective flow, Crank's equation diverges strongly from the simulated result. At about 100 min a relative mole fraction of 0.97 is calculated, while in fact acetylene is seen to stabilize at about 0.9 at the end of the simulated period. Molecular nitrogen of atmospheric origin is partially removed from the soil profile. A maximum of 9% of the nitrogen initially present is removed at the time of the minimum in the N₂^{at} curve. After this time the profile is partially replenished with atmospheric nitrogen. The time of occurrence of the minimum in the N₂^{at} curve does not coincide with the time of maximum convective flow. However, the minimum in the N₂^{at} curve coincides with the maxima in the CO₂ and N₂O curves. This implies that the overall movement of N₂^{at} is not mainly determined by convective flow, but rather by the accumulation of gases as CO₂ and N₂O. The fact that both N₂^{at} and C₂H₂ do not reach their atmospheric values in the long run may also be explained by the accumulation of CO₂ in the profile, as convective flow

MULTINARY DIFFUSION PROBLEMS

has become negligible by then. At the onset of denitrification the relative mole fractions of N_2O and N_2 increase rapidly. N_2 is hardly formed as the level of 1% of C_2H_2 is quickly reached. Therefore, mainly N_2O is formed. Observe that the maximum mole fraction of nitrous oxide appears much later than the maximum convective flow. As nitrous oxide is the principle cause of convective flow, both maxima would be expected to coincide. This result demonstrates the complex behavior of gas mixtures with mutually dependent diffusion fluxes and convective flow due to source/sink terms.

The questions stated earlier can now be answered. (1) Effective concentrations of acetylene may be reached in soil to inhibit the conversion of nitrous oxide into molecular nitrogen without severely disturbing the soil atmosphere. (2) The time to reach this concentration is about 12% longer compared with the usual calculations, e.g., Eq. (4.17) of Crank (1975). (3) Overall gas movement due to gas production and accumulation of gases as carbon dioxide and nitrous oxide amount to a maximum of 10% for atmospheric nitrogen. These figures show that acetylene diffusion is not seriously affected by describing the diffusion process by the Stefan-Maxwell equations.

The case study of denitrification was also used to test the simplified theory of gas diffusion as summarized in Eqs. (8) through (10). Results (data not reported) are very similar to those of the rigorous theory. The largest difference was found for the maximum nitrous oxide concentration, which was 8% lower, compared with the rigorous theory. This remarkable agreement may be ascribed to the similarity of binary diffusion coefficients, which do not differ by more than a factor of 2. As a result, the correction term in Eq. (9) will be small compared with the concentration diffusion term, i.e., Eq. (8). This reasoning is supported by the fact that, for the limiting case of equal binary diffusion coefficients, both Eq. (2) and Eq. (9) reduce to Eq. (8). However, when diffusion of gases in multinary gas mixtures with largely different binary diffusion coefficients is to be investigated, the Stefan-Maxwell equations must be used.

CONCLUSIONS

1. The simulation model presented enables us to study the integral dynamics of diffusion processes in soil atmosphere.

2. Gas profiles showing concentration gradients may be stagnant for some components. Interpretation of such profiles in terms of calculations of gas fluxes at different depths and production terms from the differences between these gas fluxes would wrongly suggest nonzero production terms.

3. Denitrification is only slightly affected when the influence of a diffusion resistance on this process is calculated according to the Stefan-Maxwell equations, compared with Fick's law.

4. The Stefan-Maxwell equations as implemented in the simulation model must be used to study the dynamic behavior of gas mixtures whenever binary diffusion coefficients differ by more than a factor of 2.

5. Simplified theory gives satisfactory results when binary diffusion coefficients do not differ by more than a factor of 2 and when one constituent of the gas phase is abundantly present, so that binary diffusion coefficients may be related to this component.

SUMMARY

Results of a dynamic simulation model describing diffusion of gases in multinary gas mixtures agree well with analytical steady-state solutions for ternary diffusion. This confirms the correct implementation of diffusion theory in the simulation model. Subsequently, the model has been used to calculate the dynamic behavior of a gas system in which denitrification takes place. Acetylene is taken as a measure of whether or not denitrification is significantly affected by describing the diffusion process by the Stefan-Maxwell equations, compared with an analytical solution to Fick's law. The case study then shows that denitrification is not significantly affected. The same case study is used to show that multinary diffusion can be well approximated by Fick's first law when modified to maintain isobaric conditions. In general, the simulation model based on the Stefan-Maxwell equations must be used to study the dynamic behavior of gas mixtures. However, simplified theory will give satisfactory results when binary diffusion coefficients do not differ by more than a factor of 2, a condition usually met in the gas phase of soil.

The model is useful to gain insight into:

1. the dynamics of diffusion in complex gas systems containing sink/source terms

LEFFELAAR

2. the length of time to attain, if possible, a steady-state situation

3. the order of magnitude of the gas fluxes through the profile

The computer program may be adapted easily to incorporate other kinetics of gas conversions, number of gases, and number of layers. The model will form part of an extended model including water flow and biological denitrification. This extended model should provide a means for calculating denitrification in soil aggregates not saturated with water and will be subject to integral verification by specially designed experiments.

NOTE

A listing of the computer program that produced these results is available from the author.

ACKNOWLEDGMENTS

I wish to express my appreciation to Prof. J. Schenk and Prof. H. J. Merk (Technical University of Delft) for stimulating discussions in the early stages of this work and to Prof. C. T. de Wit, Dr. J. Goudriaan, and Prof. G. H. Bolt for reviewing the manuscript.

LIST OF SYMBOLS

Symbol	Meaning	Unit
a, b, c	empirical constants in Eq. (7)	
a		$\text{Pa m}^2 \text{s}^{-1} (\text{K}^b)^{-1}$
c		K
c_i, c	molar concentration of component i and all components together, $c_i = \rho_i/M_i$	mol m^{-3}
	$c = \sum_{i=1}^v c_i$	
$c_{L,i}$	molar concentration of component i in layer L	mol m^{-3}
D_{ij}	binary diffusion coefficient for gas pair $i - j$	$\text{m}^2 \text{s}^{-1}$
k	Boltzmann constant, $k = R/N = 1.3806 \cdot 10^{-23}$	J K^{-1}
k_1, k_2, k_3, k_4	zeroth-order rate constant first-order rate constants lower and upper gas concentration limits where reduction factor r_i becomes 0 and 1, respectively	$\text{mol m}^{-3} \text{s}^{-1}$
l_i, h_i		mol m^{-3}
L	layer number	
M_i	molecular weight of component i , $M_i = \rho_i/c_i$	kg mol^{-1}
n_i, n	molecular concentration or number density of component i and all components together	m^{-3}
	$n_i = c_i \bar{N}$	
	$n = \sum_{i=1}^v n_i$	
N_i	molar flux of component i	$\text{mol m}^{-2} \text{s}^{-1}$
$N_{L,i}$	molar flux of component i in layer L	$\text{mol m}^{-2} \text{s}^{-1}$
\bar{N}	Avogadro's number, $\bar{N} = 6.0225 \cdot 10^{23}$	mol^{-1}
NL	maximum number of layers	
p	pressure	Pa
P_i	production term of gas i	$\text{mol m}^{-3} \text{s}^{-1}$
Q	ratio of total mole fraction of nonmoving components at $x = \delta$ and $x = 0$ of gas layer	
	$Q = (1 - X_{12})/(1 - X_{10})$	
r	ratio of diffusion coefficients, $r = D_{12}/D_{13}$	
r_i	reduction factor for component i	
R	gas constant, $R = 8.3142$	$\text{Pa m}^3 \text{mol}^{-1} \text{K}^{-1}$
t	time	s
T	absolute temperature	K
T_{ij}	reduced temperature, $T_{ij} = kT/\epsilon_{ij}$	
v	number of components	
v_0	mass average velocity of mixture with respect to stationary coordinates	m s^{-1}
	$v_0 = \left(\sum_{i=1}^v \rho_i \bar{v}_i \right) / \left(\sum_{i=1}^v \rho_i \right)$	
\bar{v}_i	velocity of component i with respect to stationary coordinates, $\bar{v}_i = \bar{N}/c_i$	m s^{-1}
∇_i	diffusion velocity of component i with respect to the mass average velocity of the mixture, $\nabla_i = \bar{v}_i - v_0$	m s^{-1}
x	distance between centers of layers or space coordinate	m
X_i, X_{10}, X_{12}	mole fraction of component i in general and at $x = 0$ and $x = \delta$ of gas layer, respectively	
X_i^0	mole fraction of component i when no moving gas is present	
α_{12}	dimensionless quantity, $\alpha_{12} = N_{12}/(c D_{12})$	
δ	total thickness of gas layer	m
Δ	finite difference of concerning symbol with respect to layers L and $L - 1$	
ϵ	gas-filled porosity	
$\epsilon_{ij}, \epsilon_{ij}$	Lennard-Jones potential parameter; maximum energy of attraction between like molecules of component i and between unlike molecules of components i and j	J
ρ_i, ρ	mass concentration of component i and all components together, $\rho_i = c_i M_i$	kg m^{-3}
	$\rho = \sum_{i=1}^v \rho_i$	
σ_{ij}, σ_{ij}	Lennard-Jones potential parameter; collision diameter for like molecules of component i and for unlike molecules of components i and j	m

MULTINARY DIFFUSION PROBLEMS

Σ_{i_1}	summation operator	J. A. S. Adams and W. M. Lowder (eds.). Univ. of Chicago Press, Chicago, pp. 191-215.
	dimensionless collision integral based on the Lennard-Jones intermolecular potential field	La Fara, R. L. 1973. Computer methods for science and engineering. Hayden, Rochelle Park, N.J.
	superscript; arithmetic spatial average of concerning symbol with respect to the layers L and $L - 1$	Leffelaar, P. A. 1979. Simulation of partial anaerobiosis in a model soil in respect to denitrification. <i>Soil Sci.</i> 128:110-120.
		Marrero, T. R., and E. A. Mason. 1972. Gaseous diffusion coefficients. <i>J. Phys. Chem. Ref. Data</i> 1:3-118.
		Mason, E. A., and L. Monchick. 1962. Transport properties of polar-gas mixtures. <i>J. Chem. Phys.</i> 36:2746-2757.
		Meiberg, J. B. M., P. M. Bruinenberg, and W. Harder. 1980. Effect of dissolved oxygen tension on the metabolism of methylated amines in <i>Hyphomicrobium X</i> in the absence and presence of nitrate: Evidence for "aerobic" denitrification. <i>J. Gen. Microbiol.</i> 120:453-463.
		Millington, R. J. 1959. Gas diffusion in porous media. <i>Science</i> 130:100-102.
		Monchick, L., and E. A. Mason. 1961. Transport properties of polar gases. <i>J. Chem. Phys.</i> 35:1676-1697.
		Ryden, J. C., L. J. Lund, J. Letey, and D. D. Focht. 1979. Direct measurement of denitrification loss from soils: 2. Development and application of field methods. <i>Soil Sci. Soc. Am. J.</i> 43:110-118.
		Smith, K. A. 1980. A model of the extent of anaerobic zones in aggregated soils, and its potential application to estimates of denitrification. <i>J. Soil Sci.</i> 31:263-277.
		Stolzy, L. H., and H. Flühler. 1978. Measurement and prediction of anaerobiosis in soils. In <i>Nitrogen in the environment</i> , vol. 1. D. R. Nielsen and J. G. MacDonald (eds.). Academic Press, New York, pp. 363-426.
		Toor, H. L. 1957. Diffusion in three component gas mixtures. <i>Appl. Ind. Chem. Eng. J.</i> 3:198-207.
		Wakao, N., S. Otani, and J. M. Smith. 1965. Significance of pressure gradients in porous materials: 1. Diffusion and flow in fine capillaries. <i>Appl. Ind. Chem. Eng. J.</i> 11:435-439.
		Wakao, N., and J. M. Smith. 1962. Diffusion in catalyst pellets. <i>Chem. Eng. Sci.</i> 17:825-834.
		Wilke, C. R. 1950. Diffusional properties of multicomponent gases. <i>Chem. Eng. Prog.</i> 46:95-104.
		Wit, C. T. de, and H. van Keulen. 1975. Simulation of transport processes in soils. <i>Simulation Monographs</i> , PUDOC, Wageningen, the Netherlands.
		Wood, J. T., and D. J. Greenwood. 1971. Distribution of carbon dioxide and oxygen in the gas phase of aerobic soils. <i>J. Soil Sci.</i> 22:280-288.
		Yoshinari, T., R. Hynes, and R. Knowles. 1977. Acetylene inhibition of nitrous oxide reduction and measurement of denitrification and nitrogen fixation in soil. <i>Soil Biol. Biochem.</i> 9:177-183.

REFERENCES

Avnimelech, Y. 1971. Nitrate transformation in peat. *Soil Sci.* 111:113-118.

Crank, J. 1975. The mathematics of diffusion, 2nd ed. Oxford Univ. Press.

Cunningham, R. E., and R. J. J. Williams. 1980. Diffusion in gases and porous media. Plenum, New York.

Delwiche, C. C. (ed.). 1981. Denitrification, nitrification, and atmospheric nitrous oxide. Wiley, New York.

Fairbanks, D. F., and C. R. Wilke. 1950. Diffusion coefficients in multicomponent gas mixtures. *Ind. Eng. Chem.* 42:471-475.

Flühler, H., and H. P. Läser. 1975. A hydrophobic membrane probe for total pressure and partial pressure measurements in the soil atmosphere. *Soil Sci.* 120:85-91.

Frissel, M. J., and P. Reiniger. 1974. Simulation of accumulation and leaching in soils. *Simulation Monographs*, PUDOC, Wageningen, the Netherlands.

Greenwood, D. J., and D. Goodman. 1964. Oxygen diffusion and aerobic respiration in soil spheres. *J. Sci. Food Agric.* 15:579-588.

Hirschfelder, J. O., C. F. Curtiss, and R. B. Bird. 1964. Molecular theory of gases and liquids. Wiley, New York.

Hsu, H. W., and R. B. Bird. 1960. Multicomponent diffusion problems. *Appl. Ind. Chem. Eng. J.* 6:516-524.

IBM Corp. 1975. Continuous system modeling program III (CSMP III). Program reference manual. SH 19-7001-3. Data Processing Division, 1133 Westchester Ave., White Plains, N.Y.

Jaynes, D. B., and A. S. Rogowski. 1983. Applicability of Fick's law to gas diffusion. *Soil Sci. Soc. Am. J.* 47:425-430.

Jong, E. de, and H. J. V. Schappert. 1972. Calculation of soil respiration and activity from CO_2 profiles in the soil. *Soil Sci.* 113:328-333.

Koorevaar, P., G. Menelik, and C. Dirksen. 1983. Elements of soil physics. Developments in Soil Science, 13. Elsevier, Amsterdam.

Kraner, H. W., G. L. Schroeder, and R. D. Evans. 1964. Measurement of the effects of atmospheric variables on radon-222 flux and soil-gas concentrations. In *The natural radiation environment*.

CHAPTER 5

DENITRIFICATION IN A HOMOGENEOUS, CLOSED SYSTEM: EXPERIMENT AND SIMULATION

P.A. LEFFELAAR ¹ and W. WESSEL ²

A simulation model describing microbial respiration and denitrification was developed for a homogeneous (i.e. spatially uniform in all phases) soil layer, in which no transport processes occurred. Major processes included were growth and maintenance of biomass at the expense of glucose carbon, and the concomitant reduction of nitrate to molecular nitrogen, via the intermediates nitrite and nitrous oxide. Growth of biomass was calculated by a first order rate equation, in which the relative growth rate was described by a double Monod equation consisting of rate limiting factors for carbon and nitrogenous substrates. The Pirt equation was used to calculate the consumption rates of substrates.

As a starting point to parameterize the model, a data set was compiled from various literature sources, and it was investigated whether it would be possible to simulate experimental observations of the sequence of denitrification products by modifying some of these literature data within reasonable limits. It was concluded that the model has a reasonable structure, since the experiments reported in this paper and one from the literature could be simulated rather well.

The objective of this paper is to describe the model with the underlying assumptions, and to compare some of its results with experimental data.

Microbial denitrification refers to the process in which nitrate (NO_3^-), nitrite (NO_2^-), and nitrous oxide (N_2O) serve as electron acceptors for essentially aerobic bacteria at low oxygen concentrations, with the result that molecular nitrogen (N_2) can be produced (Delwiche 1981; Knowles 1982). In this reductive pathway, nitric oxide (NO) may occur as intermediate between NO_2^- and N_2O , but its existence has not been assessed unambiguously (Firestone 1982).

¹ Dept. of Theoretical Production Ecology (TPE), Bornsesteeg 65, 6708 PD Wageningen, The Netherlands.

² Former graduate student at TPE, present address: Laboratory of Physical Geography and Soil Science, Dapperstraat 115, 1093 BS, University of Amsterdam, Amsterdam, The Netherlands.

Experimental studies on denitrification comprise laboratory experiments using soil columns (e.g. Rolston and Marino 1976) and soil incubation flasks (Cooper and Smith 1963; Cho and Sakdinan 1978; Cho 1982; Lind 1980), and field experiments using different techniques (Hauck and Weaver 1986). Simulation studies on denitrification appear to have been confined largely to field soil models that integrate a number of physical processes with denitrification (Frissel and van Veen 1981; Tanji 1982). The evaluation of such models was then based on comparison with data obtained in field experiments. Thus, the comparison between experiment and the submodel of denitrification was indirect only: model results were the outcome of the combined submodels, rather than that of the denitrification submodel alone. It is, however, desirable that submodels are tested more rigorously (Tanji 1982). This applies particularly to denitrification, because even in a system without transport processes, the overall process is still governed by complex interactions between bacteria, carbon substrate (electron donors), electron acceptors, and oxygen status of soil. More rigorous model testing implies testing of the denitrification submodel by comparing its results directly with simple laboratory incubation studies cited earlier. Denitrification models for homogeneous soil systems without transports have been proposed by Betlach and Tiedje (1981) and Cho and Mills (1979). The former model was used to describe incubation experiments. The latter model was not compared with experimental data. The major drawback of both models is that they do not incorporate microbial growth, though microbial growth strongly influences the nitrogen transformation kinetics.

The objective of this paper is to describe a denitrification model including microbial growth, in a homogeneous (i.e. spatially uniform in all phases) soil, incorporating the reductive pathway of $\text{NO}_3^- \rightarrow \text{NO}_2^- \rightarrow \text{N}_2\text{O} \rightarrow \text{N}_2$, and to compare model results with experimental data reported in this paper and obtained from literature.

MATERIALS AND METHODS

Denitrification is but one of the many interrelated N-transformations that occur in soil (Stevenson 1982; Legg and Meisinger 1982). To limit attention to denitrification, therefore, it is most appropriate to exclude as many N-transformations from the system as possible, or at least minimize their influence on system behavior. Therefore, nitrogen inputs with rain, capillary rize, or with organic manure were excluded from the experiment. Roots were absent, thus root uptake of nitrogen and exudation of carbohydrates (Barber and Lynch 1977) were also excluded. Minimization of ammonium fixation, volatilization, and nitrification was attained by supplying the anoxic soil with potassium nitrate. Furthermore, it is probable that dissimilatory reduction of nitrate and nitrite with ammonium as the major end product occurs hardly, because very anaerobic conditions are needed for this conversion (Knowles 1982). The major processes that occur in the soil system are then: denitrification, nitrate assimilation by bacteria, mineralization, immobilization, and diffusion of gaseous denitrification products from soil into the head space of the incubation container (Letey et al. 1980^a; Cho 1982). In the

present system, minimization of the influence of this diffusive transport on gas concentrations in the head space was achieved using petri dishes (glass, internal diameter and height about 11 and 1.7 cm, respectively), since these permit the incubation of a thin (about 0.2 cm) soil layer that still contains enough material (about 20 g) for chemical analysis. Furthermore, the small container volume (about 160 ml) assured that small amounts of evolved gases yielded detectable concentrations in gas chromatographic analysis.

Soil

A loam soil from Herveld was taken from the upper 25 cm layer and stored under field moist conditions. Some characteristics are: pH (measured in 4 g of soil suspended in 10 ml of liquid) in H_2O and KCl: 7.3 and 6.9, respectively; CaCO_3 (Scheibler's method described by Allison and Moodie 1965): 2.5 %; organic carbon (Mebius 1960): 1.3 %; total nitrogen (Novozamsky et al. 1984): 0.14 %; CEC- BaCl_2 (Bascomb 1964): 22 cmol(+) per kg of soil and soil texture (pipette method described by Day 1965) $< 2\text{ }\mu\text{m}$, $< 20\text{ }\mu\text{m}$, and $< 50\text{ }\mu\text{m}$: 22, 42, and 61 %, respectively. Treatment of soil before use in the experiment has been described in Leffelaar (1986).

Soil container

Incubation vessels were constructed from petri dishes of which the rims were flattened by grinding. Pieces of window-pane equipped with septum caps (Subseal) served as cover. Leak-proof connections were attained by greased (Dow Corning vacuum grease) viton rubber rings (0.1 cm thick) placed between petri dish and cover.

Experimental procedure

About 23.5 g of soil with gravimetric moisture content of 0.22 g g^{-1} , was transferred to a petri dish. Two ml of a solution containing potassium nitrate (KNO_3) and glucose ($\text{C}_6\text{H}_{12}\text{O}_6$) was added and thoroughly mixed with a spatula. Concentrations were chosen to obtain C and N additions of about 520 and 175 mg kg^{-1} dry soil, respectively. Total initial N content of the soil was then about 315 mg kg^{-1} , because some endogenous nitrate-N was present. The incubation vessel was covered and air was replaced by neon (Ne) (Matheson Gas Products, Oevel, Belgium) by flushing through a needle pierced through the septum, while a second needle was installed to remove excess gas. Soil atmosphere was analysed for (traces of) oxygen (O_2), carbon dioxide (CO_2), N_2O , N_2 , and Ne by gas chromatography. Chemical analysis for NO_3^- , NO_2^- , and ammonium (NH_4^+) were performed at termination of incubation. All analytical procedures were described in Leffelaar (1986). Gas percentages were converted to mg of gas using the gas-filled volume of the incubation vessel and a correction for pressure build up due to the evolved gases. The correction was calculated as the ratio of the percentages of Ne at time zero and at sampling time. Treatments were duplicated. Experiments were done in a constant-temperature room ($22.7 \pm 1.5\text{ }^\circ\text{C}$).

DENITRIFICATION MODEL

Major processes that occur in the experimental system used to measure denitrification were given in the previous sections. In principle, these processes also occur in the model. A model, however, remains a simplified representation of a system (de Wit 1982), and numerous choices and assumptions have to be made during its development. The choices made with respect to the state variables included in the model, and with respect to the degree of detail of the description of their rates of change, are reflected in the differential equations, Eqs. (1) through (16), given in Table 1. All symbols are defined in Table 2. State variables distinguished are: bacteria (B), glucose carbon (C), CO_2 , O_2 , NO_3^- -N, NO_2^- -N, N_2O -N, N_2 -N, assimilated N (N_{ass}), mineralized carbon and nitrogen from dead biomass (C_{min} and N_{min}), and immobilized carbon and nitrogen in resistant organic matter (C_{imm} and N_{imm}). The equations in Table 1 show that the processes directly related to denitrification, i.e. growth of biomass, and consumption of electron acceptors, were calculated in a detailed fashion, while other processes like mineralization and immobilization of carbon and nitrogen were calculated more roughly. Furthermore, three main types of equations may be distinguished: first order rate equations for biomass, Eqs. (2, 3), double Monod equations for relative growth rates, Eq. (5), and the Pirt equation for substrate and electron acceptor consumption, Eqs. (6, 10). An account of the choices and assumptions made during the development of the model now follows on the basis of the differential equations.

Bacteria

Two groups of heterotrophic strictly aerobic bacteria are considered, i.e. bacteria that can only grow with oxygen as electron acceptor (further called strict aerobes), and bacteria that can grow with oxygen as electron acceptor under aerobic conditions or with nitrate, nitrite, and nitrous oxide as electron acceptor under anoxic conditions (further called denitrifiers). The number of microbial groups distinguished is kept small, because the model need be initiated for each group by quantitative data that are difficult to obtain (Focht and Verstraete 1977). Since denitrifiers usually form a portion of the total microbial population in soil (Focht and Verstraete 1977; Woldendorp 1981; Tiedje et al. 1982), however, the distinction of two groups represents the absolute minimum. The chemical composition of the bacteria, needed to calculate carbon nitrogen ratios (Eqs. 12, 14, 16), was set at $\text{C}_{6}\text{H}_{10.8}\text{N}_{1.5}\text{O}_{2.9}$, in accordance with data reported for Paracoccus denitrificans (van Verseveld and Stouthamer 1978). All bacteria are assumed to be active, and they are the only organisms that occupy the soil. The bacteria were homogeneously distributed in the model soil, and immobility of the organisms was assumed (Woldendorp 1981). Growth rates of both groups of bacteria are taken proportional to their respective amounts of biomass, Eq. (2), (van Veen and Frissel 1981; Schlegel 1972). Thus, it is assumed that the population densities of the bacteria never limit their growth, as would be presented by the logistic growth

equation (Schmidt et al. 1985). Low population densities with respect to the carrying capacity of the soil surface area (0.1-0.2 %) were reported by Woldendorp (1981). Relative growth rates depending on the concentrations of carbon and electron acceptor, were calculated by double Monod kinetics, Eq. (5), (Megee et al. 1972; Shah and Coulman 1978; Bader et al. 1975; Bader 1978). The double Monod model assumes that the reductant (C) and the oxidant (O_2 or one of the N-oxides) combine in the same organism. This assumption is based on the existence of different enzymes that catalyse the respective reductions within the same organism (Knowles 1982). Denitrifying enzymes were assumed to be already present or immediately induced after the onset of anaerobic conditions. This is supported by the relative short (1 to 10 hours) lag periods before denitrification started (Tiedje 1978; Smith and Tiedje 1979). Total simulation time lasted over 100 hours. The total relative growth rate of the denitrifiers under anaerobic conditions is simply calculated as the sum of the single relative growth rates, Eq. (4). Equation (5) also shows that independency of relative growth rates with different electron acceptors was assumed, and that competition between the two groups of bacteria took place via the common carbon substrate. When aerobic conditions prevail, both groups use oxygen as electron acceptor. Death rates of both groups of bacteria were taken proportional to their respective amounts of biomass, Eq. (3). Relative death rates were assumed constant and numerically equal to the product of maintenance coefficient and growth yield (Verstraete 1977). Cell decay is interpreted as lysis of the cell (Painter 1970). The products of the decay process are discussed in the section on mineralization.

Consumption of carbon substrate and electron acceptors

The consumption of carbon (glucose) is described by an equation by Pirt (1965, 1975), Eq. (6). The first term of this equation represents the use of substrate for cell synthesis and growth energy, whereas the second term represents the maintenance requirements of the organism for e.g. turnover of cell materials and osmotic work to maintain concentration gradients between the cell and the surroundings (Pirt 1975). The carbon substrate in the model serves both as carbon and energy source for the bacteria. Complete oxidation is assumed if it is used as energy source. Thus, carbon dioxide production can be calculated as the difference between the total amount of carbon consumed and the amount used for cell synthesis, Eq. (8). Calculations of the consumption of electron acceptors were also done with Pirt's equation, i.e. Eq. (10). The maintenance coefficients in Eq. (10), however, were multiplied with the relative presence of each electron acceptor in the water phase. This correction was introduced because the maintenance data derived from the literature for each reductive step suffice to maintain the whole of the biomass. Without the correction, therefore, the bacteria would consume too much electron acceptor for their maintenance.

Nitrate assimilation

Besides the use of nitrate in denitrification, also nitrate assimilation will

TABLE 1
Differential equations of the denitrification model

net growth of bacteria:	
$\frac{dB}{dt} = \left(\frac{dB}{dt} \right)_g - \left(\frac{dB}{dt} \right)_d$	(1)
$\left(\frac{dB}{dt} \right)_g = \mu B$	(2)
$\left(\frac{dB}{dt} \right)_d = m_c \gamma_c^{\max} B$	(3)
relative growth rates:	
$\mu = \sum_i \mu_{E_i}$ for $i = 2, 3, 4$	(4)
$\mu_{E_i} = \mu_{E_i}^{\max} \frac{[C]}{K_c + [C]} \frac{[E_i]}{K_{E_i} + [E_i]}$ $i = 1, 2, 3, 4$ refers to O_2, NO_3^-N, NO_2^-N , and N_2O-N , respectively	(5)
consumption of glucose carbon:	
$\frac{dC}{dt} = \left(\frac{\mu}{\gamma_c^{\max}} + m_c \right) B$	(6)
net rate of change of glucose carbon:	
$\frac{dC}{dt} = \frac{dC_{\min}}{dt} + \left(\frac{dC}{dt} \right)_d$	(7)
production of carbon dioxide:	
$\frac{dCO_2}{dt} = \left(\left(\frac{dC}{dt} \right)_d - \left(\frac{dB}{dt} \right)_g \right) / N_c$	(8)
consumption of electron acceptor:	
$E = \sum_i E_i$ for $i = 2, 3, 4$	(9)
$\frac{dE_i}{dt} = \left(\frac{\mu_{E_i}}{\gamma_{E_i}^{\max}} + m_{E_i} \frac{E_i}{E} \right) B$ $i = 1, 2, 3, 4$ refers to O_2, NO_3^-N, NO_2^-N , and N_2O-N , respectively	(10)
net rates of change of electron acceptors:	
$\frac{dO_2}{dt} = - \left(\frac{dE_1}{dt} \right) / M_{O_2}$; $\frac{dNO_3^-N}{dt} = \frac{dN_{\min}}{dt} - \frac{dE_2}{dt} - \frac{dN_{ass}}{dt}$;	
$\frac{dNO_2^-N}{dt} = \frac{dE_2}{dt} - \frac{dE_3}{dt}$;	
$\frac{dN_2O}{dt} = \left(\frac{dE_3}{dt} - \frac{dE_4}{dt} \right) / 2 M_n$; $\frac{dN_2}{dt} = \left(\frac{dE_4}{dt} \right) / 2 M_n$	(11)
nitrate assimilation:	
$\frac{dN_{ass}}{dt} = F_{nb} \left(\frac{dB}{dt} \right)_d$	(12)
carbon mineralization from dead biomass:	
$\frac{dC_{\min}}{dt} = F_c \left(\frac{dB}{dt} \right)_d$	(13)
nitrogen mineralization from dead biomass:	
$\frac{dN_{\min}}{dt} = F_n \frac{F_{nb}}{F_{cb}} \left(\frac{dB}{dt} \right)_d$	(14)
immobilization of carbon:	
$\frac{dC_{imm}}{dt} = (1 - F_c) \left(\frac{dB}{dt} \right)_d$	(15)
immobilization of nitrogen:	
$\frac{dN_{imm}}{dt} = (1 - F_n) \frac{F_{nb}}{F_{cb}} \left(\frac{dB}{dt} \right)_d$	(16)

TABLE 2
List of symbols

Symbol	Meaning	Unit
B	amount of bacterial carbon. Refers either to strict aerobes that cannot denitrify or to denitrifiers	kg C
C, E	amount of glucose-C	kg C
F_{den}	total amount of electron acceptor (O ₂ or nitrogenous compounds), and amount of individual electron acceptor, respectively. i=1,2,3,4 refers to O ₂ , NO ₃ ⁻ , NO ₂ ⁻ , and N ₂ O ₃	kg O ₂ kg O ₂ kg N ₂ O ₃
F_c, F_n	mass fraction of carbon and nitrogen in biomass	-
F_{ch}	initial mass fraction of denitrifiers with respect to total bacterial biomass	-
F_{den}	mass fraction of carbon and nitrogen that mineralizes from the dead biomass	-
K, K _c	half saturation value in Monod model with respect to carbon and electron acceptor, respectively	kg m ⁻³ H ₂ O ²
m_c, m_e	maintenance coefficients with respect to carbon and electron acceptor, respectively	kg kg ⁻¹ B s ⁻¹
N_c, N_n, N_o	molecular weight of carbon, nitrogen, and oxygen, respectively	kg mol ⁻¹
t	time	s
Y_{max}	maximum growth yield on glucose-C and on electron acceptor E, where no substrate would be used for maintenance	kg B kg ⁻¹
μ_i	subscript that refers to assimilated	-
μ_b	subscript referring to bacteria	-
μ_s	subscript referring to carbon substrate	-
μ_d, μ_g	subscripts indicating death or decrease, and growth, respectively	-
μ_h	subscript referring to high critical level	-
μ_m	subscript that refers to immobilized	-
μ_l	subscript referring to low critical level	-
μ_{min}	subscript that refers to mineralized	-
μ	total relative growth rate on oxygen or on all N-electron acceptors together	s ⁻¹
$\mu_{E_i}^a, \mu_{E_i}^A$	actual and maximum relative growth rate on electron acceptor E _i , respectively, with glucose-C as carbon limiting substrate	s ⁻¹
\sum	summation operator	-
[]	brackets around an amount convert it to a concentration, either with respect to dry soil (e.g. for bacteria) or with respect to volume of water (e.g. for substrates or electron acceptors)	-

TABLE 3
Total concentration of biomass ([B]), initial fraction denitrifiers (F_{den}), maximum relative growth rates (μ), half saturation values (K), maximum growth yields (Y), and maintenance coefficients (m), with respect to carbon and different electron acceptors at 20°C

symbol	unit	sub- stra- te	parameter values used in simulation runs		
			as derived directly from literature compilation	modified values used for closer comparison with experiments	in this paper
[B] $\times 10^4$	kg C		1	1	1
F_{den}	kg		0.02	0.02	0.6
$\mu \times 10^6$	s ⁻¹	NO ₃ ⁻	4.8	3.9	4.8
		NO ₂ ⁻	4.8	2.4	2.4
		N ₂ O	2.4	1.2	1.2
K $\times 10$	kg C		0.17	0.17	0.17
or N	kg C	NO ₃ ⁻	0.83	0.83	0.83
μ^3	kg C	NO ₂ ⁻	0.83	0.83	0.83
μ^4	kg C	N ₂ O	0.83	0.83	0.83
Y $\times 10^2$	kg B	c	50.3	50.3	50.3
	kg C	NO ₃ ⁻	40.1	10.0	30.0
	or N	NO ₂ ⁻	42.6	5.4	22.5
		N ₂ O	15.1	0.38	1.9
$m \times 10^5$	kg C		0.21	0.21	0.21
or N	kg C	NO ₃ ⁻	2.5	2.5	2.5
	kg B s	NO ₂ ⁻	0.97	0.97	0.97
		N ₂ O	2.2	2.2	2.2

occur in the system. The process of assimilation goes via nitrite to ammonium at the rate required for the synthesis of organic nitrogen compounds (Boogerd 1984). This characteristic of the process is reflected by Eq. (12), through the stoichiometric relation of assimilation rate to the gross growth rate of the bacteria via the inverse of the carbon-nitrogen ratio. Enzymes that are active in the assimilatory process are different from those of the dissimilatory process, and they are not affected by oxygen (Focht and Verstraete 1977; Bryan 1981). Therefore, nitrate assimilation was similarly calculated under aerobic and anaerobic conditions for both groups of bacteria. The absence in the model of assimilation of nitrite (Boogerd 1984) and possibly nitrous oxide means that growth and maintenance cease as soon as nitrate is depleted. A more complete description of nitrogen assimilation would be possible by incorporating bacterial growth on these nitrogenous compounds. However, this would also introduce new problems with respect to which nitrogenous form would be preferentially assimilated; therefore, it was not attempted.

Mineralization and immobilization

Products from cell decay (see section about bacteria) or mineralization will, partially, enter the surroundings, and may be used again as substrates for growth and maintenance. Under aerobic conditions it was assumed that certain fractions of the carbon and nitrogen, F_c and F_n in Eqs. (13) and (14), respectively, were liberated from the dying cells. The carbon and nitrogen released were considered equivalent to glucose carbon and nitrate nitrogen, as expressed by Eq. (7) and (11), where the glucose-C pool and the nitrate-N pool are replenished by these liberated products. Thus, it was implicitly assumed that both sequential processes in mineralization, i.e. ammonification and nitrification (Russell 1973) occurred. Under anoxic conditions nitrification can not occur, because oxygen is needed for this process (Patrick 1982). Therefore, under anaerobic conditions mineralization was assumed not to occur, by taking F_c and F_n equal to zero. By these simplifications, model descriptions of ammonification, ammonium assimilation, nitrification, and inhibition of assimilatory nitrate reductase by ammonia (Bryan 1981; Payne 1973) were avoided. The remaining carbon and nitrogen from dying cells were added to the pools of immobilized carbon and nitrogen, C_{imm} and N_{imm} in Eqs. (15) and (16), respectively: this carbon and nitrogen did not participate anymore in the dynamic processes.

Environmental conditions

Major environmental conditions affecting denitrification are concentrations of water soluble carbon (Burford and Bremner 1975; Stanford et al. 1975^a), and electron acceptor in the soil water where the bacteria live. These variables affect relative growth rates by means of Eq. (5). Growth of both groups of bacteria was similarly described by Eqs. (1) through (16). In case of the strict aerobes, E_i in Eqs. (5) and (10) always refers to oxygen ($i = 1$). In case of the denitrifiers three situations were distinguished. First, when ample oxygen is available, i.e.

$[O_2] > [O_2]_b$, growth of denitrifiers was described similarly to that of the strict aerobes. Second, when the oxygen concentration is lower than a certain limit, $[O_2]_i$, the N-oxides are used as electron acceptors, and i equals 2, 3, or 4 in Eqs. (5) and (10). The third situation occurs in the transition zone where the oxygen concentration is between the lower and upper limits, i.e. $[O_2]_i < [O_2] < [O_2]_b$: both oxygen and N-oxides are used as electron acceptors (Meiberg et al. 1980). Because the gaseous electron acceptors oxygen and nitrous oxide occur in both the soil water and gas phase, their concentrations and thus the pattern of denitrification will be affected by their solubility in the water phase. Growth and maintenance of both groups of bacteria was assumed to cease whenever either the appropriate electron acceptor (oxygen for strict aerobes or oxygen and nitrogenous electron acceptors for denitrifiers) or nitrate and/or carbon for assimilation were depleted.

Other environmental conditions, e.g. soil acidity (Bremner and Shaw 1958; Stanford et al. 1975^a), temperature (McKenney et al. 1984; Stanford et al. 1975^b; Bremner and Shaw 1958), and soil water potential (Harris 1981; Griffin 1981) merely determine overall bacterial activity. Though empirical relationships between microbial activity and soil pH, temperature, and water potential could be incorporated in the model, it is believed that these incorporations would not significantly contribute to a better understanding of the principal processes now reflected in Eqs. (1) through (16). Therefore, they were omitted. This, however, implies that the buffer capacity of soil was considered high and that pH would remain between 6 and 8, a range that is reported to have little effect on denitrification (Burford and Bremner 1975; Stanford et al. 1975^a). Furthermore, data that were known to be temperature dependent, e.g. relative growth rates, maintenance coefficients, and solubility coefficients, were converted to 20 °C, whereas water potential was assumed not to affect microbial activity: Griffin (1981) reported that bacterial activities in soil decrease sharply when the matric potential falls to values between -50 and -300 kPa. Though the assumption of a negligible effect of water potential on microbial activity seems reasonable at the water content used (about 0.32 g g⁻¹), no soil water characteristic was available for this loosely packed soil to substantiate this assumption. Therefore, effects of water potential may be hidden in the parameterization of the model with respect to relative growth rates.

Bacteria are subjected to the concentrations of substrates as these occur in the water phase of soil. Soil water content will thus have a profound influence on these concentrations. This has a number of consequences. First, different concentrations directly affect relative growth rates through Eq. (5). Second, substrate concentrations strongly affect the maintenance coefficients in the Pirt equation (Pirt 1975). Third, low water contents will decrease the rate of diffusion over short distances (microdiffusion) of nutrients to bacterial colonies or cells. It was already stated that low population densities with respect to the surface area of soil exist (Woldendorp 1981). Woldendorp also stated that the microorganisms on the soil particles were seen as isolated cells or small colonies. Thus, even when nutrients are homogeneously distributed, microdiffusion must occur to transport nutrients to

these patches of growing cells. It is not feasible to model microdiffusion, however, and it seems unavoidable to incorporate its effect on bacterial activity through "effective" half saturation values, that have larger values than those measured in pure culture studies (Shieh 1979). Half saturation values found in soil are indeed much higher than those obtained with pure cultures (Firestone 1982).

Computer program

Numerical calculations were done by a program written in Continuous System Modeling Program III (CSMP III) language (IBM 1975), and executed on a VAX machine. The program was developed and written with three targets in mind (apart from the purpose to simulate the respiration and denitrification process): 1) to facilitate the communication of the model and the program to others; 2) to enable the author to incorporate the program in a very large program including transport processes of water, solutes, and gases in an unsaturated soil aggregate; 3) to minimize programming errors. Therefore, the calculation sequence has been summarized in terms of call's to (FORTRAN) subroutines in the main (CSMP) program. The main program contains three major sections: 1) a parameter section, summarizing all biological, soil physical, chemical, and run time control parameters; 2) an initial section, mainly to calculate the amounts of the state variables at time zero, and to convert a number of parameters to SI-units and to 20 °C; all actual input parameters for the dynamic section are printed for control purposes; 3) a dynamic section, starting with the state variables in terms of amounts contained in integrals. The latter is followed by subsections to calculate: a) derived quantities from the state variables (material balances, and concentrations), b) production terms, c) gross rates of change of each integral value, and d) net rates of change of each integral value. A last subsection contains the routines for printing results. The types of subroutines that are called from the dynamic section can be classified similarly to the subsections distinguished there. In addition, however, a subroutine that contains only the control structure to choose the correct calculation subroutines, i.e. on basis of the actual environmental conditions, is distinguished. Thus, the extensively structured program enables one to get a quick overview of the calculations, whereas details may be studied in the separate subroutines. Care has been taken to maintain the recognizability of the rate equations in the subroutines. Units and abbreviations of variables have been given in a separate listing. A system to abbreviate variables was designed and applied to improve the recognizability of the variables, and the readability of the program.

All results presented have been obtained by the variable time step integration method of Runge-Kutta Simpson. Material balances of nitrogen and carbon were computed during the simulation runs, and were found to be correct. To prevent adverse numerical effects of the occurrence in the simulations of slightly negative amounts or concentrations of substances that were consumed, small (< 0.5 % with respect to maximum of variable) threshold values were introduced. Below these threshold values, the appropriate consumption rates were set to zero. The program gives results in terms of rates of respiration and denitrification, concentrations of

biomass (with respect to dry soil mass) and substrates (with respect to soil water), and concentrations and pressures of gases in the soil container.

Model parameters

The microbiological and physicochemical parameters that are needed to test the model should, ideally, originate from soil batch culture studies in which the parameters summarized in Eqs. (1) through (16) are reported. If the sequence of denitrification products could be simulated by using these parameters, it would be warranted to conclude that the model is a very reasonable representation of the soil biological system. Such data sets do not exist to date, however. Another way to come to a judgment about the model is to use data from different authors, and to investigate whether it is possible to simulate the experimental sequence of denitrification products by modifying some of these data within reasonable limits, i.e. within the limits found for representative denitrifying organisms. For this purpose a data set was compiled from the literature (Table 3, that is placed directly after Table 2) that is discussed below.

Biomass contains about 1-2 % of total soil carbon (Woldendorp 1981). When the organic carbon content of soil is about 1 %, this results in 10^{-4} to $2 \cdot 10^{-4}$ kg of biomass-C kg^{-1} dry soil. The lower value has been used throughout this study.

The (initial) fraction of bacteria that is able to denitrify, F_{den} , may vary from decimal fractions of a percent to half of the soil bacterial flora, depending on the medium used in enumeration by the most probable number method (Focht and Verstraete 1977). Therefore, it seems not unreasonable to use this fraction to tune the model results to those of experiments. Note, however, that this fraction is only specified at the start of the simulation, since it will change in the course of time due to different growth rates of the strict aerobes and denitrifiers.

Maximum relative growth rates on three N-electron acceptors for an organism that can grow on glucose are needed in the model. Koike and Hattori (1975^a) reported maximum relative growth rates for *Pseudomonas denitrificans* grown in liquid batch culture under aerobic and anaerobic conditions with glucose and glutamate ($\text{C}_5\text{H}_9\text{NO}_4$) as carbon source and oxygen or nitrate as electron acceptor. The organism could grow aerobically, but not anaerobically, on glucose; anaerobically it needed glutamate. The data for the maximum relative growth rates in Table 3 were derived as follows. The ratio of relative growth rates on glutamate under anaerobic conditions to that under aerobic conditions was 0.14/0.66 (Koike and Hattori 1975^a, their Table 1). The aerobic relative growth rate on glucose was $5.694 \cdot 10^{-5} \text{ s}^{-1}$ at 20 °C, using a Q_{10} value of 2. Assuming that the ratios of relative growth rates on nitrate, nitrite, and nitrous oxide equal those of the number of electrons accepted by the nitrogen atom in each reduction step, the value for e.g. the relative growth rate on nitrate becomes $0.14/0.66 \times 5.694 \cdot 10^{-5} \times 2/5$.

Half saturation values for heterogeneous microbial populations obtained from soil extracts grown in continuous cultures with glucose and nitrate were reported by

Shah and Coulman (1978), and are given in Table 3. The half saturation values for nitrite and nitrous oxide nitrogen were taken equal to that of nitrate nitrogen, so that relative growth rates retain similar ratios as the maximum relative growth rates when equal electron acceptor concentrations would be present.

Maximum growth yields and maintenance coefficients on glucose and on three N-electron acceptors are needed in the model. Van Verseveld et al. (1977) reported values for Paracoccus denitrificans grown in continuous culture under anaerobic conditions with gluconate ($C_6H_{12}O_7$) as carbon source and nitrate as electron acceptor. Their data show some variation when gluconate or nitrate is the limiting growth factor. Therefore, mean values of Y_c^{\max} and m_c were used. The data were converted to the units reported in Table 3 using the elementary composition of Paracoccus denitrificans, $C_6H_{10.8}N_{1.5}O_{2.9}$ (van Verseveld and Stouthamer 1978). Koike and Hattori (1975^b) reported maximum growth yields and maintenance coefficients on glutamate and on all three nitrogenous electron acceptors for Pseudomonas denitrificans grown in continuous culture. Since the maximum growth yields on nitrate in both the studies of van Verseveld et al. (1977) and Koike and Hattori (1975^b) differed but 10 %, the electron acceptor data for growth yield from Koike and Hattori were used. The maintenance value from Koike and Hattori for nitrate was about 3.7 times as high as the corresponding value of van Verseveld et al. The maintenance data are used, however, because they form part of a consistent data set with the maximum growth yields, and no other data are known to be reported.

The data for the maximum growth yields on the three electron acceptors as reported in Table 3 were derived as follows. The growth yields reported by Koike and Hattori on nitrate, nitrite, and nitrous oxide refer to the reduction of each electron acceptor to molecular nitrogen. Growth yields for each separate reduction step, as needed in the model, were therefore calculated as the difference between the values of two consecutive reductions. The resulting values were converted to the units reported in Table 3 using the elementary composition of Paracoccus denitrificans.

The data for the maintenance coefficients on the three electron acceptors reported in Table 3 were derived as follows. The maintenance coefficients on nitrate, nitrite, and nitrous oxide from Koike and Hattori again refer to the reduction of the electron acceptor to molecular nitrogen. In one time unit the amount of biomass maintained per unit nitrate electron acceptor that is reduced to molecular nitrogen, is the inverse of the maintenance coefficient for nitrate as reported by Koike and Hattori. The same holds for nitrite and nitrous oxide. In analogy with the derivation of growth yields for each separate reduction step, the amount of biomass that is maintained when e.g. nitrate is reduced to nitrite will be the difference between the inverse maintenance coefficients: $1/mNO_3^- = (1/m'NO_3^-) - (1/m'NO_2^-)$, where m' values are those from Koike and Hattori expressed in $kg\ N\ kg^{-1}\ biomass\ s^{-1}$ at $30\ ^\circ C$, and mNO_3^- is the desired maintenance coefficient for the reduction of nitrate to nitrite. The latter value was converted to the units in Table 3 using the elementary composition of Paracoccus denitrificans and a Q_{10} value of 2.

The mineralization parameters, F_c and F_n , were taken zero under anaerobic

conditions for reasons outlined in the section about mineralization and immobilization.

Gas solubility values ($\text{m}^3 \text{ gas m}^{-3} \text{ water}$) at 1 atm and 20 °C for nitrous oxide (0.6788) and molecular nitrogen (0.01686) were taken from Wilhelm et al. (1977).

The remaining parameters used to simulate the experiment, i.e. amount of soil, moisture content, and concentrations of added substrates, were taken according to the description in the section about materials and methods.

Parameter values for μ , K, Y, and m under aerobic conditions are not reported in the present study, because no experimental data that give the full time course of the development of anaerobiosis and the subsequent reduction of nitrate to molecular nitrogen via the intermediates nitrite and nitrous oxide were found in the literature; as a consequence, no simulation runs under aerobic conditions were made.

The denitrification model will form part of an extended model that includes the dynamic interactions between denitrification and the physical transport processes of water, gases, and ions in a partially saturated soil aggregate that is surrounded by air. The extended model and the parameters needed for aerobic growth conditions will be described in a following paper.

RESULTS AND DISCUSSION

Model results are presented in terms of the reduction sequence nitrate, nitrite, nitrous oxide, and molecular nitrogen. In Figs. 1, 2, and 3 the simulation results are compared with the experimental data obtained in this paper (Fig. 1 and 2), and those from Cooper and Smith (1963) (Fig. 3), without (Fig. 1) and with (Fig. 2 and 3) modifications of the data as compiled from the literature. Finally, Fig. 4 gives some results of a sensitivity analysis of the model. Values of the microbiological parameters used in the simulations are given in Table 3.

Figure 1 shows the experimental data from this study, with bars indicating one standard deviation, and the results of the simulation using the unmodified literature data. Comparing these simulated and experimental results, makes clear that model structure is reasonable: denitrification products appear in the right sequence, and the time course of the simulated and experimental denitrification process is rather similar. In particular the simulated nitrate and nitrite curves are close to the experimental curves. Major differences are the delayed start of the evolution of molecular nitrogen in the simulated results, and the fact that no reduction of nitrite and nitrous oxide takes place when nitrate is depleted. The latter feature is found in all figures. It is the direct consequence of the "practical", but not necessary, assumption that growth and maintenance cease, when nitrate for assimilation is depleted.

Figure 2 shows results of a simulation using modified literature data, and again the experimental results from this paper (only the smoothed dashed curves are given for readability). The input data to obtain the simulated results in Fig. 2 were modified with respect to those from the literature compilation by factors of 0.5 and 0.8 for the maximum relative growth rates, and 0.25, 0.125, and 0.025 for the maximum

growth yields on nitrate, nitrite, and nitrous oxide, respectively. The changes in

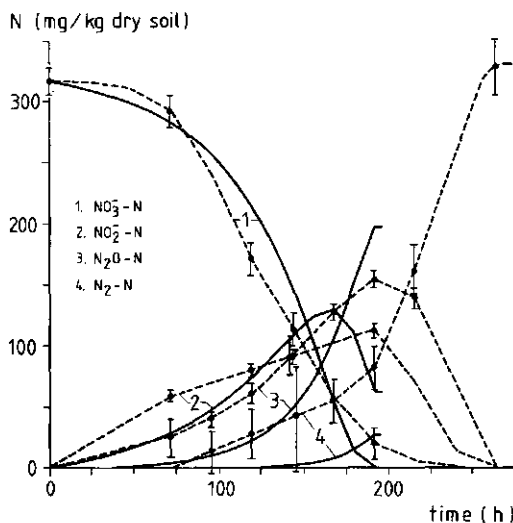


Fig.1. Experimental (this paper, bars indicate one standard deviation; dashed curves) and simulated (based on unmodified literature data, Table 3 4th column; continuous curves) concentrations of nitrate, nitrite, nitrous oxide, and molecular nitrogen as function of time.

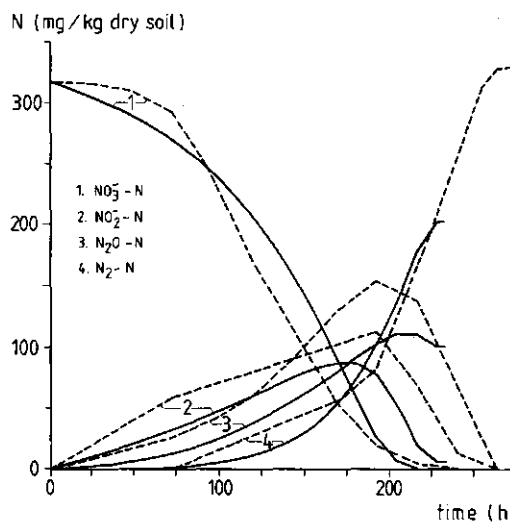


Fig.2. Experimental (this paper, dashed curves) and simulated (based on modified literature data, Table 3 5th column; continuous curves) concentrations of nitrate, nitrite, nitrous oxide, and molecular nitrogen as function of time.

the maximum relative growth rates are supported by data from Koike and Hattori (1975^a), who reported such values for Pseudomonas denitrificans under anaerobic conditions on different substrates, that differed by a factor of 0.43. The changes that were introduced for the maximum growth yields on nitrogenous electron acceptors could not be substantiated by data from literature: only Koike and Hattori (1975^b) have reported on these three parameters. The similarity between the simulated and experimental results is judged good. Especially the disappearance of nitrate and the evolution of molecular nitrogen are almost quantitatively described. The maxima of nitrite and nitrous oxide are about 25 % too low compared to the experimental values, but they appear at about the right moment. It is likely, that similar or even better results would have been obtained when the maintenance coefficients on nitrogenous oxides had been included in the modifications. Then, the modification of e.g. growth yield on nitrous oxide could have been smaller, because a larger maintenance value would take over part of the adaptation of the model results to those of the experiment. It must be stressed, however, that no parameter optimization has been carried out, rather it was investigated whether the model structure had the potential to describe experimental data. All modified parameters to obtain the simulated results are lower than in the compiled literature data. This was to be expected, since growth and yield of bacteria in soil will not be as efficient as in liquid batch and continuous culture studies.

Figure 3 shows experimental results from Cooper and Smith (1963, results at

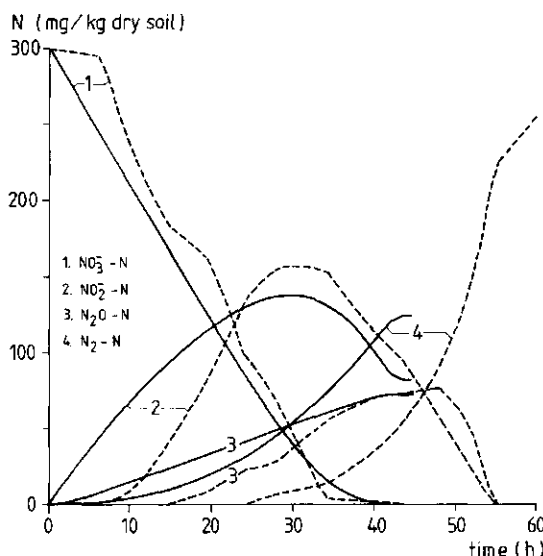


Fig.3. Experimental (paper Cooper and Smith, dashed curves) and simulated (based on modified literature data, Table 3 last column; continuous curves) concentrations of nitrate, nitrite, nitrous oxide, and molecular nitrogen as function of time.

the case of Cooper and Smith. These authors, however, had installed a tube with 4 N KOH in their experimental flasks to trap the carbon dioxide produced. In the model calculations the contribution of carbon dioxide to overpressure was 9.6 %. The result that pressure affects significantly the time course of gaseous denitrification products, indicates that it would have been better to run the model with a zero carbon dioxide production rate: momentarily, the pressure influence is hidden in the parameter for maximum growth yield on nitrous oxide. The importance of these theoretical observations is twofold. First, denitrification patterns reported by different workers should be measured at similar gas pressures (preferably 1 atm), if they are to be mutually compared. Second, differences in local gas pressures in field soils will affect the ratio N_2O/N_2 , and thus not only the biochemistry of the denitrification process is a determining factor for the numerical value of this ratio. The N_2O/N_2 ratio is the subject of research in connection with the possible contribution of nitrous oxide to destruction of the ozone layer in the stratosphere (Letey et al. 1980^b, 1980^c).

Nearly similar simulation results were obtained when the solubility of nitrous oxide in soil water was doubled (data not shown).

CONCLUDING REMARKS

The presented simulation model proved to give a satisfactory description of the denitrification process measured in laboratory incubation vessels. A major difficulty, however, is that no coherent data sets exist to date to parameterize the model. Simulation results obtained with such data sets would enable one to put forward more definite conclusions about the quality of the model. Therefore, besides the introduction of minor improvements in the present model, e.g. the consumption of other electron acceptors than nitrate for growth and for maintenance processes after the depletion of nitrate, it neither seems appropriate to principally modify the model, nor to develop more complicated models, e.g. that of Cho and Mills (1979), that are inherently more difficult to parameterize. Rather, attention should be given to gather coherent data sets including both determinations of the parameters needed in the present model and the time course of denitrification products. Such data should be used to further test the model to be able to judge its predictive value in ecological studies concerning denitrification.

Sensitivity analysis of the presented model may help to design the experiments that are needed to determine these parameters.

ACKNOWLEDGMENTS

Thanks are due to Professor G.H. Bolt and his staff of the department of Soil Science and Plant Nutrition, who have given the opportunity to carry out the experimental work in their laboratory. We wish to thank Mr. W. Otten, who carried out the experimental work reported in this paper, and Ir. R. Baas and Ir. J. Reijerink, who developed preliminary versions of the present model. Mr. C. Rijpma is thanked for drawing the illustrations. Dr. J.L.M. Huntjens, Prof.

A.J.B. Zehnder, Ir. J.H.G. Verhagen, Prof. G.H. Bolt, and Dr. B.H. Janssen kindly commented on the long list of assumptions underlying the denitrification model. Prof. Zehnder, Prof. Bolt, Prof. C.T. de Wit, and Ir. J.H.G. Verhagen gave their constructive criticism on the manuscript.

REFERENCES

Allison, L.E., and C.D. Moodie. 1965. Carbonate. In *Methods of soil analysis*, pt. 2. C.A. Black (ed.). *Agronomy* 9. American Society of Agronomy, Madison, Wis., pp. 1379-1396.

Bader, F.G. 1978. Analysis of double-substrate limited growth. *Biotechnol. Bioeng.* 20:183-202.

Bader, F.G., J.S. Meyer, A.G. Fredrickson, and H.M. Tsuchiya. 1975. Comments on microbial growth rate. *Biotechnol. Bioeng.* 17:279-283.

Barber, D.A., and J.M. Lynch. 1977. Microbial growth in the rhizosphere. *Soil Biol. Biochem.* 9:305-308.

Bascomb, C.L. 1964. Rapid method for the determination of cation exchange capacity of calcareous and non-calcareous soils. *J. Sci. Food Agric.* 15:821-823.

Betlach, R.M., and J.M. Tiedje. 1981. Kinetic explanation for accumulation of nitrite, nitric oxide, and nitrous oxide during bacterial denitrification. *Appl. Environ. Microbiol.* 42:1074-1084.

Birch, H.F. 1958. The effect of soil drying on humus decomposition and nitrogen availability. *Plant Soil* 10:9-31.

Birch, H.F. 1959. Further observations on humus decomposition and nitrification. *Plant Soil* 11:262-286.

Boogerd, F.C. 1984. Energetic aspects of denitrification in Paracoccus denitrificans. Ph.D. thesis. Vrije Universiteit, Amsterdam, p. 132.

Bryan, B.A. 1981. Physiology and biochemistry of denitrification. In *Denitrification, nitrification, and atmospheric nitrous oxide*. C.C. Delwiche (ed.). Wiley, New York, pp. 67-84.

Bremner, J.M., and K. Shaw. 1958. Denitrification in soil. II. Factors affecting denitrification. *J. Agric. Sci.* 51:40-52.

Burford, J.R., and J.M. Bremner. 1975. Relationships between the denitrification capacities of soils and total, water-soluble and readily decomposable soil organic matter. *Soil Biol. Biochem.* 7:389-394.

Cho, C.M. 1982. Oxygen consumption and denitrification kinetics in soil. *Soil Sci. Soc. Am. J.* 46:756-762.

Cho, C.M., and J.G. Mills. 1979. Kinetic formulation of the denitrification process in soil. *Can. J. Soil Sci.* 59:249-257.

Cho, C.M., and L. Sakdinan. 1978. Mass spectrometric investigation on denitrification. *Can. J. Soil Sci.* 58:443-457.

Cooper, G.S., and R.L. Smith. 1963. Sequence of products formed during denitrification in some diverse western soils. *Soil Sci. Soc. Am. Proc.* 27:659-662.

Day, P.R. 1965. Particle fractionation and particle-size analysis. In *Methods of soil analysis*, pt. 1. C.A. Black (ed.). *Agronomy* 9. American Society of Agronomy, Madison, Wis., pp. 545-567.

Delwiche, C.C. (ed.). 1981. *Denitrification, nitrification, and atmospheric nitrous oxide*. Wiley, New York, p. 286.

Fillery, I.R.P. 1983. Biological denitrification. In *Gaseous loss of nitrogen from plant-soil systems*. J.R. Freney and J.R. Simpson (eds.). Martinus Nijhoff, The Hague, pp. 33-64.

Firestone, M.K. 1982. Biological denitrification. In *Nitrogen in agricultural soils*. F.J. Stevenson (ed.). Agronomy 22. American Society of Agronomy, Madison, Wis., pp. 289-326.

Focht, D.D., and W. Verstraete. 1977. Biochemical ecology of nitrification and denitrification. In *Advances in microbial ecology*, vol 1. M. Alexander (ed.). Plenum Press, New York, pp. 135-214.

Frissel, M.J., and J.A. van Veen (eds.). 1981. *Simulation of nitrogen behaviour of soil-plant systems*. PUDOC, Wageningen, p. 277.

Griffin, D.M. 1981. Water potential as a selective factor in the microbial ecology of soils. In *Water potential relations in soil microbiology*. Soil Sci. Soc. Am. special publication no. 9, Madison, Wis., pp. 141-151.

Harris, R.F. 1981. Effect of water potential on microbial growth and activity. In *Water potential relations in soil microbiology*. Soil Sci. Soc. Am. special publication no. 9, Madison, Wis., pp. 23-95.

Hauck, R.D., and R.W. Weaver (eds.). 1986. *Field measurement of dinitrogen fixation and denitrification*. Soil Sci. Soc. Am. special publication no. 18, Madison, Wis., p. 115.

IBM Corp. 1975. *Continuous system modeling program III (CSMP III)*. Program reference manual. SH 19-7001-3. Data Processing Division, 1133 Westchester Ave., White Plains, N.Y.

Knowles, R. 1982. Denitrification. *Microbiological reviews* 46:43-70.

Koike, I., and A. Hattori. 1975^a. Growth yield of a denitrifying bacterium, Pseudomonas denitrificans, under aerobic and denitrifying conditions. *J. Gen. Microbiol.* 88:1-10.

Koike, I., and A. Hattori. 1975^b. Energy yield of denitrification: An estimate from growth yield in continuous cultures of Pseudomonas denitrificans under nitrate-, nitrite- and nitrous oxide-limited conditions. *J. Gen. Microbiol.* 88:11-19.

Leffelaar, P.A. 1986. Dynamics of partial anaerobiosis, denitrification, and water in a soil aggregate: experimental. *Soil Sci.* 142:352-366.

Legg, J.O., and J.J. Meisinger. 1982. Soil nitrogen budgets. In *Nitrogen in agricultural soils*. F.J. Stevenson (ed.). Agronomy 22. American Society of Agronomy, Madison, Wis., pp. 503-566.

Letey, J., W.A. Jury, A. Hadas, and N. Valoras. 1980^a. Gas diffusion as a factor in laboratory incubation studies on denitrification. *J. Environ. Qual.* 9:223-227.

Letey, J., N. Valoras, A. Hadas, and D.D. Focht. 1980^b. Effect of air-filled porosity, nitrate concentration, and time on the ratio of N_2O/N_2 evolution during denitrification. *J. Environ. Qual.* 9:227-231.

Letey, J., A. Hadas, N. Valoras, and D.D. Focht. 1980^c. Effect of preincubation treatments on the ratio of N_2O/N_2 evolution. *J. Environ. Qual.* 9:232-235.

Lind, A-M. 1980. Denitrification in the root zone. *Danish J. of Plant and Soil Sci.* 84:101-110.

MacGregor, A.N. 1972. Gaseous losses of nitrogen from freshly wetted desert soils. *Soil Sci. Soc. Am. Proc.* 36:594-596.

Megee, R.D.III, J.F. Drake, A.G. Fredrickson, and H.M. Tsuchiya. 1972. Studies in intermicrobial symbiosis. Saccharomyces cerevisiae and Lactobacillus casei. *Can. J. Microbiol.* 18:1733-1742.

McKenney, D.J., G.P. Johnson, and W.I. Findlay. 1984. Effect of temperature on consecutive denitrification reactions in Brookston clay and Fox sandy loam. *Appl. Environ. Microbiol.* 47:919-926.

Mebius, L.J. 1960. A rapid method for the determination of organic carbon in soil. *Anal. Chim. Acta* 22:120-124.

Meijberg, J.B.M., P.M. Bruinenberg, and W. Harder. 1980. Effect of dissolved oxygen tension on the metabolism of methylated amines in Hyphomicrobium X in the absence and presence of nitrate: Evidence for 'aerobic' denitrification. *J. Gen. Microbiol.* 120:453-463.

Novozamsky, I., V.J.G. Houba, E. Temminghoff, and J.J. van der Lee. 1984. Determination of "total" N and "total" P in a single soil digest. *Neth. J. Agric. Sci.* 32:322-324.

Painter, H.A. 1970. A review of literature on inorganic nitrogen metabolism in microorganisms. *Water Res.* 4:393-450.

Patrick, W.H., Jr. 1982. Nitrogen transformations in submerged soils. In *Nitrogen in agricultural soils*. F.J. Stevenson (ed.). Agronomy 22. American Society of Agronomy, Madison, Wis., pp. 449-465.

Payne, 1973. Reduction of nitrogenous oxides by microorganisms. *Bacteriol. Rev.* 37:409-452.

Pirt, S.J. 1965. The maintenance energy of bacteria in growing cultures. *Proc. roy. Soc. London, Series B* 163:224-231.

Pirt, S.J. 1975. Principles of microbe and cell cultivation. Blackwell, Oxford, p. 274.

Rolston, D.E., and M.A. Marino. 1976. Simultaneous transport of nitrate and gaseous denitrification products in soil. *Soil Sci. Soc. Am. J.* 40:860-865.

Russell, E.W. 1973. Soil conditions and plant growth. Longman, London, p. 849.

Schlegel, H.G. 1972. *Allgemeine Microbiologie*. Georg Thieme Verlag Stuttgart, p. 461.

Schmidt, S.K., S. Simkins, and M. Alexander. 1985. Models for the kinetics of biodegradation of organic compounds not supporting growth. *Appl. Environ. Microbiol.* 50:323-331.

Shah, D.B., and G.A. Coulman. 1978. Kinetics of nitrification and denitrification reactions. *Biotechnol. Bioeng.* 20:43-72.

Shieh, W.K. 1979. Theoretical analysis of the effect of mass-transfer resistances on the Lineweaver-Burk plot. *Biotechnol. Bioeng.* 21:503-504.

Smith, M.S., and J.M. Tiedje. 1979. Phases of denitrification following oxygen depletion in soil. *Soil Biol. Biochem.* 11:261-267.

Stanford, G., R.A. Vander Pol, and S. Dzienia. 1975^a. Denitrification rates in relation to total and extractable soil carbon. *Soil Sci. Soc. Am. Proc.* 39:284-289.

Stanford, G., S. Dzienia, and R.A. Vander Pol. 1975^b. Effect of temperature on denitrification rate in soils. *Soil Sci. Soc. Am. Proc.* 39:867-870.

Stevenson, F.J. 1982. Origin and distribution of nitrogen in soil. In *Nitrogen in agricultural soils*. F.J. Stevenson (ed.). Agronomy 22. American Society of Agronomy, Madison, Wis., pp. 1-42.

Tanji, K.K. 1982. Modeling of the soil nitrogen cycle. In *Nitrogen in agricultural soils*. F.J. Stevenson (ed.). Agronomy 22. American Society of Agronomy, Madison, Wis., pp. 721-772.

Tiedje, J.M. 1978. Denitrification in soil. In *Microbiology*. D. Schlessinger (ed.). American Society of Microbiology. Washington, D.C., pp. 362-366.

Tiedje, J.M., A.J. Sextone, D.D. Myrold, and J.A. Robinson. 1982. Denitrification: ecological niches, competition and survival. *Antonie van Leeuwenhoek* 48:569-583.

Veen, J.A. van, and M.J. Frissel. 1981. Simulation model of the behaviour of N in soil. In *Simulation of nitrogen behaviour of soil-plant systems*. M.J. Frissel and J.A. van Veen (eds.). PUDOC, Wageningen, pp. 126-144.

Verseveld, H.W. van, and A.H. Stouthamer. 1978. Growth yields and the efficiency of oxidative phosphorylation during autotrophic growth of Paracoccus denitrificans on methanol and

formate. *Arch. Microbiol.* 118:21-26.

Verseveld, H.W. van, E.M. Meijer, and A.H. Stouthamer. 1977. Energy conservation during nitrate respiration in *Paracoccus denitrificans*. *Arch. Microbiol.* 112:17-23.

Verstraete, W. 1977. Fundamentele studie van de opbouw- en omzettingsprocessen in microbiele gemeenschappen. Univ. Gent, Gent, Belgic, p. 444.

Wilhelm, E., R. Battino, and R. J. Wilcock. 1977. Low-pressure solubility of gases in liquid water. *Chem. Rev.* 77:219-262.

Wit, C.T. de. 1982. Simulation of living systems. In *Simulation of plant growth and crop production*. F.W.T. Penning de Vries, and H.H. van Laar (eds.). PUDOC, Wageningen, The Netherlands, pp. 3-8.

Woldendorp, J.W. 1981. Nutrients in the rhizosphere. Agricultural yield potentials in continental climates. *Proc. 16th Coll. Int. Potash Institute, Bern*, pp. 99-125.

CHAPTER 6

DYNAMICS OF PARTIAL ANAEROBIOSIS, DENITRIFICATION, AND WATER IN A SOIL AGGREGATE: SIMULATION.

P.A. LEFFELAAR ¹

A simulation model was developed to study the dynamics of partial anaerobiosis and denitrification in unsaturated soil. The model enables one to calculate simultaneously the distribution of water, bacteria, oxygen, carbon dioxide, nitrous oxide, molecular nitrogen, neon, absolute soil atmospheric pressure, nitrate, nitrite, and glucose as a function of space and time in an unsaturated, homogeneous, cylindrical aggregate, and the changes in atmospheric composition as a function of time in the chamber that contains the aggregate. Except for water transport, these processes are caused by microbial activity, because roots are not present in the aggregate. The simulation model is the theoretical counterpart of the experimental "soil aggregate system" as studied in a previously described respirometer setup.

The simulated results showed a satisfactory agreement with experimental data: part of the experimental results could be described quantitatively, whereas other data that deviated from the experimental data could be understood by studying the dynamic behaviour of the model. Hysteresis in the soil water retention curve resulted in low values of the gas-filled porosities in the outer shell of the partially wetted aggregate, permitting only gaseous exchange through the water phase of soil. As a result anaerobiosis and denitrification occurred.

A major conclusion was that appropriate model parameterization was needed first. To that purpose the model will be used to plan respirometer experiments, to help interpret the experimental data so obtained, and to investigate the relative importance of a number of parameters in a sensitivity analysis. Furthermore, it was concluded that only the interaction of experiment and theory will ultimately lead to a full understanding of the complex soil biological system described.

The objective of this paper is to describe the

¹ Department of Theoretical Production Ecology, Bornsesteeg 65, 6708 PD Wageningen, The Netherlands.

simulation model, to discuss its parameterization, and to compare some of the simulated results with those of the experimental system described previously.

The release of nitrous oxide and molecular nitrogen by biological denitrification occurs when bacteria capable of denitrification colonize a location where oxygen is absent and water, nitrate, and decomposable organic compounds are present (Delwiche 1981; Ingraham 1981). In aggregated unsaturated soils anaerobiosis, and hence denitrification, is mainly confined to within the aggregates (Currie 1961; Greenwood 1961). In principle, therefore, denitrification losses from aggregated field soils can be predicted when denitrification losses from individual aggregates and their size distribution are known (Smith 1977, 1980). Denitrification losses from a single aggregate can be predicted successfully only when the spatial distributions of denitrifiers, oxygen, water, nitrate, and decomposable organic compounds can be measured or calculated as a function of time and when these distributions are subsequently combined so that zones of denitrification show up.

Figure 1 depicts some schematic oxygen and water distributions as expected in field aggregates under the assumption of a homogeneous distribution of bacteria and organic compounds and a negligible nitrate production due to nitrification. When oxygen consumption rate does not exceed oxygen supply rate, anoxic conditions will not develop, and equimolar respiration occurs as indicated by arrows (Fig. 1a). Just after rainfall, mainly the outer shell of an aggregate will be wetted (Leffelaar 1979). The oxygen diffusion rate in the outer shell is then seriously impeded, and when oxygen consumption rate exceeds oxygen supply rate, anoxic conditions arise locally (Fig. 1b). When nitrate from fertilizer has been absorbed

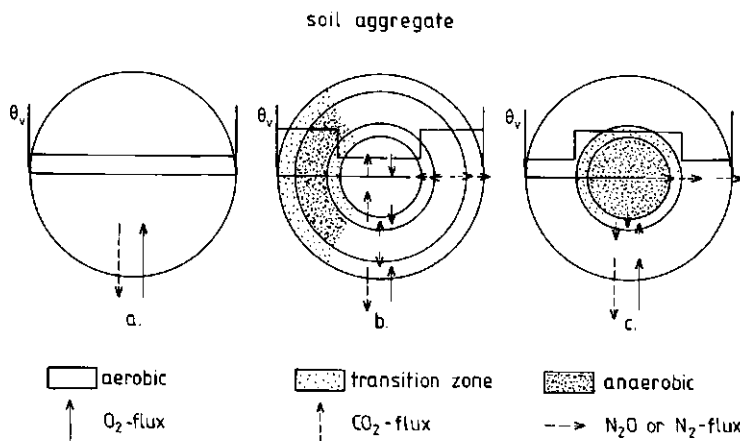


Fig.1. Schematic of water and oxygen distributions in soil aggregates. a, in a dry period; b, just after a rain shower; c, some time after rainfall.

Lengths of arrows indicate relative magnitudes of molar source or sink terms.

with the rainwater, denitrification occurs in the wetted shell. In the center of the aggregate equimolar respiration continues to take place until the oxygen from the enclosed air has been consumed. Then most of the aggregate volume is anaerobic, but denitrification does not necessarily increase, for the nitrate is mainly concentrated in the wetted shell. The arrows in Fig. 1b indicate a net gas production caused by denitrification. Subsequent redistribution of water may result in a decrease of the anaerobic aggregate volume, and hence of denitrification, when the water content in the wetted shell becomes low enough to get continuous gas-filled pores permitting rapid oxygen diffusion into the aggregate. The distribution of oxygen in Fig. 1c will be found in initially water-saturated aggregates that are drying. Upon further drying their oxygen distributions will adjust to that of Fig. 1a.

These complicated dynamic interactions between biological and physical processes determining denitrification are studied best through the development of a sufficiently detailed explanatory simulation model. Such a model should include a description of microbial activity, movement of gases, water, nitrate, and nitrite, and decomposition of organic compounds in an individual aggregate. The objective of the present paper is to describe such an explanatory simulation model, to discuss its parameterization, and to compare the model results with experimental data presented in a previous paper (Leffelaar 1986).

SIMULATION MODEL INTEGRATING SUBMODELS FOR DENITRIFICATION, WATER, SOLUTES, AND GASES

The explanatory simulation model was developed to calculate the distribution of the relevant state variables, here bacteria, water, solutes, and gases, as a function of space and time. As to the geometry, the model refers to an unsaturated cylindrical aggregate in which transport processes are radial. Also the changes in atmospheric composition as a function of time, in the chamber that contains the aggregate, were to be calculated. The cylindrical geometry is a model representation of a soil aggregate from which the upper and lower sides are removed and originates directly from Fig. 1. The simulation model is the theoretical counterpart of an experimental system described previously (Leffelaar 1986). This system consisted of a "macro soil aggregate" with variable water content, placed in a specially designed respirometer. The experimental system was developed at the time to evaluate the present theoretical model; conversely, the theoretical model was developed for full interpretation of the measured data.

The simulation model exposed here comprises four submodels: one for the biological processes of respiration and denitrification, and three for the transport processes of water, solutes (nitrate, nitrite, and decomposable organic compounds, i.e. glucose), and gases (oxygen, carbon dioxide, nitrous oxide, molecular nitrogen, and neon), respectively. To calculate the spatial distribution of the various state variables, the system was divided into a number of concentric layers (Frissel and Reiniger 1974; de Wit and van Keulen 1975). The interaction between the four submodels may be demonstrated by the equation of continuity that is solved for each mobile substance in each layer, i.e. Eq.(1),

$$\frac{\partial C_i}{\partial t} = - \frac{\partial J_i}{\partial x} + P_i \quad (1)$$

All symbols are defined in the appended list of symbols. For instance, the denitrification submodel calculates different production rates (P_i) in adjacent aggregate layers, because the bacteria in these layers are subjected to different environmental conditions. Different production rates result in gradients in concentration of substance i . When it concerns a gaseous substance, in principle also gradients in absolute pressure result. The diffusive, dispersive, and mass flow transports that will now occur are contained in the flux (J_i). Integration of Eq.(1) with respect to time will give the time course of substance i in a layer as a result of the interactions of microbial activity and physical transport processes, and the environmental conditions for the bacteria in the layer change. When a substance is inert, e.g. neon, or immobile, e.g. biomass, the production term or the flux term in Eq.(1) equals zero, respectively.

Models remain simplified representations of the real system (de Wit 1982). This, however, does not imply that all models are simple and concise. During the present study it became clear that e.g. interactions between submodels could impose difficulties that are normally not envisaged when such models are developed or used separately. Such interactions, in conjunction with the use of four submodels have resulted in a large, rather complicated computer program (110 pages of code and 120 subroutines) that needed much CPU-time (100 minutes for a typical run on a VAX-8700 machine). To develop the (sub)models, numerous assumptions had to be made. A great part of these assumptions has been described elsewhere: the denitrification model by Leffelaar and Wessel; the water flow model by Dane and Wierenga (1975); and the solute transport model by Bolt (1979). Therefore, these models are merely summarized below. The gas diffusion model for multinary gas mixtures was also previously discussed (Leffelaar 1987). However, in the integrated model, the interaction of the gases with the water, and with the gas production terms due to respiration and denitrification, complicated the description of the gas transport model. Therefore, the gas transport model, and the assumptions made for its development will be detailed in the present paper.

Respiration and denitrification submodel

The submodel describing respiration and denitrification was discussed in detail in a previous paper (Leffelaar and Wessel). Summarizing, growth of two groups of heterotrophic strict aerobic bacteria of which a part is capable to denitrify was calculated by a first order rate equation. The relative growth rate was described by a double Monod equation consisting of rate limiting factors for carbon substrate and oxygen or nitrogenous electron acceptor. Changes in the amounts of glucose carbon, carbon dioxide, oxygen, nitrate, nitrite, nitrous oxide, and molecular nitrogen were described by Pirt's equation, where growth yields and maintenance coefficients of the

bacteria are distinguished. The submodel was developed for a homogeneous soil layer. In the simulation model each concentric layer of the aggregate was also assumed homogeneous. Therefore, the denitrification submodel was simply applied in each layer of the aggregate to yield all of the production terms P_i in Eq.(1).

Water transport submodel

Water redistribution in the aggregate was calculated by combining Darcy's law, Eq.(2)

$$J_w = - k \frac{dh}{dx} \quad (2)$$

with the equation of continuity, Eq.(1), where the production term cancelled because roots were absent. Since only horizontal transport of water occurred in the aggregate, gravitational head was omitted in Eq.(2). Both hydraulic conductivity (k) and pressure head of soil water (h) were functions of volumetric water content.

In author's experiments (Leffelaar 1986, Fig. 4) it appeared that redistribution of water with an initial (schematic) distribution as depicted in Fig. 1b, resulted finally in a non-homogeneous water distribution. This was attributed to the hysteresis phenomenon that may occur in both the water retention curve (Koorevaar et al. 1983), and the hydraulic conductivity-water content curve (Staple 1966; Dane and Wierenga 1975), although others maintain that the latter curve is essentially nonhysteretic (Kool and Parker 1987). Preliminary attempts to model the redistribution process of water in the aggregate without taking hysteresis into account failed: water content was always finally homogeneously distributed. Thus, the submodel for water redistribution had to include hysteresis.

A simulation model describing soil water flow including hysteresis in the water retention curve and in the hydraulic conductivity-water content relationship was reported by Dane (1972)² and Dane and Wierenga (1975). Essentially, the scanning curve for wetting (or drying) was forced to converge to the main wetting (or main drying) curve as function of the difference between the water content at which a reversal of drying to wetting (or wetting to drying) occurred, and the actual water content. Dane's model was attractive to use because it combined a reasonable description of the hysteresis phenomenon with an explicit computational scheme similar to that used in the present simulation model. Although other models (e.g. Hopmans and Dane 1986; Kool and Parker 1987) may have a more rigorous theoretical basis than the one of Dane, these models have implicit computational schemes that are difficult to adapt to the needs of the present simulation model. The model of Dane and Wierenga (1975) was reformulated so that variable time step integration methods

² Dane, J.H. 1972. Effect of hysteresis on the prediction of infiltration, redistribution and drainage of water in large soil columns. Thesis, New Mexico State University, Las Cruces, N.M.

could be used to save computer time. Furthermore, the tabular data input of the main drying and main wetting water retention curves and the hydraulic conductivity-water content curves in the model was replaced by equations described by van Genuchten (1980). The parameters in these equations were estimated from the measurements described in the model parameters section below by optimization procedures outlined by van Genuchten (1978).

The water submodel is not affected by the results of other submodels, though in real soil hydraulic characteristics may be affected by entrapped air and gas pressure (Chahal 1966), resulting from e.g. respiration and denitrification processes; the water submodel, however, directly affects the submodels for the transport processes of solutes and gases.

Solute transport submodel

Solute transport in the aggregate was calculated by combining Eq.(3),

$$J_s = - D_0 \lambda_w \theta \frac{dc_s}{dx} - L_d |J_w| \frac{dc_s}{dx} + J_w c_s \quad (3)$$

with the equation of continuity, Eq.(1). The three terms in Eq.(3) represent Fick's first law for diffusive transport, convective dispersion, and convective transport of the solute, respectively. Diffusive flux in soil is reduced compared with that in free water, because the water phase occupies only a fraction of the soil volume (θ), and the diffusion path has a tortuous geometry (λ_w). The product $D_0 \lambda_w \theta$ is often called effective diffusion coefficient, though it would seem conceptually more appropriate to call $\lambda_w \theta$ the flux reduction factor, since the use of D_0 assumes that in the water phase of soil diffusion occurs as in free water. The tortuosity factor, λ_w , was a function of volumetric water content. The convective dispersion coefficient, $L_d |J_w|$, is linearly related to the average water flow velocity, $|J_w|$, Bolt (1979). Concentration of solute (c_s) refers to the water phase of the soil, since no adsorption of solutes to the solid phase was assumed to occur. Numerical dispersion was reduced in the simulation program by computing the convective transport (third term in Eq.(3)) using the linearly interpolated value for c_s at the transition between adjacent compartments (Goudriaan 1973).

Equation (3) was derived and extensively discussed by Bolt (1979), and applied in numerous simulation studies, e.g. de Wit and van Keulen (1975), Frissel and Reiniger (1974), Leistra (1972; 1980), Leistra et al. (1980), and Boesten (1986).

It follows directly from Eq.(3) that the water flow submodel affects the transport of the solutes as long as the redistribution process continues; diffusive transport, however, will always be present in moist soil, since bacterial activity will hardly ever be similar in adjacent compartments.

Gas transport submodel

Gas transport in the aggregate was calculated by combining Eq.(4),

$$J_g = - D_{ij} \lambda_g \epsilon_g \frac{dc_g}{dx} + J_p \frac{c_g}{c} \quad (4)$$

with the equation of continuity, Eq.(1). The first term in Eq.(4) represents Fick's first law for diffusive transport incorporating area reduction (ϵ_g) and tortuosity (λ_g), similar to solute transport, but now referring to the gas phase of soil. The binary diffusion coefficients, D_{ij} , were calculated as described previously (Leffelaar 1987) with respect to neon (Ne), because in the experiments nitrogen was replaced by Ne to have the opportunity to measure small quantities of N_2 (Leffelaar 1986). When eventually pressure changes occurred, the binary diffusion coefficients were pressure corrected. Diffusive transports through the water phase of soil were calculated according to Fick's first law, i.e. the first term in Eq.(4), under the assumption that no coupling of gas fluxes will occur in water. This seems plausible, since the main interactions of dissolved gases will be with the water molecules: water density is very high compared with dissolved gas densities.

The second term is the product of the pressure adjustment flux (J_p) and the relative presence of gas g (c_g/c), that serves to maintain equal total gas pressures on either side of adjacent soil layers. In fact, the second term in Eq.(4) embodies the coupling of fluxes in multinary gas mixtures where water is absent (Leffelaar 1987). The description of diffusion of gases by Eq.(4) in multinary, isothermal, isobaric, ideal-gas mixtures, where in principle differences in total gas pressure were caused solely by unequal binary diffusion coefficients (D_{ij}), agreed to within 10 % with results of the rigorous gas kinetic theory for such systems (Leffelaar 1987). The pressure adjustment flux in that case was calculated as the sum of the individual gas fluxes. The integration of the multinary gas diffusion model with the models for water flow and denitrification complicates the calculation of the pressure adjustment flux. This is so, because in a wet soil, where water movement occurs, differences in total gas pressure could also be caused by different gas solubilities in water, mass flow of gas due to water movement, and different source/sink terms in adjacent soil layers, aside from the effect of unequal binary diffusion coefficients. To calculate the pressure adjustment flux in the integrated model, the previously used assumption that total gas pressure gradients will not occur in adjacent soil layers (Leffelaar 1987), was supplemented with the assumption that partitioning of gases over the water and the gas phase is instantaneous and given by the gas solubility coefficients in water. The details to solve the pressure adjustment flux in the integrated model will be given below. Since pressures and concentrations are interrelated through $c = p/(RT)$, concentrations have been used for convenience in the derivations.

Consider a series of soil layers as depicted in Fig. 2, that have equal total gas concentrations, $c(l)$, with $l=1,2,\dots,n$. To maintain these mutually similar total gas concentrations, the rate of change of $c(l)$ should be equal in each layer:

$$\frac{\Delta c(l)}{\Delta t} = \frac{\Delta c(l+1)}{\Delta t} \quad , \quad l=1,2,\dots,n \quad (5)$$

with

$$\frac{\Delta c(l)}{\Delta t} = \sum_g \frac{\Delta c'(g,l)}{\Delta t} \quad , \quad g=1,2,\dots,m, \text{ and } l=1,2,\dots,n \quad (6)$$

The rate of change of concentration of gas g in layer l is defined by the continuity equation written in finite difference form:

$$\frac{\Delta c'(g,l)}{\Delta t} = (J(g,l) + J_p(l) \frac{\bar{c}(g,l)}{c(l)}) \frac{A(l)}{V(g,l)} - (J(g,l+1) + J_p(l+1) \frac{\bar{c}(g,l+1)}{c(l+1)}) \frac{A(l+1)}{V(g,l)} + \frac{S(g,l)}{V(g,l)} \quad (7)$$

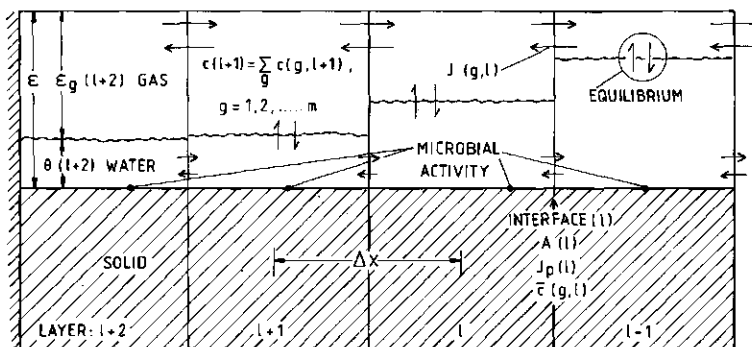


Fig. 2. Geometry of soil system.

where $J(g,l)$ represents Fick's first law, and $V(g,l)$ is the volume that is occupied by gas g in layer l :

$$V(g,l) = (\bar{\epsilon}_g(l) + K(g) \bar{\theta}(l)) V(l) \quad (8)$$

The assumption of instantaneous partitioning of gas over the gas and water phase is contained in $V(g,l)$. A bar above a symbol indicates the linearly interpolated spatial average of that symbol with respect to the layer in brackets and the previous one. Note that index l may denote the number of the layer or the number of the layer-interface with the previous one. When water would be stationary, Eqs.(5) through (8) would suffice to solve the pressure adjustment flux as explained below.

Water movement into a layer will induce a counter current of gas mixture in its gas phase. Since concentration is amount ($A_m(g,l)$) per unit volume, the rate of change of the concentration of $c(g,l)$ can be written as:

$$\frac{\Delta c(g,l)}{\Delta t} = \frac{\Delta}{\Delta t} \left\{ \frac{A_m(g,l)}{V(g,l)} \right\} \quad (9)$$

Differentiating the right hand side of Eq.(9) gives

$$\begin{aligned} \frac{\Delta c(g,l)}{\Delta t} &= \frac{1}{V(g,l)} \frac{\Delta A_m(g,l)}{\Delta t} - \frac{A_m(g,l)}{V(g,l)} \frac{1}{V(g,l)} \frac{\Delta V(g,l)}{\Delta t} = \\ &= \frac{\Delta c'(g,l)}{\Delta t} - c(g,l) \frac{1}{V(g,l)} \frac{\Delta V(g,l)}{\Delta t} \end{aligned} \quad (10)$$

The term $\Delta c'(g,l)/\Delta t$ of Eq.(10) is defined by Eq.(7); the second term needs further explanation, in particular the rate of change of $V(g,l)$. In Eq.(8), that defines $V(g,l)$, the gas-filled porosity, $\bar{\epsilon}_g(l)$, can be eliminated by the identity: $\bar{\epsilon}_g(l) = \epsilon - \theta(l)$. Differentiating the resulting expression yields

$$\frac{\Delta V(g,l)}{\Delta t} = (K(g) - 1) V(l) \frac{\Delta \theta(l)}{\Delta t} \quad (11)$$

The last derivative represents the net rate of change of water content, that follows directly from the water flow submodel: $(J_w(l) A(l) - J_w(l+1) A(l+1))/V(l)$. The principal equation for the rate of

change of total gas concentration in layer l is obtained by substituting this last expression in Eq.(11), then substituting Eq.(7) and Eq.(11) in Eq.(10), and finally taking the sum over the rates of change of all gases as meant by Eq.(6):

$$\begin{aligned}
 \frac{\Delta c(l)}{\Delta t} = & \sum_g \left\{ \frac{A(l)}{V(g,l)} (J(g,l) + J_p(l) \frac{\bar{c}(g,l)}{c(l)}) \right\} - \\
 & \sum_g \left\{ \frac{A(l+1)}{V(g,l)} (J(g,l+1) + J_p(l+1) \frac{\bar{c}(g,l+1)}{c(l+1)}) \right\} + \\
 & \sum_g \frac{S(g,l)}{V(g,l)} - \\
 & \sum_g \left\{ \frac{(K(g) - 1) (J_w(l) A(l) - J_w(l+1) A(l+1))}{V(g,l)} \right\} \quad (12)
 \end{aligned}$$

To take account of the diffusive, dispersive, and mass transports of gases in the water phase of soil, these were summed and added to the terms $J(g,l)$ and $J(g,l+1)$ as if they formed part of the gas phase fluxes. These transports were calculated by Eq.(3) in which the appropriate constants were substituted.

To solve Eq.(12) for the pressure adjustment fluxes $J_p(l)$, two situations need be distinguished for the present simulation model:

- 1) all layers have gas-filled porosities exceeding a certain critical value $\epsilon_{g,crit}$, and exchange of gases between soil and atmosphere takes place via both gas and water phase. $\epsilon_{g,crit}$ is assumed to be the value where air permeability is just measurable (Le Van Phuc and Morel-Seytoux 1972); such layers are further referred to as gas-continuous layers.
- 2) a number of consecutive layers is gas-continuous, but they are sealed from the atmosphere by one or more layers that have gas-filled porosities smaller than $\epsilon_{g,crit}$.

When the first situation occurs, atmospheric pressure is maintained and $\Delta c(l)/\Delta t = 0$ for all layers.

The set of linear equations needed to solve $J_p(l)$ was obtained as follows: equate Eq.(12) to zero for all layers; rewrite the summation terms to separate the terms containing $J_p(l)$ from other terms, and bring all terms containing $J_p(l)$ to the left of the equal sign. No outflow of gas occurs from the last layer, e.g. the $(l+2)$ nd layer in Fig. 2, because it is the center of the cylindrical aggregate, and $J(g,l+1)$, $J_p(l+1)$, and $J_w(l+1)$ in Eq.(12) equal zero. Each equation (except the

last) of the set of linear equations now contains terms with $J_p(l)$ and $J_p(l+1)$, and the set may be written in matrix notation from which the vector of pressure adjustment fluxes can be solved.

When the second situation occurs in which a number of gas-continuous layers is enclosed by layers that have very small gas-filled porosities, exchange of gases between soil and atmosphere takes place via the water-phase (Fig. 1b). When net gas production differs from the gas transport through the water phase, the total gas pressure in the enclosed layers will change, and the difference between the rates of change in consecutive layers must be zero. The set of linear equations needed to solve $J_p(l)$ was obtained similarly to the previous situation with the modification that at first the difference between each pair of adjacent layers was equated to zero: $\Delta c(l)/\Delta t - \Delta c(l+1)/\Delta t = 0$, for all l .

The J_p -vector was solved for each time step during the simulation using the mathematical libraries of IMSL (IMSL 1982). Subsequently, the pressure adjustment fluxes $J_p(l)$ were used in Eq.(4).

One problem remains to be solved. Suppose that the initial distribution of water in soil is (schematically) given by Fig. 1b. In the outer layers, where $\epsilon_g < \epsilon_g^{crit}$, gas exchange takes place via the water phase, and the total gas concentrations in these layers will undoubtedly be different from the enclosed gas-continuous layers. Since water redistributes, layers at the water front will become gas-continuous, and a jump in total gas concentration will appear. Moreover, when the outer layer becomes gas-continuous, such a jump in total gas concentration will occur at the interface of the aggregate and the surroundings. The principle assumption in this study was, however, that no gradients in total gas concentration could occur in soil when $\epsilon_g > \epsilon_g^{crit}$. Therefore, such differences in total gas concentration were adjusted instantaneously, the production terms from the denitrification submodel and the gas transport parameters were recalculated, and then the usual calculations as described above were continued. The following equations were derived to achieve this adjustment, resulting in equal total gas concentrations in all adjacent gas-continuous soil layers.

Assume that layer (l-1) (see Fig. 2) has just become gas-continuous, and that it contains a larger total gas concentration with respect to the adjacent layers l, l+1, etc. The amount of gas from layer (l-1) that will expand into layer l is defined by Eq.(13):

$$\Delta A_m(l-1) = \sum_g \Delta A_m(g, l-1) = \sum_g A_p(l) \frac{c(g, l-1)}{c(l-1)} \quad (13)$$

A_p denotes the amount of gas needed to adjust the pressures in adjacent layers. Since all consecutive layers, i.e. l, l+1, etc, have similar total gas concentrations, a certain amount of gas from layer l will expand into the next layer and so on. The final total gas concentration (i.e. after the adjustments) in, for instance, layer l, is defined by Eq.(14):

$$c(l) = \sum_g \frac{A_m(g, l) + A_p(l) \frac{c(g, l-1)}{c(l-1)} - A_p(l+1) \frac{c(g, l)}{c(l)}}{V(g, l)} \quad (14)$$

To solve Eq.(14) for the amounts of gas transferred due to pressure adjustment, the difference between each pair of adjacent layers was equated to zero, similar to the case where a number of gas-continuous layers was enclosed by layers that had gas-filled porosities smaller than ϵ_g^{crit} .

The procedure to obtain the set of linear equations from which the vector A_p was solved, was similar to the one to solve the pressure adjustment fluxes described above.

When the new gas-continuous layer contained a smaller total gas concentration with respect to adjacent layers, the direction of the adjustment was reversed, and Eq.(14) was formulated slightly different. All principles remain unchanged, however.

In the case that the outer soil layer became gas-continuous, total gas concentration in the aggregate was adjusted to that of the surroundings, and, since the chamber that contained the experimental aggregate was always kept at atmospheric pressure (Leffelaar 1986), this was also done in the simulation.

Computer program

Numerical calculations were done by a program written in Continuous System Modeling Program III (CSMP III) language (IBM 1975), and executed on a VAX machine. The program was developed and written with two targets in mind (apart from the purpose to simulate the processes of respiration and denitrification in the unsaturated soil aggregate): 1) to facilitate the communication of the model and the very large program to others; 2) to minimize programming errors. Therefore, the calculation sequence has been summarized in terms of call's to (FORTRAN) subroutines in the main (CSMP) program. The main program contains three major sections: 1) a parameter section, summarizing all biological, soil physical, chemical, and run time control parameters; 2) an initial section, mainly to calculate the amounts of the state variables at time zero, and to convert a number of parameters to SI-units and to 20 °C; all actual input parameters for the dynamic section are printed for control purposes; 3) a dynamic section, starting with the state variables in terms of amounts contained in integrals. The latter is followed by subsections to calculate: a) derived quantities from the state variables (material balances, concentrations, gradients, conductivities, diffusion coefficients, and reduction factors due to tortuosity), b) production terms, c) gross rates of change of each integral value, and d) net rates of change of each integral value. A last subsection contains the routines for printing results. The types of subroutines that are called from the dynamic section can be classified similarly to the subsections distinguished there. In addition, however, subroutines that contain only the control structures to choose the correct calculation subroutines, i.e. on basis of the actual environmental conditions, are distinguished. Thus, the extensively structured program enables one to get a quick overview of the calculations, whereas details may be studied in the separate subroutines. Care has been taken to maintain the recognizability of the rate equations in the subroutines. The program contains 120 subroutines and 110 pages of code. Process descriptions of respiration and denitrification, gastransport, watertransport, and solute transport take about 20, 55, 20, and 5 % of the program code, respectively. The simulations reported in this work took about 100 and 300 minutes CPU-time on a VAX-8700 and VAX-785 machine, respectively, for a 45

hours real time simulation. Few comments have been given in the program code, except for the subroutines that contain the control structures. Instead, units and abbreviations of all variables, and short subroutine descriptions have been given in a separate listing (45 pages). A system to abbreviate variables was designed and applied to improve the recognizability of the variables, and the readability of the program.

All results presented have been obtained by the variable time step integration method of Runge-Kutta Simpson, that is especially provided for continuous processes. During a simulation, however, discontinuities in total gas pressure may occur when a layer has become gas-continuous. At such events and when the preceding integration is successfully completed, as indicated by the CSMP integration status variable, the pressure adjustment algorithm is executed and the values of the state variables in the integrals are adjusted. Just before and after the adjustment procedure, the values of the gas pressures and concentrations in the aggregate layers and in the chamber that contained the aggregate, are printed in a separate file for control purposes. Material balances of water, nitrogen, and carbon were computed during the simulation runs, and were found to be correct. To prevent adverse numerical effects of the occurrence in the simulations of slightly negative amounts or concentrations of substances that were consumed, small ($< 0.5\%$ with respect to maximum of variable) threshold values were introduced. Below these threshold values, the appropriate consumption rates were set to zero. The program gives results in terms of rates of respiration and denitrification; fluxes of gases, water, and substrates; concentrations of biomass (with respect to dry soil mass), water (with respect to volume of soil), and substrates (with respect to volume of water); and concentrations and pressures of gases in the aggregate layers and in the chamber that contains the aggregate.

Model parameters

The procedure followed to come to a judgment about the simulation model was similar to the one proposed by Leffelaar and Wessel: data not measured during the present study were gathered from different authors, and then it was investigated whether it was possible to simulate the overall picture of the experiment by modifying some of the gathered data within reasonable limits.

Pertinent data of aggregate

The initial volume of the chamber that contained the aggregate for the reported experiment was 530 cm^3 .

Aggregate dimensions were those of the experimental system: height and diameter 2.59 and 9.8 cm, respectively (Leffelaar 1986). Fourteen concentric layers were distinguished to characterize the space coordinate of the model aggregate: 5 layers of 0.2 cm, 2 of 0.3 cm, 2 of 0.4 cm, and 5 of 0.5 cm. The choice of both number and grouping of layers was based on a compromise between the need to simulate the expected large gas concentration gradients in the wet outer soil layers with

reasonable accuracy, and to optimize the time step used for the Runge-Kutta Simpson integration method both with respect to maintaining numerical stability and to minimize round-off errors in this single precision integration algorithm. Soil porosity, $0.478 \text{ cm}^3 \text{ cm}^{-3}$, was calculated from the volume and amount of soil, using a particle density of 2.65 g cm^{-3} . Gas pressures in the soil layers and in the chamber that contained the aggregate were initiated according to the gas composition used to flush the respirometer system (Leffelaar 1986): 19.525 kPa and 81.8 kPa for oxygen and neon, respectively. The amount of solution added to the aggregate at the start of the simulation was 43.2 cm^3 ; it contained 3.0 g/l of glucose and 8.44 g/l of potassium nitrate, so that the amounts of C and N applied were similar to those in the experiment.

Microbiological characteristics

Microbiological parameters for bacteria that can grow with oxygen as electron acceptor under aerobic conditions or with nitrate, nitrite, and nitrous oxide as electron acceptor under anoxic conditions (further called denitrifiers), were discussed by Leffelaar and Wessel with respect to anoxic conditions. The data reported in their Table 2 (column 5) with respect to biomass concentration ($[B]$), maximum relative growth rates (μ), half saturation values (K), maximum growth yields (Y), and maintenance coefficients (m) on different electron acceptors were used as a starting point in the present study; these data are not repeated here. The data could not be used directly because, unfortunately, Leffelaar and Wessel used loam soil from Herveld, whereas Leffelaar (1986) used sandy loam soil from Lelystad. After some preliminary simulation runs, it appeared that reasonable results were obtained with respect to the experimental data (Leffelaar 1986), when $[B]$ was set at $10^{-5} \text{ kg C per kg of dry soil}$ (0.1), the initial mass fraction of denitrifiers with respect to total biomass (F_{den}) was set at 0.8 (40), and the maximum growth yield, Y , on nitrate and nitrite was set at 0.025 (0.25) and 0.214 (4), respectively, where bracketed numbers indicate the factors with which the data of Leffelaar and Wessel were multiplied to arrive at the present data. Other previously reported microbiological parameters remained unchanged.

Maximum relative growth rates with oxygen as electron acceptor are needed for both the bacteria that can only grow with oxygen as electron acceptor (further called strict aerobes) and the denitrifiers. As a first estimate for both groups of bacteria, this value was taken equal to the sum of the maximum relative growth rates on the nitrogenous electron acceptors, i.e. $0.75 \text{ } 10^{-5} \text{ s}^{-1}$.

A half saturation value (K) for oxygen respiration in water saturated soil crumbs was reported by Greenwood (1961): $10^{-3} \text{ mol O}_2 \text{ m}^{-3} \text{ H}_2\text{O}$. This value was used for the aerobic respiration of the strict aerobes. The half saturation values on glucose for strict aerobes and denitrifiers under aerobic conditions were taken similar to the value for the denitrifiers under anaerobic conditions: $0.0174 \text{ kg C m}^{-3} \text{ H}_2\text{O}$ (Shah and Coulman 1978).

Maximum growth yields, Y , and maintenance coefficients, m , on glucose as carbon source and oxygen as electron acceptor are needed in the model. Van Verseveld et al.

(1977) and Meijer et al. (1977) reported values for Paracoccus denitrificans grown in continuous culture under respectively anaerobic and aerobic conditions on gluconate ($C_6H_{12}O_7$) as carbon source and nitrate or oxygen as electron acceptor. Y_c and m_c values in both studies were very similar. Therefore, the values for glucose under aerobic conditions were taken identical to those under anaerobic conditions: $0.503 \text{ kg B kg}^{-1} \text{ C}$ and $0.212 \text{ } 10^{-5} \text{ kg C kg}^{-1} \text{ B s}^{-1}$. The values used for Y_{O_2} and m_{O_2} were $0.65 \text{ kg B kg}^{-1} \text{ O}_2$ and $0.382 \text{ } 10^{-5} \text{ kg O}_2 \text{ kg}^{-1} \text{ B s}^{-1}$, respectively. These values were obtained by converting the values reported by Meijer et al. (1977), using the elementary composition of Paracoccus denitrificans as explained previously (Leffelaar and Wessel). After the preliminary simulation runs a value of $0.16 \text{ kg B per kg O}_2$ was adopted for Y_{O_2} : this is the value of Meijer et al. (1977) multiplied with the ratio (0.25) of the sum of the maximum growth yields on nitrogenous compounds as used in the present study to the sum of the literature compilation by Leffelaar and Wessel (their Table 2, 4th column).

The mineralization parameters, F_c and F_n , were taken 0.6 under aerobic conditions.

The oxygen pressures that delimit the transition zone where denitrifiers may utilize both oxygen and nitrogenous compounds as electron acceptor were 101 ($[O_2]_i$) and 1013 ($[O_2]_h$) Pa, respectively (Leffelaar 1987).

Hydraulic characteristics

Initial water distribution was given by the water content measurement at the start of the experiment reported previously (Leffelaar 1986); it is reproduced here in Fig. 4 in the section about results and discussion. The main water retention curves and the hydraulic conductivity curves for the sandy loam soil from Lelystad are depicted in Fig. 3. The data points for the main water retention curves were obtained for uniformly packed soil samples contained in perspex rings (diameter and height 2.7 and 1 cm, respectively) of which the bottom was closed by a gauze. The soil used was pulverized to pass a 0.5-mm sieve, similar to the soil used to prepare the experimental aggregate (Leffelaar 1986). Soil pressure heads for the desorption curve were applied using a Blokzijl sand box (0, 10, 31.5, and 100 cm), a kaolin box (270, 520, and 1000 cm), and a pressure membrane apparatus (16000 cm) according to procedures described by Stakman (1974). Soil water pressure heads for the main sorption curves were started at a pressure head of 520 cm using initially air-dry soil. Treatments were quintuplicated. The dashed water retention curves in Fig. 3 were obtained by the optimization procedures by van Genuchten (1978); the continuous hand drawn envelop curves produced the best agreement between measured and simulated water contents, however. Therefore, these were used to produce the data presented below. Assuming that the aggregate followed the main drying curve before the solution was added, initiation of pressure head in each compartment was carried out according to the primary wetting scanning curve that is also shown in Fig. 3. To calculate the scanning curves, a hyperbolic type of equation, $y = a / (|\theta - \theta_r| + a)$, was used (Dane and Wierenga 1975): when the difference

between the water content where a reversal from e.g. drying to wetting occurs (θ_r) and the actual water content (θ) equals a, the scanning curve is halfway between the main water retention curves. The pressure head at the actual water content is then given by the sum of the pressure head at the main drying curve times y , and the main wetting curve times $(1-y)$. Parameter a in the hyperbola was taken $0.01 \text{ m}^3 \text{ m}^{-3}$ (Dane and Wierenga 1975).

The hydraulic conductivity- water content curves in Fig. 3 were calculated from the envelop water retention curves by procedures outlined by van Genuchten (1978): these calculations gave the relative hydraulic conductivity curves, however, and a matching point was needed, e.g. the saturated hydraulic conductivity. Saturated hydraulic conductivity was obtained using similarly prepared soil samples as used for the water retention curves in small perspex cylinders (diameter and height 1.6 and 10 cm, respectively), following the constant head method described by Kessler and Oosterbaan (1974). The value obtained, $5 \text{ } 10^{-7} \text{ m s}^{-1}$, was determined in quadruplicate. The preliminary simulation runs showed that the rate of water redistribution hardly affected the course of other processes since gas-continuity between the aggregate and the surroundings did not occur at the final water distribution. Therefore, solely to reduce computer time, the saturated hydraulic conductivity was taken 5 times smaller.

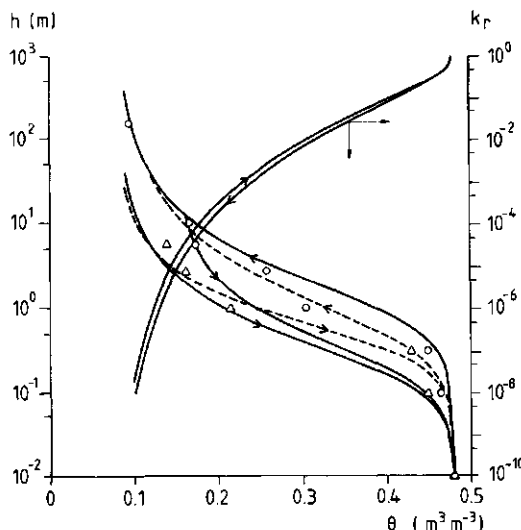


Fig.3. Experimental (o: desorption; Δ : sorption), curve-fitted (---, van Genuchten 1978), and hand drawn envelope (—) soil water retention curves that produced the best agreement between measured and simulated water contents, and primary wetting scanning curve used for initiation of model; calculated (—, van Genuchten 1978) relative hydraulic conductivity curves based on hand drawn water retention curves, for Lelystad sandy loam.

Transports characteristics in the water phase

Diffusion coefficients for nitrate and glucose at 25 °C were $19 \cdot 10^{-10}$, and $6.7 \cdot 10^{-10} \text{ m}^2 \text{ s}^{-1}$, respectively (Harremoës 1978). (Correction of data to 20 °C would not exceed 3 %, and was neglected.) The value for nitrite was not reported; it was taken equal to the one for nitrate.

Diffusion coefficients at about 20 °C for oxygen, carbon dioxide, and molecular nitrogen in water were $20 \cdot 10^{-10}$, $16.5 \cdot 10^{-10}$, and $22 \cdot 10^{-10} \text{ m}^2 \text{ s}^{-1}$, respectively (Harremoës 1978). The values for nitrous oxide and neon were not reported; they were taken equal to those of carbon dioxide and molecular nitrogen because of their respective similarities in molecular weights. From the preliminary simulation runs it appeared that hardly any gaseous exchange between the interior of the aggregate and the surroundings occurred when these literature data were used. The experimental findings (Leffelaar 1986), however, showed that exchange of gases between the aggregate and the surroundings was much more pronounced. Therefore, assuming that gaseous transports through the water phase of soil were well described, it seems probable that in the experimental aggregate these transports were enhanced, e.g. through small cracks in the outer part of the aggregate. In an attempt to take account of this enhancement in gaseous exchange, the diffusion coefficients of gases in water were set 10 times higher compared with the literature values for pure water. Gas solubility coefficients at 20 °C and 1 atmosphere for oxygen, carbon dioxide, nitrous oxide, molecular nitrogen, and neon were reported by Wilhelm et al. (1977): 0.033, 0.937, 0.679, 0.017, and $0.011 \text{ m}^3 \text{ gas m}^{-3} \text{ water}$, respectively. The relationship between the tortuosity factor for diffusion of solutes and gases in the water phase and soil water content were taken from a literature compilation by Leistra (1978): values for λ_w were 0.03, 0.1, 0.2, 0.34, and 0.5 for θ -values of 0.1, 0.2, 0.3, 0.4, and $0.5 \text{ m}^3 \text{ m}^{-3}$, respectively. The value for the dispersion length (L_d) for this fine packed soil was suggested by Prof. G.H. Bolt (personal communication): 0.001 m.

Transport characteristics in the gas phase

Parameters and equations needed to calculate binary diffusion coefficients were reported previously (Leffelaar 1987). The resulting values for D_{iNe} at 20 °C and atmospheric pressure were: $0.32 \cdot 10^{-4}$, $0.24 \cdot 10^{-4}$, $0.24 \cdot 10^{-4}$, $0.31 \cdot 10^{-4}$, and $0.49 \cdot 10^{-4} \text{ m}^2 \text{ s}^{-1}$ when i stands for oxygen, carbon dioxide, nitrous oxide, molecular nitrogen and neon, respectively. As a first approximation, the tortuosity factor for diffusion of gases in the gas phase, λ_g , was represented by the same relationship as the one used for solutes in the water phase: for the gases it was related to the gas-filled porosity, however. The value for the gas-filled porosity where soil was considered gas-continuous, $\varepsilon_g^{\text{crit}}$, was taken $0.063 \text{ m}^3 \text{ m}^{-3}$. This value was simply just sufficient to prevent gas continuity throughout the aggregate. The preliminary simulations showed that when $\varepsilon_g^{\text{crit}}$ was taken slightly smaller, gas continuity occurred, anaerobiosis quickly disappeared, and denitrification ceased: such results were contradictory to

the experimental findings (Leffelaar 1986) and it was thus concluded that no gas-continuity had occurred in the experiment. The value of about 6 % for the critical gas-filled porosity was near to experimental values found by Le Van Phuc and Morel-Seytoux (1972), and Corey (1957).

RESULTS AND DISCUSSION

A representative experimental data set on the distribution of water, gases, and nitrogen species was discussed by Leffelaar (1986). Present simulation results are compared with that particular data set in the Figs. 4 through 7. The experimental results from Leffelaar (1986) are represented by the smooth curves as previously drawn through the data points. Actual data points have been omitted here to improve readability of the figures; for an assessment of the quality of experimental curves and data points, reference is made to the original paper.

Figure 4 shows the volumetric water distribution at the start of the simulation and at the end, after 45 hours: simulated redistribution was essentially completed after 12 hours. Simulated curves are not smooth, since plotted water contents were obtained by weighing and summing the water contents of the concentric layers that coincided with a measuring location: thus plotted data refer to the rectangular geometry of the water measurements obtained by gamma radiation (de Swart and Groenevelt 1971). The major portion of the simulated and experimental curves match very well. The simulated curve at 45 hours was fully determined by the initial water distribution and the water retention curves shown in Fig. 3. At the outside of the

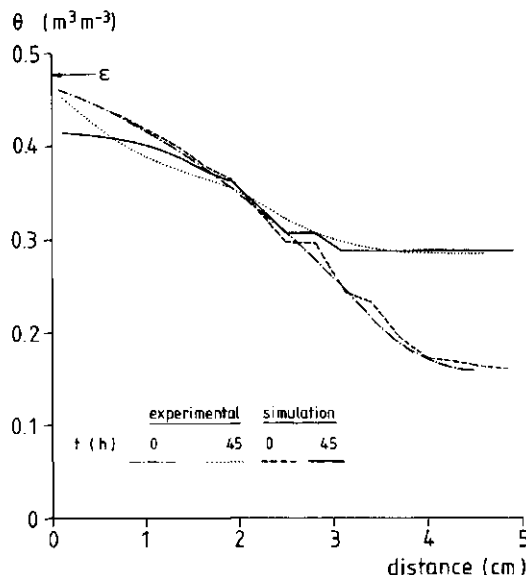


Fig.4. Simulated and experimental volumetric water distribution in soil aggregate (center at distance 4.9 cm) at time zero and after 45 hours.

aggregate, however, the simulated water content is about 1-3 % lower than the experimental value, and consequently the air-filled porosity at the outside was that much higher. The critical air-filled porosity in the simulation was so chosen, that no gas continuity would occur after redistribution of water, in accordance with the experimental findings. When the critical air-filled porosity was taken slightly lower, however, the aggregate became gas-continuous, anaerobiosis disappeared quickly, and denitrification ceased. It thus appears that air-filled porosity is a determining factor in the regulation of oxygen status of soil and with this in the regulation of denitrification.

Figure 5 shows oxygen pressures (left y-axis) in the aggregate center and the periphery to equal about zero after 14 h. The oxygen pressure curves show satisfactory similarity to the experimental findings. (The experimental results of peripheral (dotted line) and central (short-dash line) electrodes coincided up to about 10 hours; after about 14 hours the experimental results of the central electrode coincided with the simulated results.) The simulated results show an interesting feature of the model: when the layer where the peripheral oxygen electrode is located becomes gas-continuous, a pressure jump occurs. This feature has a number of aspects. First, the oxygen pressure in the layer that has become gas continuous was about 4 kPa lower than in the adjacent series of gas-continuous layers before the pressure jump occurred; hardly any gradient in oxygen pressure occurred in

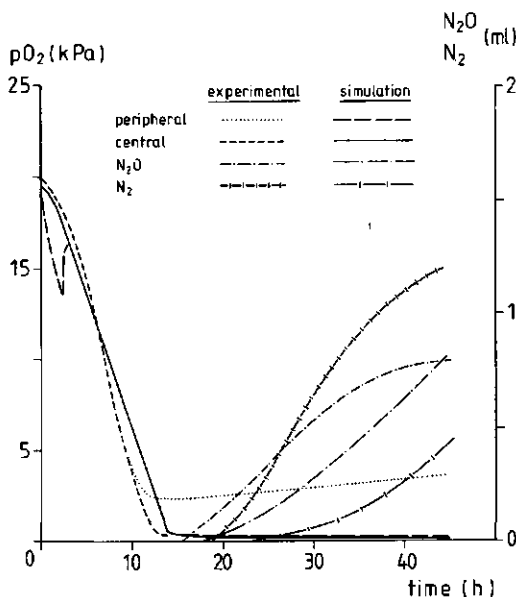


Fig.5. Simulated and experimental oxygen pressure (left y-axis) in center and 4 cm from center (peripheral) of soil aggregate and volumes of nitrous oxide and molecular nitrogen in chamber that contains the aggregate (right y-axis) as function of time.

the adjacent series of layers. Thus, gaseous transport through the water phase was very limited. Second, this jump or a more gradual change in oxygen pressure was not found in the experimental results. Therefore, it is very probable that gas-continuity has been present in the layers where the oxygen electrodes were located in the experiment, resulting in similar electrode readings. Third, such pressure jumps focus attention to the practical problem of measuring oxygen pressure by polarographic Clark-type oxygen electrodes (Leffelaar 1986). The calculated absolute pressure in the layer that has become gas-continuous was 86.9 and 103.9 kPa before and after the jump, respectively. Since changes in absolute pressure cause proportional changes in oxygen pressure, Clark-type oxygen electrode measurements will be directly affected (Fatt 1976). The simulated results were obtained using diffusion values for gases in water that were 10 times higher than those reported in the literature, to take account of possible enhancement of gaseous exchange between the aggregate and the surroundings, as explained in the section about model parameters. When the literature values were used, however, the results of the oxygen electrodes were hardly affected after the pressure jump; before that moment, oxygen pressure at the location of the peripheral electrode had decreased to 11.5 kPa instead of 13.4 kPa (Fig. 5). This result would mean that the time course of the oxygen pressure is mainly determined by the actual soil respiration rate and the amount of oxygen present at time zero, and to a lesser extent by gaseous transport through the water phase.

Figure 6 shows that the oxygen outside the aggregate decreased much slower than in the experiment. Oxygen decrease will be determined by the respiration rate and

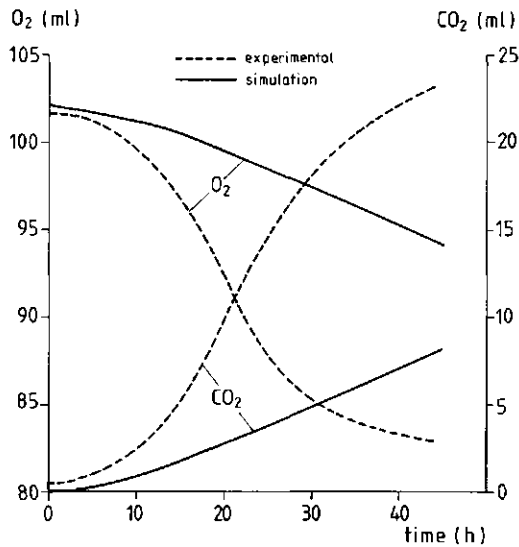


Fig.6. Simulated and experimental volumes of oxygen (left y-axis) and carbon dioxide (right y-axis) in chamber that contains the aggregate as function of time.

the volume of the aerobic outer shell of the aggregate, Fig. 1b. Introduction of higher aerobic respiration rates in an attempt to better match the experimental decrease of oxygen in the soil container, however, caused a proportionally faster decrease of the oxygen pressures at the locations of the electrodes. Thus, the enhancement in gaseous exchange between the aggregate and the surroundings was stronger than represented by the 10 times higher diffusion coefficients in the water phase, and a greater part of the soil volume did participate in oxygen respiration in the experiment. The ratio of oxygen flux density at 21 h in the experiment ($2.7 \text{ L O}_2 \text{ m}^{-2} \text{ d}^{-1}$, Leffelaar 1986) to that of the simulation ($0.61 \text{ L O}_2 \text{ m}^{-2} \text{ d}^{-1}$) would suggest that the order of magnitude of the aerobic shell in the experiment was about four times larger compared with the simulation. Since oxygen penetration in the simulation equalled about 0.2 cm, this would mean that in the experiment oxygen penetrated into the aggregate to a depth of about 0.8 cm. This is very near to the peripheral electrode, that in fact stabilized at about 2 kPa in the experiment, Fig. 5.

Figure 6 also shows the development of carbon dioxide. Though the simulated curve lags behind compared with the experimental one, it is near complementary to the simulated oxygen curve, resulting in a respiration quotient of about one. In fact, the respiration quotient behaved as a damped oscillation ($0.4(1\text{h}) \rightarrow 1.27(8\text{h}) \rightarrow 1.44(12\text{h}) \rightarrow 0.97(23\text{h}) \rightarrow 1.0(28\text{h})$) and stabilized after 28 hours. A respiration quotient of 1 was also found in the experiment (Leffelaar 1986). One would expect higher final values, however, since the whole of the aggregate was producing carbon dioxide, while only the outer shell consumed oxygen. When the literature values of the gas diffusion coefficients were used the sequence of respiration quotients was ($0.4(1\text{h}) \rightarrow 0.6(3\text{h}) \rightarrow 0.9(11\text{h}) \rightarrow 1.66(16\text{h}) \rightarrow 2.44(45\text{h})$), and no stabilization occurred. These simulated findings demonstrate a strong influence of transport processes on the respiration quotient of soil. Furthermore, the conclusion that the respiration quotient is not a sensitive measure to decide whether a soil is partially anaerobic, as suggested earlier on the basis of experimental results (Leffelaar 1986), is supported by these theoretical findings. The discrepancy between a respiration quotient of about 1 and the knowledge that soil is partially anaerobic was previously ascribed to the higher solubility of CO_2 in water compared with O_2 , with the expectation that CO_2 would be released slower from the soil than O_2 . As a consequence, the respiration quotient would be underestimated as long as no steady rates of exchange of CO_2 and O_2 were established (Leffelaar 1986). The above reasoning was not confirmed by theory: a simulation where the solubility of carbon dioxide in water was set 10 times smaller than the literature value, revealed that the respiration quotient was about halved before steady rates of exchange of CO_2 and O_2 were established. After 28 h it stabilized at about 1 again.

Production of nitrous oxide and molecular nitrogen is shown in Fig. 5. Though simulated curves lag behind with respect to the experimental curves, the flux densities of nitrous oxide and molecular nitrogen at 40 h, equalled 1.4 and 1.1 $\text{kg N ha}^{-1} \text{ d}^{-1}$, which was rather similar to the experimental values: 1.3 and 1.9 $\text{kg N ha}^{-1} \text{ d}^{-1}$, respectively. The curves of the development of nitrous

oxide and molecular nitrogen did not decrease as suggested by the experimental curves. On second thoughts, this suggestion might be misleading, since much nitrite, and some nitrate, was still found inside the experimental aggregate and denitrification probably continued (Leffelaar 1986). The linear increase of nitrous oxide and the curvilinear increase of molecular nitrogen with time in the simulation, can be explained by the fact that the pressure of nitrous oxide hardly changed inside the aggregate after 30 h, while that of molecular nitrogen increased by about 0.3-0.4 kPa per hour: thus the driving force for diffusive transport for N_2O remained similar, while that of N_2 increased.

Figure 7 depicts the simulated and measured distributions of nitrate and nitrite in the soil aggregate after 45 hours. The calculated nitrate distribution deviates strongly from the measured distribution: simulated concentrations decrease from outside to the center of the aggregate, whereas experimental concentrations increase. Note, however, that the model results are consistent with the assumption that reduction of nitrate due to denitrification will be less in regions where oxygen is present, i.e. the outer shell of the aggregate. In this respect the experimental results were rather unexpected: nitrate was depleted in a region where oxygen could probably penetrate (see above discussion with respect to oxygen in Fig. 6). It might be that the upper limit of oxygen pressure below which both denitrification and oxygen consumption may take place was actually higher in the experiment, causing more nitrate to be denitrified in the outer shell. The picture of the calculated nitrite

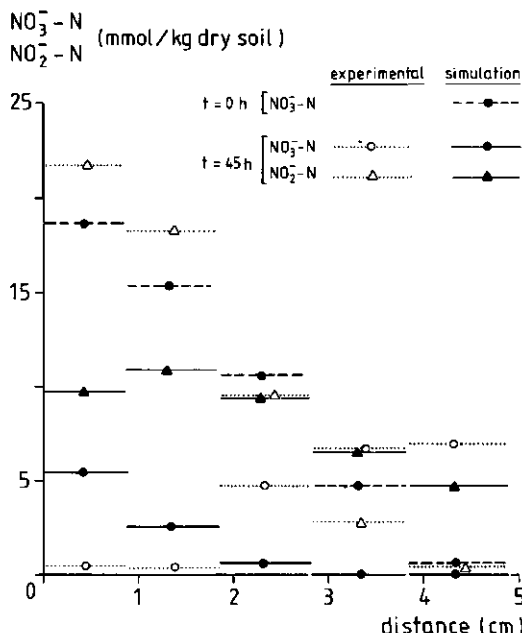


Fig.7. Simulated and experimental distributions of nitrate and nitrite in soil aggregate (center at distance of 4.9 cm) at time zero and after 45 hours.

concentrations resembled the measured data better. The influence of water redistribution on the simulated nitrite concentration is demonstrated in the center of the aggregate, where nitrite-N is much higher than the initial nitrate-N concentration. Thus either nitrate was leached into the center and subsequently denitrified to nitrite, and/or nitrite formed in adjacent soil layers was transported to the center.

CONCLUSIONS

It was concluded from the above discussion that the simulation model presented gives a satisfactory description of the soil biological system studied: part of the experimental results could be described quantitatively, e.g. water distribution and the time course of the oxygen pressure at the experimental positions of the electrodes, whereas other data that deviated from the experimental data, e.g. consumption rate of oxygen and production rates of carbon dioxide, nitrous oxide, and molecular nitrogen, could be understood by studying the dynamic behaviour of the model.

The model gives rise to the following conclusions about a number of physical soil properties that are usually not measured or considered in soil physics literature with respect to biological processes in soil:

- 1) the critical gas-filled porosity below which gaseous transports take place through the water phase, is a determining factor in gaseous exchange in soil;
- 2) soil water hysteresis is important in causing a non-homogeneous soil water distribution at a homogeneous pressure head distribution, implying that a small amount of added water is sufficient to decrease the gas-filled porosity to values smaller than the critical gas-filled porosity;
- 3) the rate at which water redistributes hardly affects the course of the biological processes if the final water distribution does not allow for gas-continuity between aggregate and surroundings;
- 4) the rate of water redistribution is very important, however, if gas-continuity does occur during the redistribution process: then, this rate determines the time period in which anaerobiosis and possibly denitrification can occur;
- 5) soil respiration may cause differences in soil atmospheric pressure of the order of magnitude of $\pm 10\%$ in the enclosed gas continuous part of the soil, which may affect soil hydraulic characteristics (Chahal 1966);
- 6) the exchange of gases between aggregate and surroundings is seriously underestimated when it is fully ascribed to diffusion through the water phase of gas-discontinuous soil layers: the model suggests that enhancement of gas exchange occurs, perhaps through small cracks in the outer part of the aggregate;
- 7) total gas pressure jumps, as simulated by the model, will affect the measurement of oxygen pressure by polarographic oxygen electrodes, though it remains to be investigated whether such pressure jumps will actually occur in field soil.

This study showed that the parameterization of the model formed the major problem that needs attention first. Therefore, a more extensive exploration of both

the experimental respirometer system (Leffelaar 1986) and the theoretical simulation model is intended for the near future: the model will be used first to plan experiments with respect to the respirometer system, second to help interpret the data so obtained, and third to investigate the relative importance of a number of parameters in a sensitivity analysis.

Finally, it was concluded that only the interaction between experiment and theory will ultimately lead to a full understanding of the complex soil biological system described.

ACKNOWLEDGMENTS

I wish to thank Ir. J.H.G. Verhagen and Dr. J. Goudriaan for their indispensable help to develop the equations to maintain equal total gas pressures in adjacent gas-continuous soil layers. Mr. A.J. Koster and Mr. G. Klein of the computer center of the University were so kind to provide the necessary memory space and CPU time to execute the program on the VAX. Mr. E. Korzilius is thanked for the determination of the hydraulic characteristics of the Lelystad soil, and for the development of the preliminary version of the soil water submodel. Mr. C. Rijpma skilfully prepared the figures. Prof. G.H. Bolt, Prof. C.T. de Wit, and Ir. J.H.G. Verhagen reviewed the manuscript.

LIST OF SYMBOLS

Symbol	Meaning	Unit
a	half transition constant in hysteresis hyperbola: when $ \theta - \theta_T = a$, half the transition to the main drying or wetting curve is completed	m^{-3}
$A(1)$	interfacial total soil area between adjacent layers; index refers to interface with previous layer	m^2
$A_m(g, 1)$	amount of gas g in layer 1	mol
$A(1)$	amount of gas transferred to adjust the pressure in layer 1 to that of adjacent layers; index refers to interface with previous layer	mol
B	amount of bacterial carbon. Refers either to strict aerobes or denitrifiers	kg C
$[B]$	concentration of bacterial carbon. Refers either to strict aerobes or denitrifiers	$\text{kg C kg}^{-1} \text{ dry soil}$

trifiers		
c_i	concentration of substance i . When $i=g$, it refers to gas, and units are either mol m^{-3} of gas phase or $\text{mol m}^{-3} \text{H}_2\text{O}$; when $i=s$, it refers to solute, and unit is $\text{kg m}^{-3} \text{H}_2\text{O}$	amount m^{-3}
$c, c(1)$	total molar gas concentration in general, $c = \sum_g c_g$, and with respect to layer 1, respectively	mol m^{-3}
$c(g,1), c'(g,1)$	molar concentration of gas g in layer 1; second concentration is defined by Eq.(7) and it is included in first concentration, Eq.(10)	mol m^{-3}
c_i	concentration of substance i with respect to volume of soil. When $i=g$, it refers to gas, and amount is mol; when $i=s$, it refers to solute, and amount is kg; when $i=w$, it refers to water, and amount is $\text{m}^3 \text{H}_2\text{O}$. Symbol is only used in the equation of continuity, Eq.(1)	amount m^{-3} of soil
D_0	diffusion coefficient of solute or gas in free liquid water	$\text{m}^2 \text{s}^{-1}$
D_{ij}	binary diffusion coefficient of gas pair $i-j$ in free air	$\text{m}^2 \text{s}^{-1}$
F_c, F_n	mass fraction of carbon and nitrogen that mineralizes from the dead biomass	-
F_{den}	initial mass fraction of denitrifiers with respect to total bacterial biomass	-
h	pressure head of soil water. h is a function of volumetric water content	m

h	subscript referring to high critical level	
J_i	flux of substance i . When $i=g$, it refers to gas, and amount is mol; when $i=s$, it refers to solute, and amount is kg; when $i=w$, it refers to water, and amount is $m^3 H_2O$	amount $m^{-2} s^{-1}$
$J(g,1)$	molar flux of gas g into layer 1	$mol m^{-2} s^{-1}$
$J_p, J_p(1)$	pressure adjustment flux in general and for the gas flux into layer 1, respectively; index 1 refers to interface with previous layer	$mol m^{-2} s^{-1}$
$J_w(1)$	flux of water into layer 1	$m^3 m^{-2} s^{-1}$
k	hydraulic conductivity. k is a function of volumetric water content	$m s^{-1}$
K	half saturation value with respect to carbon or electron acceptor	$kg m^{-3} H_2O$
$K(g)$	gas solubility coefficient in liquid water at 20 °C and one atmosphere	$m^3 gas m^{-3} H_2O$
l	subscript referring to low critical level, or bracketed index to indicate layer number	
L_d	dispersion length parameter	m
m_c, m_c	maintenance coefficients with respect to carbon or electron acceptor, and for carbon specifically, respectively	$kg kg^{-1} B s^{-1}$
p	pressure	Pa
P_i	net production term of substance i . When $i=g$, it refers to gas, and amount is mol; when $i=s$, it refers to solute, and amount is kg. For a gas in layer 1: $P_g = S(g,1)/V(1)$	amount $m^{-3} s^{-1}$

R	gas constant	$\text{Pa m mol}^{-1} \text{K}^{-1}$
$S(g,1)$	gas production term of gas g in layer 1	mol s^{-1}
t	time	s
T	absolute temperature	K
$V(1)$	volume of a soil layer, i.e. sum of volumes of gas, water and solids	m^3
$V(g,1)$	gas volume occupied by gas g in layer 1 with reference to both gas and water phases. $V(g,1)$ is defined by Eq.(8).	m^3
x	space coordinate	m
y	weight factor: outcome of hyperbolic equation that forces a scanning curve towards one of the main water retention curves ($0 \leq y \leq 1$)	-
y_c	maximum growth yield on carbon or electron acceptor, and on carbon specifically, respectively, when no substrate would be used for maintenance	kg B kg^{-1}
Δ	finite difference of concerning symbol	
$\varepsilon, \varepsilon_g$	total soil porosity, and actual volumetric gas content in general, and in layer 1, respectively: $\varepsilon_g = \varepsilon - \theta$	$\text{m}^3 \text{m}^{-3}$
$\varepsilon_g^{\text{crit}}$	critical gas content where gas phase in layers is just discontinuous	$\text{m}^3 \text{m}^{-3}$
$\theta, \theta(1), \theta_T$	volumetric water content in general, in layer 1, and at a transition point on wetting or drying curve where scanning drying or scanning wetting curve starts, respectively	$\text{m}^3 \text{m}^{-3}$
λ_i	tortuosity factor. When $i=w$, tortuosity in water phase; when $i=g$, tortuosity in gas phase. λ_w and λ_g are functions of θ or ε_g , respectively	-

μ	maximum relative growth rate on oxygen s^{-1} with glucose-C as carbon source
\sum	summation operator
\parallel	bars around a variable means absolute value
$\bar{-}$	superscript; linearly interpolated spa- tial average of concerning symbol with respect to the layer in brackets and the previous one

REFERENCES

Boesten, J.J.T.I. 1986. Behaviour of herbicides in soil: simulation and experimental assessment. Dissertation, Agricultural university, Wageningen, p.263.

Bolt, G.H. 1979. Movement of solutes in soil: principles of adsorption/ exchange chromatography. In Soil Chemistry B. Physico-chemical models. G.H. Bolt (ed.). Developments in Soil Science, SB. Elsevier, Amsterdam, pp.285-348.

Chahal, R.S. 1966. Effect of entrapped air and pressure on matric suction. *Soil Sci.* 102:131-134.

Corey, A.T. 1957. Measurement of water and air permeability in unsaturated soil. *Soil Sci. Soc. Am. Proc.* 21:7-10.

Currie, J.A. 1961. Gaseous diffusion in the aeration of aggregated soils. *Soil Sci.* 92:40-45.

Dane, J.H., and P.J. Wierenga. 1975. Effect of hysteresis on the prediction of infiltration, redistribution and drainage of water in a layered soil. *J. of Hydrol.* 25:229-242.

Delwiche, C.C. 1981. The nitrogen cycle and nitrous oxide. In Denitrification, nitrification, and atmospheric nitrous oxide. C.C. Delwiche (ed.). Wiley, New York, pp.1-15.

Fatt, I. 1976. Polarographic oxygen sensors. CRC Press, Cleveland, Ohio, p.278.

Frissel, M.J., and P. Reiniger. 1974. Simulation of accumulation and leaching in soils. *Simulation Monographs*, PUDOC, Wageningen, The Netherlands, p.116.

Genuchten, M.Th. van. 1980. A closed-form equation for predicting the hydraulic conductivity of unsaturated soils. *Soil Sci. Soc. Am. J.* 44:892-898.

Genuchten, R. van. 1978. Calculating the unsaturated hydraulic conductivity with a new, closed-form analytical model. Research Report 78-WR-08, Water Resources Program, Dep. of Civil Engineering, Princeton Univ., Princeton, NJ.

Goudriaan, J. 1973. Dispersion in simulation models of population growth and salt movement in the soil. *Neth. J. agric. Sci.* 21:269-281.

Greenwood, D.J. 1961. The effect of oxygen concentration on the decomposition of organic materials in soil. *Plant Soil* 14:360-376.

Harremoës, P. 1978. Biofilm kinetics. In *Water pollution microbiology*, vol 2. R. Mitchell (ed.). Wiley, New York, pp.71-109.

Hopmans, J.W., and J.H. Dane. 1986. Combined effect of hysteresis and temperature on soil-water movement. *J. of Hydrol.* 83:161-171.

IBM Corp. 1975. Continuous system modeling program III (CSMP III). Program reference manual. SH 19-7001-3. Data Processing Division, 1133 Westchester Ave., White Plains, N.Y.

IMSL. 1982. International mathematical and statistical libraries, Inc. Reference manual, edition 9. Customer relations, sixth floor, NBC building, 7500 Bellaire Boulevard, Houston, Texas, USA.

Ingraham, J.L. 1981. Microbiology and genetics of denitrifiers. In Denitrification, nitrification, and atmospheric nitrous oxide. C.C. Delwiche (ed.). Wiley, New York, pp.45-65.

Kessler, J., and R.J. Oosterbaan. 1974. Determining hydraulic conductivity of soils. In Drainage principles and applications. III. Surveys and investigations. ILRI, Wageningen, The Netherlands, pp.253-296.

Kool, J.B., and J.C. Parker. 1987. Development and evaluation of closed-form expressions for hysteretic soil hydraulic properties. *Water Resour. Res.* 23:105-114.

Koorevaar, P., G. Menelik, and C. Dirksen. 1983. Elements of soil physics. Developments in Soil Science, 13. Elsevier, Amsterdam, p.228.

Leffelaar, P.A. 1979. Simulation of partial anaerobiosis in a model soil in respect to denitrification. *Soil Sci.* 128:110-120.

Leffelaar, P.A. 1986. Dynamics of partial anaerobiosis, denitrification, and water in a soil aggregate: experimental. *Soil Sci.* 142:352-366.

Leffelaar, P.A. 1987. Dynamic simulation of multinary diffusion problems related to soil. *Soil Sci.* 143:79-91.

Leffelaar, P.A., and W. Wessel. Denitrification in a homogeneous, closed system: experiment and simulation. Submitted; chapter 5 of this dissertation.

Leistra, M. 1972. Diffusion and adsorption of the nematicide 1,3-dichloropropene in soil. PUDOC, Wageningen, p.105.

Leistra, M. 1978. Computed redistribution of pesticides in the root zone of an arable crop. *Plant Soil* 49:569-580.

Leistra, M. 1980. Transport in solution. In *Interactions between herbicides and the soil*. R.J. Hance (ed.). Academic Press, London, pp.31-58.

Leistra, M., R.H. Bromilow, and J.J.T.I. Boesten. 1980. Measured and simulated behaviour of oxamyl in fallow soils. *Pestic. Sci.* 11:379-388.

Le Van Phuc, and H.J. Morel-Seytoux. 1972. Effect of soil air movement and compressibility on infiltration rates. *Soil Sci. Soc. Am. Proc.* 36:237-241.

Meijer, E.M., H.W. van Verseveld, E.G. van der Beek, and A.H. Stouthamer. 1977. Energy conservation during aerobic growth in Paracoccus denitrificans. *Arch. Microbiol.* 112:25-34.

Shah, D.B., and G.A. Coulman. 1978. Kinetics of nitrification and denitrification reactions. *Biotechnol. Bioeng.* 20:43-72.

Smith, K.A. 1977. Soil aeration. *Soil Sci.* 123:284-291.

Smith, K.A. 1980. A model of the extent of anaerobic zones in aggregated soils and its potential to estimates of denitrification. *J. Soil Sci.* 31:263-277.

Stakman, W.P. 1974. Measuring soil moisture. In Drainage principles and applications. III. Surveys and investigations. ILRI, Wageningen, The Netherlands, pp.221-251.

Staple, W.J. 1966. Infiltration and redistribution of water in vertical columns of loam soil. *Soil Sci. Soc. Am. Proc.* 30:553-558.

Swart, J.G. de, and P.H. Groeneveld. 1971. Column scanning with 60 KeV gamma radiation. *Soil Sci.* 112:419-424.

Verseveld, H.W. van, E.M. Meijer, and A.H. Stouthamer. 1977. Energy conservation during nitrate

respiration in Paracoccus denitrificans. Arch. Microbiol. 112:17-23.

Wilhelm, E., R. Battino, and R. J. Wilcock. 1977. Low-pressure solubility of gases in liquid water. Chem. Rev. 77:219-262.

Wit, C.T. de. 1982. Simulation of living systems. In Simulation of plant growth and crop production. F.W.T. Penning de Vries, and H.H. van Laar (eds.). PUDOC, Wageningen, The Netherlands, pp.3-8.

Wit, C.T. de, and H. van Keulen. 1975. Simulation of transport processes in soils. Simulation Monographs, PUDOC, Wageningen, The Netherlands, p.100.

SUMMARY

Estimates of nitrogen losses by microbial denitrification from aerated, structured, partly water saturated agricultural soils, are reported to be substantial and to vary tremendously. Nitrogen losses form a waste of energy, labour, and money for the agricultural practice, whilst they also form a threat for the protective ozone layer of the stratosphere. The variation in the estimates of these nitrogen losses can partly be ascribed to indirect assessment of denitrification, for instance by N-balance methods, and partly by the complex nature of the process. A better understanding of the dynamic interactions between the biological and physical processes determining denitrification is expected to eventually lead to improved management practices involving timing and intensity of fertilizer application and irrigation, form of N-fertilizer, and tillage techniques.

Therefore, this study aimed at integrating existing knowledge about the major processes that were known to cause and affect denitrification by means of a mathematical explanatory dynamic simulation model, and at developing capability to test such a model by experiments in which denitrification could be assessed directly.

A preliminary simulation study (chapter 2) was conducted to assess where the bulk of anaerobiosis, and hence possibly denitrification, would be located in well structured soil. To this purpose, the dynamics of the volume of anoxic soil was studied as a function of respiratory activity and water distribution in a model soil composed of spherical aggregates in a hexagonal packing. This schematized geometry implied that two types of soil pores were distinguished: intra- and interaggregate pores.

Major conclusions obtained for an aggregate radius of 0.5 cm and a respiratory activity of about $10 \text{ L O}_2 \text{ m}^{-2} \text{ d}^{-1}$ for cropped soil, were that anaerobiosis always occurred to some extent within the aggregates, and that the lowest interaggregate soil pore oxygen pressure was about 20 kPa in the 0.25 m deep soil profile. The major difficulty of the model was to obtain experimental data to test it.

The knowledge that anoxity was mainly confined to within the aggregates and that gaseous nitrogen losses through denitrification will occur at such anoxic locations only when bacteria capable of denitrification, water, nitrate, and decomposable organic compounds are present there, has resulted in the experimental study of these state variables in an unsaturated, cylindrical soil aggregate, in which transport processes were radial (chapter 3). This geometry is a model representation of a soil aggregate from which the upper and lower sides are removed. The experimental aggregate was studied in a respirometer system that was specially designed for this purpose. The respirometer system enables one to measure simultaneously the distribution of water, oxygen, nitrate, nitrite, ammonium, and pH as a function of space and time in the unsaturated, artificially made, aggregate and the changes in atmospheric composition as a function of time in the chamber that contains the aggregate. Except for water transport, these processes are caused by microbial activity, because roots are not present in the aggregate. Nondestructive

measurements during an experiment involved gamma-ray attenuation, gas chromatography, and polarography. Destructive measurements were executed at the end of an experiment in the form of chemical analyses of soil.

A major conclusion was that hysteresis in the soil water retention curve had such a strong influence on the water distribution in the aggregate, that a small amount of added water was sufficient to cause permanent gas-discontinuity in the soil pores of the outer shell of the aggregate. As a result, the oxygen supply to the interior of the aggregate was severely decreased, and anaerobiosis occurred. Furthermore, large amounts of nitrite were found, whereas the release of gaseous denitrification products was underestimated due to the slow diffusion in the partially wet soil.

Therefore, assessment of denitrification through the measurement of nitrate alone will overestimate nitrogen losses, while the measurement of nitrous oxide and molecular nitrogen alone will give an underestimation. The consumption rate of oxygen ($2.7 \text{ L O}_2 \text{ m}^{-2} \text{ d}^{-1}$) and the production rates of carbon dioxide ($3.7 \text{ L CO}_2 \text{ m}^{-2} \text{ d}^{-1}$), nitrous oxide ($1.3 \text{ kg N ha}^{-1} \text{ d}^{-1}$), and molecular nitrogen ($1.9 \text{ kg N ha}^{-1} \text{ d}^{-1}$) compared well with field data for bare soil.

Finally, it was concluded that though the respirometer system yielded valuable coherent data to test the simulation model, full account of the interrelationships among these data could only be achieved by the same simulation model, because the measured variables reflect the integrated effect of biological activity and transport processes.

The cylindrical geometry of the experimental aggregate had the advantage that for the same geometry a simulation model could be developed. The model contains four submodels: 1) biological respiration and denitrification, 2) water transport including a description to account for hysteresis, 3) solute transport, and 4) gas transport including a new approach to maintain equal total gas pressures in adjacent gas-continuous soil layers. These submodels were separately developed and (partially) tested, before the integrated model was composed.

The submodel describing microbial respiration and denitrification for a homogeneous (i.e. spatially uniform in all phases) soil (chapter 5), includes growth and maintenance of biomass at the expense of glucose, and the concomitant reduction of nitrate to molecular nitrogen, via the intermediates nitrite and nitrous oxide, when anoxic conditions occur. Two groups of heterotrophic strict aerobic bacteria were considered, i.e. bacteria that can only grow with oxygen as electron acceptor, and bacteria that can grow with oxygen as electron acceptor under aerobic conditions or with nitrate, nitrite, and nitrous oxide as electron acceptor under anoxic conditions. Growth of both groups of biomass was calculated by a first order rate equation, in which the relative growth rate was described by a double Monod equation consisting of rate limiting factors for carbon and oxygen or nitrogenous substrates. The Pirt equation was used to calculate the consumption rates of substrates for growth and maintenance. As a starting point to parameterize the submodel, a data set was compiled from various literature sources, and it was investigated whether it would be possible to simulate experimental observations of the sequence of denitrification products by modifying some of these literature data within reasonable limits.

It was concluded that the model gave a satisfactory description of the denitrification process as measured in laboratory incubation vessels, but also that more definite conclusions about the quality of the model could only be obtained when biological data obtained from soil systems would become available.

The submodel describing diffusion of gases in multinary, isothermal, isobaric, ideal-gas mixtures such as the soil atmosphere, was based on Fick's first law that was extended with a flux term to maintain equal total gas pressures in adjacent soil layers. Pressure differences are in principle caused by unequal binary diffusion coefficients, different gas solubilities in water, mass flow of gas due to water movement, and unequal net gas production terms in adjacent soil layers. Fick's extended equation was tested for the simplified situation of a gas layer (which is comparable with a dry soil layer) in which respiration and denitrification took place, and where pressure differences were in principle caused solely by differences in binary diffusion coefficients: results agreed to within 10 % with the rigorous gas kinetic theory based on the Stefan-Maxwell equations (chapter 4). Binary diffusion coefficients were calculated using expressions from the rigorous gas kinetic theory. These compared to within 10 % with a number of experimental data that were relevant for soil aeration research, and it was decided to use the theoretical formula throughout the study.

A major conclusion was that the extended first law of Fick gives good results when binary diffusion coefficients do not differ by more than a factor of 2, and when one constituent of the gas phase is abundantly present, so that binary diffusion coefficients may be related to this component. Whenever such conditions do not hold, however, the Stefan-Maxwell equations must be used to study diffusion in gas mixtures.

The submodel describing water flow was directly tested against the data obtained from the respirometer system and appeared to agree well (chapter 6). The submodel for solute transport was not tested separately and may thus contain accumulated errors of other submodels.

The integrated simulation model (chapter 6) enables one to calculate simultaneously the distribution of bacteria, water, nitrate, nitrite, glucose, oxygen, carbon dioxide, nitrous oxide, molecular nitrogen, neon, and absolute soil atmospheric pressure, as a function of space and time in an unsaturated, homogeneous, cylindrical aggregate, and the changes in atmospheric composition as a function of time in the chamber that contains the aggregate. The simulation model is the theoretical counterpart of the experimental respirometer system.

The major conclusion was that the model gives a satisfactory description of the soil biological system studied: part of the experimental results could be described quantitatively, whereas other data that deviated from the experimental data could be understood by studying the dynamic behaviour of the model. Furthermore, the critical gas-filled porosity below which gaseous transport takes place only through the water phase appeared to be very important in determining soil anaerobiosis and hence possibly denitrification. Hysteresis in the soil water retention curve caused a non-homogeneous soil water distribution with the effect that a small amount of added water was sufficient to decrease the gas-filled porosity to values smaller than the

critical gas-filled porosity. This study revealed that the parameterization of the model formed a major problem that needs attention first.

Finally, it was concluded that only the interaction between experiment and theory will ultimately result in a full understanding of the complex soil biological ecosystem studied here.

SAMENVATTING

Dynamiek van partiële anaërobie, denitrificatie en water in grond: experimenten en simulatie

Schattingen van stikstofverliezen door microbiële denitrificatie uit doorluchtte, gestructureerde, gedeeltelijk met water verzadigde landbouwgrond zijn aanzienlijk en varieren flink. Stikstofverliezen vormen een verspilling van energie, arbeid en geld voor de landbouw, terwijl ze ook een bedreiging vormen voor de beschermende ozonlaag in the stratosfeer. De variatie in de schattingen van de stikstofverliezen kan deels toegeschreven worden aan het indirect vaststellen van denitrificatie, bijvoorbeeld door N-balans methodes, en deels aan de ingewikkeldheid van het proces. Een beter begrip van de dynamische wisselwerking tussen de biologische en fysische processen die denitrificatie bepalen zal uiteindelijk waarschijnlijk leiden tot een betere handelwijze met betrekking tot het tijdstip en de intensiteit van (kunst)mest toediening en irrigatie, de vorm waarin stikstof wordt gegeven en grondbewerkingstechnieken.

Daarom was deze studie gericht op het integreren van bestaande kennis omtrent de belangrijkste processen waarvan bekend was dat ze denitrificatie veroorzaken en beïnvloeden, door middel van een wiskundig verklarend dynamisch simulatiemodel, en op het ontwikkelen van de vaardigheid om zulk een model te testen met behulp van experimenten waarin denitrificatie direct kon worden vastgesteld.

Vooraf werd een simulatiestudie (hoofdstuk 2) uitgevoerd om vast te stellen waar zich het overgrote deel van anaërobie, en hiermee mogelijk denitrificatie, zou bevinden in goed gestructureerde grond. Hiertoe werd het dynamisch gedrag van het anaërobe bodemvolume bestudeerd als functie van de respiratieactiviteit en de waterverdeling in een modelgrond die opgebouwd was uit bolvormige aggregaatjes in een hexagonale staping. Door deze geometrie werden twee typen bodemporiën onderscheiden: intra- en interaggregaatporiën.

De belangrijkste conclusies, verkregen voor een aggregaatstraal van 0.5 cm en een respiratieactiviteit van ongeveer $10 \text{ L O}_2 \text{ m}^{-2} \text{ d}^{-1}$ voor begroeide grond, waren dat anaërobie altijd in zekere mate in de aggregaten voorkwam, en dat de laagste zuurstofdruk in de interaggregaatporiën ongeveer 20 kPa was in het 0.25 m diepe bodemprofiel. De belangrijkste moeilijkheid bij het model was het verkrijgen van experimentele gegevens om het te testen.

De wetenschap dat anaërobie hoofdzakelijk beperkt was tot de aggregaten en dat gasvormige stikstofverliezen door denitrificatie alleen zullen optreden op die anaërobe plekken als bacteriën welke kunnen denitrificeren, water, nitraat en afbrekbaar organisch materiaal aanwezig zijn, heeft geresulteerd in de experimentele studie van deze toestandsvariabelen in een niet met water verzadigd, cylindrisch bodemaggregaat, waarin transportprocessen radiaal waren (hoofdstuk 3). Deze geometrie is een modelvoorstelling van een bodemaggregaat waarvan de boven- en onderkant verwijderd zijn. Het experimentele aggregaat werd bestudeerd in een respirometersysteem dat speciaal voor dit doel was ontworpen. Met behulp van het

respirometersysteem kan de distributie van water, zuurstof, nitraat, nitriet, ammonium en pH worden gemeten als functie van de tijd in een niet met water verzedigd, kunstmatig samengesteld aggregaat. Bovendien kan de verandering in atmosferische samenstelling in de meetcel, waarin het aggregaat geplaatst is, gemeten worden als functie van de tijd. Met uitzondering van het watertransport, worden deze processen veroorzaakt door microbiële activiteit, omdat plantewortels niet in het aggregaat voorkomen. Metingen die uitgevoerd konden worden aan het aggregaat als geheel, betroffen metingen met gammastralen, gaschromatografie en polarografie. Metingen waarbij het aggregaat in stukjes moest worden opgedeeld, werden aan het eind van een experiment uitgevoerd in de vorm van chemische analyses van de grond. Een belangrijke conclusie was dat hysterese in de vochtcharakteristiek van de grond zo'n sterke invloed had op de waterdistributie in het aggregaat, dat een kleine hoeveelheid van buitenaf toegevoegd water al voldoende was om in de buitenste schil van het aggregaat blijvende gasdiscontinuïteit te veroorzaken in de bodemporiën. Als gevolg hiervan werd de zuurstoftoevoer naar het binnenste van het aggregaat sterk belemmerd, zodat anaërobie optrad. Verder werden grote hoeveelheden nitriet gevonden, terwijl het vrijkomen van gasvormige denitrificatieproducten onderschat werd door de langzame diffusie in de gedeeltelijk natte grond. Dit betekent dat de vaststelling van denitrificatie door middel van de meting van alleen nitraat tot een overschatting zal leiden van de stikstofverliezen, terwijl de meting van alleen lachgas en stikstofgas tot een onderschatting zal leiden. De consumptiesnelheid van zuurstof ($2.7 \text{ L O}_2 \text{ m}^{-2} \text{ d}^{-1}$) en de produktiesnelheden van koolstofdioxide ($3.7 \text{ L CO}_2 \text{ m}^{-2} \text{ d}^{-1}$), lachgas ($1.3 \text{ kg N ha}^{-1} \text{ d}^{-1}$) en stikstofgas ($1.9 \text{ kg N ha}^{-1} \text{ d}^{-1}$) lagen dicht in de buurt van veldgegevens voor onbegroeide grond. Tenslotte werd gekonkludeerd dat, hoewel het respirometersysteem waardevolle gegevens opleverde om het simulatiemodel te testen, een volledige verklaring van de onderlinge relaties tussen deze gegevens alleen bereikt zou kunnen worden met hetzelfde simulatiemodel, omdat de gemeten variabelen het geïntegreerde effect van biologische activiteit en transportprocessen weerspiegelen.

De cylindervormige geometrie van het experimentele aggregaat had het voordeel dat voor dezelfde geometrie een simulatiemodel ontwikkeld kon worden. Het model bevat vier submodellen: 1) biologische respiratie en denitrificatie, 2) watertransport met inbegrip van een beschrijving van hysterese, 3) het transport van opgeloste stoffen in water en 4) gastransport met inbegrip van een nieuwe benadering om gelijke totaal gasdrukken te handhaven in aangrenzende bodemlagen. Deze submodellen werden apart van elkaar ontwikkeld en (deels) getest, voordat het geïntegreerde model werd samengesteld.

Het submodel dat microbiële respiratie en denitrificatie beschrijft voor een homogene grond (d.w.z. ruimtelijk uniform in alle fasen) (hoofdstuk 5), omvat de groei en het onderhoud van biomassa ten koste van glucose en de daarmee, onder anaërobie omstandigheden, gepaard gaande reductie van nitraat tot stikstofgas, via de tussenprodukten nitriet en lachgas. Twee groepen heterotrofe strikt aërobe bacteriën werden onderscheiden: bacteriën die slechts kunnen groeien met zuurstof als electronacceptor en bacteriën die onder aërobe omstandigheden kunnen groeien met zuurstof als electronacceptor en onder anaërobie omstandigheden met nitraat, nitriet

en lachgas als electronacceptor. Groei van beide groepen biomassa's werd berekend met behulp van een eerste orde snelhedenvergelijking, waarin de relative groeisnelheid beschreven werd door een dubbele Monod-vergelijking met snelhedenbeperkende factoren voor koolstof en zuurstof of stikstofhoudende substraten. De Pirt-vergelijking werd gebruikt om de consumptiesnelheden van substraten voor groei en onderhoud te berekenen. Als eerste aanzet om dit submodel te parameteriseren werd een gegevensbestand samengesteld op basis van verschillende literatuurbronnen en vervolgens werd onderzocht of het mogelijk was om experimentele waarnemingen van de opeenvolging van denitrificatieprodukten te simuleren door enige van deze literatuurgegevens binnen redelijke grenzen te varieren.

De conclusie was dat het model een bevredigende beschrijving van het denitrificatieproces geeft zoals dat gemeten wordt in incubatieflesjes in het laboratorium, maar ook dat meer definitieve conclusies over de kwaliteit van het model alleen geformuleerd kunnen worden als biologische gegevens van bodemsystemen beschikbaar komen.

Het submodel dat de diffusie van gassen in multinaire, isotherme, isobare, ideale gasmengsels beschrijft zoals de bodematmosfeer, was gebaseerd op de eerste wet van Fick die was uitgebreid met een fluxterm om gelijke totaal gasdrukken te handhaven in aangrenzende bodemlagen. Ongelijke gasdrukken worden in principe veroorzaakt door verschillen in binaire diffusiecoëfficiënten, verschillende oplosbaarheden van gassen in water, massastroming van gas doordat water stroomt en ongelijke netto gasproductietermen in aangrenzende lagen. De vergelijking van Fick met de extra fluxterm werd getest voor de vereenvoudigde situatie van een gaslaag (welke vergelijkbaar is met een droge bodemlaag) waarin respiratie en denitrificatie optrad, en waar ongelijke totaal gasdrukken in principe alleen veroorzaakt werden door verschillen in binaire diffusiecoëfficiënten: de resultaten verschilden minder dan 10 % van die verkregen met de nauwkeurige kinetische gastheorie, die gebaseerd is op de Stefan-Maxwell vergelijkingen (hoofdstuk 4). Binaire diffusiecoëfficiënten werden berekend met behulp van vergelijkingen uit de kinetische gastheorie. De resultaten hiervan verschilden minder dan 10 % van een aantal experimentele gegevens die van belang waren voor het onderzoek van de bodematmosfeer, en besloten werd verder alleen de theoretische formules te gebruiken.

Een belangrijke conclusie was dat de eerste wet van Fick met de extra fluxterm goede resultaten geeft wanneer binaire diffusiecoëfficiënten niet meer dan een factor 2 verschillen en wanneer één gascomponent in overmaat aanwezig is, zodat binaire diffusiecoëfficiënten aan deze component gerelateerd kunnen worden. Als zulke omstandigheden zich echter niet voordoen, moeten de Stefan-Maxwell vergelijkingen worden gebruikt om diffusie in gasmengsels te bestuderen.

Het submodel dat waterstroming beschrijft werd direct getest met behulp van de gegevens uit het respirometersysteem en de resultaten bleken hiermee goed overeen te komen (hoofdstuk 6). Het submodel voor het transport van opgeloste stoffen werd niet apart getest en kan dus de geaccumuleerde fouten van de andere submodellen bevatten.

Met het geïntegreerde simulatiemodel (hoofdstuk 6) kan de ruimtelijke verdeling van bacteriën, water, nitraat, nitriet, glucose, zuurstof, kooldioxide, lachgas, stikstofgas, neon en de absolute druk van de bodematmosfeer berekend worden als

functie van de tijd, in een onverzadigd, homogeen, cylindrisch aggregaat. Bovendien kan de verandering in atmosferische samenstelling in de meetcel waarin het aggregaat is geplaatst, berekend worden als functie van de tijd. Het simulatiemodel is de theoretische tegenhanger van het experimentele respirometersysteem. De belangrijkste conclusie was dat het model een bevredigende beschrijving geeft van het bestudeerde biologische systeem: een deel van de experimentele resultaten kon kwantitatief beschreven worden, terwijl andere gegevens, die afweken van de experimentele gegevens, begrepen konden worden door het bestuderen van het dynamisch gedrag van het model. Bovendien bleek dat het al of niet aanwezig zijn van gascontinuïteit in de bodemporiën, dat bepaalt of gastransport door zowel de gasfase als de waterfase van de grond plaatsvindt of alleen door de waterfase, een zeer sterke invloed had op het optreden van anaërobie en dus mogelijk denitrificatie. Hysterese in de vochtkarakteristiek veroorzaakte een niet homogene waterverdeling in de grond met het gevolg dat een kleine hoeveelheid toegevoegd water voldoende was om gas-discontinuïteit te veroorzaken in de bodemporiën. Deze studie maakt duidelijk dat de parameterisatie van het model een belangrijk probleem vormt dat als eerste aandacht vraagt.

Tenslotte werd gekonkludeerd dat alleen de wisselwerking tussen experiment en theorie uiteindelijk zal leiden tot een volledig begrip van het ingewikkelde ecosysteem dat hier bestudeerd werd.

Curriculum vitae

1950 8 december: geboorte Peter Albert Leffelaar, te Amsterdam.

1970 eindexamen HBS-B aan het Amsterdams Lyceum te Amsterdam; aanvang landbouwkundige studie aan de Landbouwhogeschool (thans Landbouwuniversiteit) te Wageningen, vanaf september 1971 in de studierichting Bodemkunde en Bemestingsleer.

1974 september: kandidaatsexamen Bodemkunde en Bemestingsleer.

1975 april t/m december: praktijktaid aan Haryana Agricultural University te Hissar, Haryana, India. (Dr. Ray Pal Sharma).

1978 januari: doctoraalexamen Bodemkunde en Bemestingsleer (met lof) met drie hoofdvakken:
de Bodemscheikunde (Prof.Dr.Ir. G.H. Bolt; Dr.Ir. F.F.R. Koenigs),
de Cultuurtechniek (Prof.Dr.Ir. W.H. van der Molen; Dr.Ir. J.W. van Hoorn),
de Theoretische Teeltkunde (Prof.Dr.Ir. C.T. de Wit; Dr.Ir. J. Goudriaan).
Januari t/m mei: verbonden aan de vakgroep Theoretische Teeltkunde (thans Theoretische produktie-ecologie) als studentassistent.
September: aanstelling als promotieassistent bij de vakgroep Theoretische produktie-ecologie; aanvang van het hier beschreven onderzoek en detachering bij de vakgroep Bodemkunde en Bemestingsleer (thans Bodemkunde en Plantenvoeding) in verband met het opzetten en uitvoeren van het bij het onderzoek behorende experimentele werk.

1980 september: aanstelling als wetenschappelijk medewerker bij de vakgroep Theoretische produktie-ecologie met hoofdtaken: het leveren van een bijdrage aan het onderwijs van de vakgroep Theoretische produktie-ecologie en voortzetting van het hier beschreven onderzoek; blijvende detachering bij de vakgroep Bodemkunde en Plantenvoeding.